

1978

# Toward the production of large-particle-size monodisperse latex A feasibility study- the photoinitiated emulsion polymerization of styrene

David E. Sudol  
*Lehigh University*

Follow this and additional works at: <https://preserve.lehigh.edu/etd>

 Part of the [Chemical Engineering Commons](#)

---

## Recommended Citation

Sudol, David E., "Toward the production of large-particle-size monodisperse latex A feasibility study- the photoinitiated emulsion polymerization of styrene" (1978). *Theses and Dissertations*. 5137.  
<https://preserve.lehigh.edu/etd/5137>

This Thesis is brought to you for free and open access by Lehigh Preserve. It has been accepted for inclusion in Theses and Dissertations by an authorized administrator of Lehigh Preserve. For more information, please contact [preserve@lehigh.edu](mailto:preserve@lehigh.edu).

Toward the Production of Large-Particle-Size  
Monodisperse Latex  
A Feasibility Study -  
The Photoinitiated Emulsion Polymerization of Styrene

by  
E. David Sudol

A Research Report  
Presented to the Graduate Committee  
of Lehigh University  
In Candidacy for the Degree of  
Master of Science  
In Chemical Engineering

Lehigh University

1978

CERTIFICATE OF APPROVAL

This research report is accepted and approved in partial fulfillment of the requirements for the degree of Master of Science in Chemical Engineering.

Professors in Charge

M. L. Aaberg

V. J. Miele

J. W. Vandekhoff

Head of Department

A. J. Hengst

Date March 20, 1979

ACKNOWLEDGEMENTS

I wish to express my sincere appreciation to:

Dr. Mohamed El-Aasser, for his continuing interest, support, and guidance throughout this work and especially for his friendship.

Drs. F.J. Micale and J.W. Vanderhoff, for their interest and encouragement.

Joe Hojsak, for providing me with his time, tools, and machinery.

Syed Ahmed, for teaching me the serum replacement technique.

Dennis Nagy and Cesar Silebi, for their help in obtaining particle size via hydrodynamic chromatography and light scattering.

The Emulsion Polymers Institute and the National Aeronautics and Space Administration for their financial support during my research assistantship.

The Textile Veterans Association, for providing the Raymond T. Anderson Honor Award, presented to me as a result of the efforts contained in this report.

TABLE OF CONTENTS

	PAGE
CERTIFICATE OF APPROVAL	i
ACKNOWLEDGEMENTS	ii
TABLE OF CONTENTS	iii
LIST OF TABLES	v
LIST OF FIGURES	vi
ABSTRACT	1
I - INTRODUCTION	3
II - THEORETICAL BACKGROUND	9
III - EXPERIMENTAL	
A. Polymerization Vessels	14
B. Polymerization Procedure	20
C. Analysis of Polymerized Samples	
1. Conversion	23
(a) Dilatometry	23
(b) Gravimetric	24
2. Particle Size	24
(a) Hydrodynamic Chromatography	25
(b) Electron Microscopy	25
(c) Light Scattering	27
3. Molecular Weight	28
IV - RESULTS AND DISCUSSION	
A. LU cell	30
1. Variation in the Recipe for Photoinitiated Emulsion Polymerization.	31

	PAGE
B. Transition of Experimentation to the GE Laboratory Prototype.	52
1. Scale-up	52
2. Time Restriction Check	57
3. Choice of Recipe for Further Investigations	60
4. Investigation of the One-to-one Mole Ratio of Styrene to SLS.	62
(a) Rate of Polymerization and Degree of Conversion	62
(b) Particle Size and Molecular Weight	75
5. Other Kinetic Considerations.	
(a) Temperature Effect	80
(b) Dependency of the Rate on Monomer and Initiator Concentrations	86
V - SUMMARY AND CONCLUSIONS	91
VI - POSTSCRIPT	93
REFERENCES	94
APPENDICES	96
A. Determination of Average Particle Size from Light Scattering	97
B. Determination of $\bar{M}_n$ and $\bar{M}_w$ by Gel Permeation Chromatography (GPC)	100
C. Reproducibility Studies	102

LIST OF TABLES

TABLE		PAGE
I	Photoinitiated Emulsion Polymerization of Styrene in the LU cell as a Function of Recipe Parameters (3% styrene monomer)	33
II	Photoinitiated Emulsion Polymerization of Styrene as a Function of Conditions and Recipe Parameters (3% styrene monomer)	59
III	Photoinitiated Emulsion Polymerization of Styrene in the GE vessel as a Function of the Initiator Concentration (3% styrene monomer)	66

LIST OF FIGURES

FIGURE		PAGE
3.1	Cross-sectional view of the cylindrical vessel proposed for photoinitiated emulsion polymerizations in SPAR experiments. V1, V2, and V3 are valves, RTD is a resistance temperature detector, PD, a photo-diode light sensor, and D, a flexible diaphragm sensor for volume change measurement (General Electric).	15
3.2	Design specifications and dimensions of the LU laboratory vessel for initial photoinitiated emulsion polymerization experiments. Front and side views.	17
3.3	LU laboratory polymerization vessel - exploded diagram.	18
3.4	Schematic of the LU cell with equipment necessary for conducting kinetic studies of photoinitiated emulsion polymerizations.	19
3.5	GE laboratory prototype polymerization vessel, a modified version of Figure 3.1 (General Electric)	21
3.6	Calibration curve for Hydrodynamic Chromatography (HDC) through packed porous silica. Eluting solution is 0.55mM SLS in deionized water. Standards are Dow uniform latexes.	26
3.7	Calibration curves for Gel Permeation Chromatography (GPC) illustrating the changing calibration. Eluting liquid is toluene.	29
4.1a	Relative absorbance of the photoinitiator, DEAP, showing peak at 252nm.	32
4.1b	Typical irradiance of a UV lamp, similar to that used for photoinitiated polymerizations.	32
4.2	Rate of capillary fall versus time for an emulsion consisting of 3% styrene and 3% SLS as a function of the percent photoinitiator, DEAP, based on styrene (samples 10, 12, 13, 14).	35



- 4.3 Capillary height-time relationships for the data in Figure 4.2, percent conversion is represented in the right hand axis. The solid points represent the results of constant leakage corrections and the percentages above each curve are the gravimetrically determined minimum conversions (samples 10, 12, 13, 14). 36
- 4.4 Reproducibility experiment of a system consisting of 3% styrene, 3% SLS, and 10% DEAP based on styrene, showing good agreement despite dilatometric inaccuracy. Solid points correspond to right hand axis. (samples 13, 13-2) 38
- 4.5 Reproducibility experiment of a system consisting of 3% styrene, 3% SLS, and 15% DEAP based on styrene. Differences are primarily due to the instability of the system, one having been agitated just prior to the experiment (14-2,  $\square$ ), while the other was used having evidence of separation (14,  $\circ$ ). Solid points correspond to capillary height. 39
- 4.6 Effect of co-emulsifier content on the polymerization rate of a system consisting of 3% styrene, 3% SLS, and 10% DEAP based on styrene with varying amounts of hexadecane (samples 13, 15, 18). 40
- 4.7 Rate of capillary fall as a function of the percent DEAP based on styrene for a system consisting of 3% styrene, 3% SLS, and 1.5% decanol co-emulsifier (samples 19, 21-2, 23, 27). 42
- 4.8 Capillary height-time as a function of the percent DEAP based on styrene for the data in Figure 4.7. Solid points represent the results of constant leakage corrections. 43
- 4.9 Rate-time relationships for capillary height ( $\circ$ ) and UV intensity transmitted through the cell ( $\square$ ) during polymerization (sample 22). 45
- 4.10 Capillary height and UV intensity-time relationships for the data in Figure 4.9. Solid line is the capillary height curve corrected for a constant leakage rate. 46

FIGURE	PAGE	
4.11	UV intensity versus time measured through the LU cell containing deionized water. For comparison, data from Figure 4.10 are also given. Arrow indicates intensity recorded at the end of the experiment.	48
4.12	Capillary height (○, ●) and its rate of change (□, ■) for a system consisting of 3% styrene and 20% DEAP based on styrene with a 1:2 ratio of SLS to decanol (sample 24, 1.5% SLS, ●, ■, sample 25, 0.75% SLS, ○, □).	50
4.13	Rate of capillary height change as a function of the SLS content, the system containing 3% styrene, 0.05% decanol, and 10% DEAP based on styrene, with 3% SLS (△) or 1.5% SLS (○) (samples 15 and 16, respectively).	51
4.14	Rate of capillary height change (□, ■) and percent conversion (○, ●) for a system consisting of 3% styrene, 8.3% SLS, and 20% DEAP based on styrene. Solid points represent corrected data (sample 28).	53
4.15	Polymerization rate, $R_p$ , (□, ■) and percent conversion (○, ●), obtained from the GE vessel, for comparison to Figure 4.14 (LU cell), same recipe. Solid points represent corrected data (sample 32).	55
4.16	Comparison of rate data from the LU cell and the GE vessel, for the same polymerization recipe (samples 28 and 32).	56
4.17	Comparison of polymerization rate (□, ○) and conversion (■, ●) data for samples 32 (□) and 33 (○), obtained from the GE vessel.	61
4.18	Temperature-time and the corresponding capillary change for water, used as a control in the GE vessel.	63
4.19	Percent conversion as a function of photoinitiator content, DEAP, for the micellized system consisting of 3% styrene and 8.3% SLS. Circles indicate dilatometric conversion while bars are the limits of conversion determined gravimetrically.	65
4.20	Polymerization rate curves for increasing photoinitiator DEAP, in the micellized system (samples 52, 43, 37, 44, 45).	68

FIGURE	PAGE
4.21 Conversion histories corresponding to the data in Figure 4.20 .	69
4.22 Polymerization rate curves for increasing photoinitiator, DEAP, in the micellized system (samples 43, 37, 35, 39, 38, 36).	70
4.23 Rate of polymerization, $R_p$ , at 1.5 minutes as a function of the photoinitiator content, DEAP, for the micellized system consisting of 3% styrene and 8.3% SLS.	71
4.24 Intensity of UV radiation transmitted through the micellized system, no styrene present, as a function of the photoinitiator content, DEAP.	74
4.25 Average particle size as a function of the photoinitiator content, DEAP. Circles represent values obtained from HDC, the bars indicating the limits on these measurements. Squares were obtained from light scattering.	76
4.26a,b Electron micrographs of the latex particles produced in the system consisting of 3% styrene, 8.3% SLS, and 1.1% DEAP based on styrene (sample 52).	78
4.27 Examples of GPC chromatograms obtained for the micellized system with increasing photoinitiator content, DEAP.	79
4.28 Number ( $\square, \blacksquare$ ) and weight ( $\circ, \bullet$ ) average molecular weights determined as a function of photoinitiator content, DEAP, for the micellized system.	81
4.29 Polymerization rate curves as a function of the polymerization temperature for the system, 3% styrene, 8.3% SLS, and 17.6% DEAP based on styrene.	83
4.30 Conversions histories corresponding the the data in Figure 4.29.	84
4.31 Percent conversion and rate of polymerization, $R_p$ , at 1.5 minutes, as a function of temperature, obtained from the data in Figures 4.29 and 4.30.	85
4.32 Arrhenius dependance of the rate of polymerization on the temperature. The line represents the least squares fit of the data.	87

FIGURE

PAGE

- 4.33 Rate of polymerization,  $R_p$ , as a function of the percent conversion ( or monomer concentration) for varying amounts of DEAP in the micellized system, 3% styrene, 8.3% SLS. 89
- 4.34 Rate of polymerization,  $R_p$ , at 1.5 minutes, as a function of the square root of the initial photo-initiator concentration, DEAP, in the micellized system, 3% styrene and 8.3% SLS. 90

## ABSTRACT

An Experimental Definition Study, designed to investigate the feasibility of carrying out a photoinitiated emulsion polymerization to a significant conversion in a SPAR (Space Processing Applications Rocket) prototype polymerization vessel within the five minutes approximating the free-fall, microgravity time, has been accomplished. This is the first step in a proposed sequence of events leading to the production of large-particle-size monodisperse latexes (2-40 $\mu$ m) aboard Space Lab in the early 1980's.

In order to provide specifications for the construction of the cylindrical SPAR vessel by the General Electric Space Sciences Lab, a flat cell, designated the LU (Lehigh University) cell, was designed and assembled. Preliminary polymerization recipes, consisting of styrene monomer, sodium lauryl sulphate (SLS) emulsifier, a co-emulsifier, and  $\alpha,\alpha$ -diethoxyacetophenone (DEAP) photoinitiator, were investigated using this vessel. Subsequently, specification of the ultraviolet light source and vessel dimensions were provided to GE.

Polymerization kinetics were determined by dilatometry, a uniform diameter glass capillary being used to monitor the changing volume. The final conversions were obtained by both dilatometric and gravimetric means. The latter determination was uncertain, in that only limits could be given without knowledge of the amount of initiator incorporated into the particles.

On the basis of the emulsion and product stability, and high polymerization rate and conversion, a micellized styrene system (1:1

mole ratio styrene to SLS) was chosen for an optimization study in the GE vessel. Rate of polymerization, conversion, particle size, and molecular weight were determined as a function of the concentration of the photoinitiator. The polymerization rate was found to increase up to a maximum, then decrease with increasing initiator concentration. The maximum occurs around 23% DEAP (based on the styrene monomer phase), which corresponds to a conversion of about 70%, as measured by dilatometry. Both the average particle size and the weight-average molecular weight were found to decrease with increasing initiator.

Photoinitiation, as a means of producing a relatively high conversion in a five minute free-fall experiment, appears to be a satisfactory method for conducting an emulsion polymerization in a SPAR experiment.

## PART I - INTRODUCTION

Latexes which are used industrially in large quantities generally have a relatively broad particle size distribution (PSD). This is not usually of much concern in the manufacture of such products as latex paints, paper coatings, carpet backing, and others, in that there is no need for a specific narrow PSD. A typical example might be a latex system with a particle size of  $0.02\mu\text{m}$  with a standard deviation of  $0.05\mu\text{m}$  or 25%.

Monodisperse latexes, however, are used in much smaller quantities, primarily for scientific purposes. By definition, a monodisperse latex must have a very narrow PSD, such as  $0.20\mu\text{m}$  with a standard deviation of  $0.003\mu\text{m}$  or 1.5%. The first monodisperse latex was prepared nonintentionally in 1947 in a Dow Chemical Company pilot plant, the monodispersity being discovered later by accident<sup>1</sup>. This was the famous 580G LOT 3584 polystyrene latex. The narrow PSD was thought of as an anomaly since other batches using the same recipe had not produced similar results. Subsequently in 1951, a study deliberately aimed at preparing the same monodisperse latex was successful. A series of monodisperse latexes were then prepared, ranging in size from  $0.088\mu\text{m}$  to  $1.172\mu\text{m}$ . These consisted of both polystyrene and polyvinyltoluene latexes<sup>2,3</sup>. Conventional emulsion polymerization was used to produce the smaller sizes, while the concept of "seeding"<sup>4</sup> was successfully employed to produce the larger sizes. The latter involves the addition of monomer to a latex "seed" and polymerizing without the generation of a new crop of particles. Through this seeding

approach the PSD can be narrowed by polymerization under controlled conditions.

When ten of these monodisperse latexes were made available in 1955<sup>3</sup> many possible uses soon became apparent. They were used for calibration of scientific measuring instruments, such as electron microscopes, light scattering instruments, and ultracentrifuges, for counting virus particles, and determination of pore sizes. Also they found use in medical serological tests, such as for rheumatoid arthritis, human pregnancy, and trichinosis, and studies of the reticulo-endothelial system<sup>8</sup>. Requests for these latexes, which at first were offered without charge, soon became so great that Dow came to impose a sales price, initiating what has become a profitable business. By the early 1970's the annual sales of monodisperse latex diagnostic kits were \$30,000,000.

Currently, monodisperse latexes are available in size ranges 0.05 - 2.0 $\mu$ m and greater than about 40 $\mu$ m. The latter is about the smallest size that can be separated by elutriation or sieving. Monodisperse latexes with particle sizes between these ranges are not presently available, while the need for them is obvious. For instance, in most hospitals blood cells are counted using an electronic particle counter such as a Coulter Counter, but these counters are calibrated with standards that do not closely approximate the size of red blood cells, 7 $\mu$ m.

The reason for the gap in available sizes of monodisperse latexes lies in the difficulty of preparation. The production of monodisperse



polystyrene latex by emulsion polymerization for further use as a seed involves mixing styrene monomer, water, emulsifier, initiator, and buffer, and heating to the polymerization temperature<sup>9</sup>. Monodispersity is achieved by having a short particle nucleation stage relative to the particle growth stage. Using the seeding technique, particles can be grown from, say 0.1 $\mu$ m to 2.0 $\mu$ m in a sequence of polymerizations, each having an increased seed particle size<sup>2,3,6,7</sup>.

The limit of approximately 2 $\mu$ m diameter is reached due to the sensitivity of latexes to emulsifier concentration and mechanical shear. The emulsifier level must be high enough to maintain particle stability and yet must not exceed the amount needed to generate a new crop of particles. The latter occurs when the critical micelle concentration (c.m.c.) is reached in the aqueous phase, resulting in a bimodal PSD<sup>6,7</sup>. For small-particle-size latexes the amount of emulsifier can be anywhere in a relatively broad concentration range, such as from 1.00 to 2.57% for a seed latex of 0.257 $\mu$ m diameter<sup>6,7</sup>. As the seed size increases, however, this range narrows, until at sizes above 1 $\mu$ m, the polymerization becomes a "knife-edge" operation, for which polymerization with the same ingredients might yield partial flocculation of the latex or a stable latex with new particles.

Flocculation caused by mechanical shear also becomes a problem with increasing particle size. As the particles become larger the intensity of Brownian motion decreases thus enhancing the effect of the density difference between the particles and the aqueous phase. Creaming of polystyrene particles (density, 1.05gm/cc) swollen with styrene

monomer (density, 0.905gm/cc) occurs when a critical size, somewhere between 0.5 and 0.8 $\mu$ m, is reached with a 2:1 ratio monomer to polymer. Settling of polystyrene particles also begins to occur in this size range. Thus, at low conversions the particles tend to cream and at high conversions they settle out and since the polystyrene particles are soft until very high conversion (approaching 100%), either of these could result in sticking and coalescence of the particles. Therefore, increased agitation is used to offset these effects but often with the result of creating coagulum through the mechanical shearing action. In attempts to improve this situation, polyvinyltoluene (density, 1.027gm/cc) and vinyltoluene-tert-butylstyrene copolymer particles (density, 1.00gm/cc) have been prepared but are limited to 2.0 $\mu$ m again because of creaming at low conversion. Other attempts to alter the density of the aqueous phase have ended in coagulation due to destabilization of the latex particles.

Eliminating this gravity effect can be accomplished if the polymerization could be carried out in the microgravity environment of space. In this case, the emulsifier concentration could be kept at a level low enough to ensure that no new particles are generated while maintaining the stability of the latex. The density effects of creaming and settling during polymerization would be eliminated and agitation could be reduced to a level which minimizes flocculation due to the shearing and yet ensure good heat transfer.

To this end, technical proposals were submitted to the National Aeronautics and Space Administration (NASA) entitled: 1. "Hetero-

genious Chemical Reactions: Preparation of Monodisperse Latexes", in response to an announcement of opportunity (A.O.) for SPAR experiments; 2."Heterogenous Chemical Reactions: Preparation of Large-Particle-Size Monodisperse Latexes", in response to an A.O. for the Orbital Flight Test (OFT) missions of the Space Shuttle; and 3."Production of Large-Particle-Size Monodisperse Latexes", in response to an A.O., "Space Processing Investigations for STS (Space Transportation System) Missions".

These proposals suggest a sequential program as follows:

1. determination of the kinetics of small-particle size latexes in the approximately five minutes of microgravity available in the SPAR experiments for comparison to the same experiments on earth;
2. determination of the kinetics of seeded emulsion polymerization of large-particle-size monodisperse latexes on early tests of the Space Shuttle in order to supply data for the design and operation of a large scale production process on Space Lab;
3. developement of a production facility for operation in microgravity that will produce 1500-2000cc quantities of 30% solids large-particle-size monodisperse latexes;
4. transfer of responsibility for the manufacture and marketing to an interested company.

Subsequently, a four month Experimental Definition Study was funded by NASA in order to determine the feasibility of obtaining the kinetics of fast polymerizing small-particle-size latexes during a SPAR

flight, as mentioned in 1. above. The work reported here was begun under this contract and continued somewhat beyond the initial design. The immediate objective was to further define and develop the scientific base, flight hardware requirements, and experimental operating conditions for the proposed SPAR experiments.

## PART II - THEORETICAL BACKGROUND

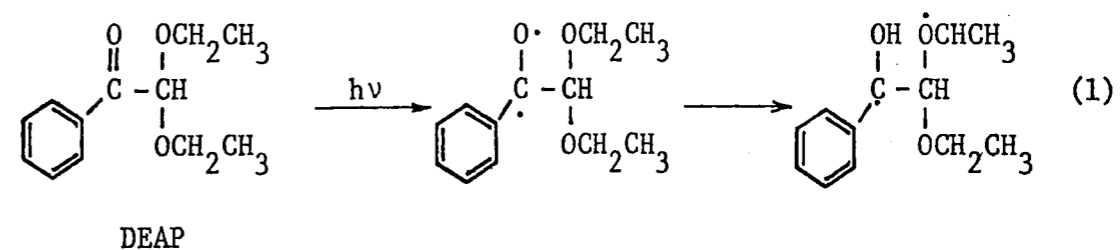
Much has been written on the subject of emulsion polymerization, its theories and practices, and no attempt will be made here to review this area. A brief description of the process in relation to its intended use in this Experimental Definition Study will be made, however.

The essential components of an emulsion polymerization system are the monomer(s), dispersing medium, emulsifying agent(s), and initiator. Under consideration for this study are combinations of styrene monomer, water, sodium lauryl sulphate (SLS) with or without a co-emulsifier, and  $\alpha,\alpha$ -diethoxyacetophenone (DEAP) photoinitiator. This system does not fit the strict definition of emulsion polymerization in that the initiator is oil (styrene) soluble rather than water soluble. Oil soluble initiators are generally used in suspension polymerizations which produce particles only as small as 1-3 $\mu$ m. Particle sizes resulting from emulsion polymerization are generally on the order of 0.05-0.2 $\mu$ m.

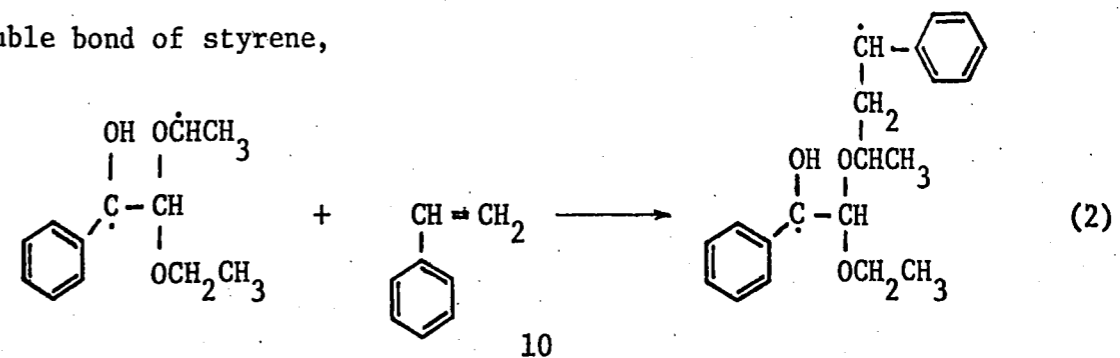
The most frequently cited theoretical mechanism of emulsion polymerization has been advanced by Harkins<sup>10</sup>. This three stage approach will be briefly described here.

The first stage is referred to as the initiation stage. When an emulsifier, such as SLS, is added to water in a concentration above its critical micelle concentration (c.m.c.), micelles are formed. A micelle is often depicted as a cluster of 50-100 of these soap molecules with their hydrophobic ends (hydrocarbon chain) pointed towards the center of the micelle. When a relatively water insoluble

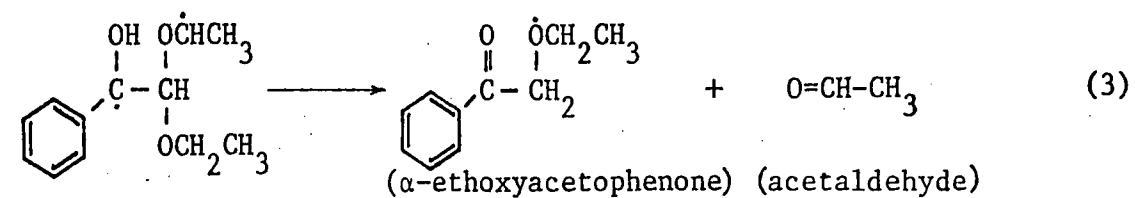
monomer, such as styrene, is added to this solution, it can be found in the form of large droplets (1 - 10  $\mu\text{m}$  in diameter) stabilized by emulsifier molecules and also solubilized inside of these micelles. The ratio of the amount of monomer in the form of droplets to the amount in the form of swollen micelles will vary depending on the concentrations of each component. An extreme would be the case where no droplets exist, all of the monomer being absorbed into the micelles, termed a micellized or solubilized system. For a typical emulsion polymerization using a water soluble initiator, such as potassium persulphate, free radicals are generated in the aqueous phase and enter the monomer swollen micelles initiating polymerization. However, due to the fact that the photoinitiator, DEAP, is relatively water insoluble and styrene soluble, free radicals will be generated in the oil phase, that is, in the monomer swollen micelles and monomer droplets. This occurs when initiator molecules are activated by photons of a particular wavelength (in the range 200-400nm) and energy, polymerization beginning as given by the the following equation for DEAP<sup>11</sup>,



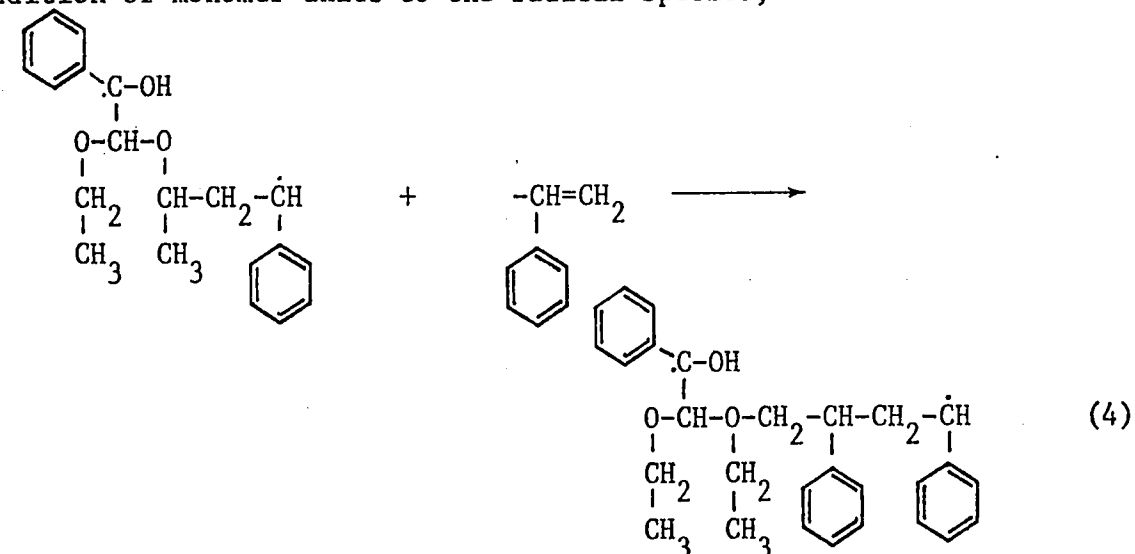
This biradical intermediate is a good attacking group for the vinyl double bond of styrene,



In the absence of a reactive site this biradical will undergo internal coupling and disproportionation<sup>11</sup> yielding,



Stage two, termed propagation and growth, involves the continued addition of monomer units to the radical species,



Radical chain polymerization continues in this manner with the addition of monomer units. The initiation stage is separated from the growth stage when new particles are no longer generated. During this stage the monomer concentration in the polymer particles is considered to be constant, the monomer being supplied to the growing particles from the droplets which act as monomer reservoirs.

In stage three, these reservoirs have disappeared resulting in a continually decreasing monomer concentration in the particles until the end of the polymerization. There is no particle growth in this stage, only shrinkage due to the density change from monomer to polymer.

The rate of polymerization in an emulsion system is determined by a number of factors. A comprehensive treatment of the kinetics and mechanisms has been given recently in a review paper by Ugelstad and Hansen<sup>12</sup>. The kinetics for each stage are described in terms of the Smith-Ewart theory, with some modifications, and also some more recent theories.

The polymerization rate is, first of all, dependant on the number of particles formed. With more particles, there is an increased number of sites for polymerization. The number of particles is determined by the rate of initiation and the emulsifier concentration in the micellar form. Smith and Ewart derived this relationship as

$$N_p = k \left( \frac{R_i}{\mu} \right)^{0.4} (a_s [S])^{0.6} \quad (5)$$

where  $k$  = constant between 0.37 and 0.53

$\mu$  = rate of increase of the volume of a polymer particle

$a_s$  = interfacial area occupied by an emulsifier molecule

$[S]$  = concentration of micellar emulsifier

For a photoinitiated system the rate of initiation is given by<sup>11</sup>

$$R_i = 2\phi I_o \left[ 1 - e^{-\epsilon [I]b} \right] \quad (6)$$

for a vessel of thickness  $b$  or

$$R_i = 2\phi\epsilon I_o [I] \quad (7)$$



when the incident light intensity does not vary significantly through the thickness of the cell,

where  $\phi$  = quantum yield for radical production

$\epsilon$  = molar absorptivity of the initiator for the particular wavelength of radiation absorbed  
(extinction coefficient)

$I_0$  = light intensity incident on the initiator  
(moles of light quanta per liter-second)

$[I]$  = concentration of the initiator (moles/liter)

For the case of an oil soluble initiator  $[I]$  would be the concentration in the monomer/polymer phase. This also assumes that both radical sites of the biradical of DEAP are equally accessible for reaction with styrene monomer.

The rate of polymerization is also dependent on the propagation rate constant,  $k_p$ , the concentration of monomer in the particles,  $[M_p]$ , and the average number of radicals per particle,  $\bar{n}$ ,

$$R_p = k_p [M_p] N_p \bar{n} \quad (8)$$

$\bar{n}$  is dependent on the rate of free radical termination in the particle, and the rates of radical adsorption and desorption.

From the standpoint of developing a system for photoinitiated polymerization, the variables that would affect rates and conversions would be the amount of monomer, the types and concentrations of emulsifiers and photoinitiator, the thickness of the reaction vessel and the intensity of the incident UV radiation.

### PART III - EXPERIMENTAL

#### A. Polymerization Vessels

Two different reaction vessels were used during the course of this investigation, each serving a specific function. The first, referred to as the LU (Lehigh University) cell, was designed in order:

1. to establish the critical dimensions of the second, the General Electric laboratory prototype polymerization vessel, this being a modification of the vessel shown in Figure 3.1;
2. to evaluate preliminary polymerization recipes consisting of styrene monomer, sodium lauryl sulphate (SLS) emulsifier, co-emulsifier, and  $\alpha,\alpha$ -diethoxyacetophenone (DEAP) photoinitiator, in order to determine which would be studied in more detail using the GE prototype vessel;
3. to determine the problems associated with this experiment, such as obtaining the kinetics of polymerization and the percent conversion of styrene to polystyrene by dilatometric and gravimetric techniques. The latter two objectives will be discussed in Part IV.

The LU cell was designed to meet a number of qualifications. First, the UV radiation pathlength through the reaction fluid and also the distance between the lamp and the Quartz cell window was necessarily adjustable. Second, in order to determine percent conversion and reaction kinetics by dilatometry, a capillary in contact with the fluid system and open to the atmosphere was incorporated. Implicit in this condition is the constraint that no leakage from the cell would be acceptable. Third, the temperature within the cell required monitoring in order that any thermal expansion of the fluid due to temperature rise could be accounted for. Fourth, a provision was needed for meas-

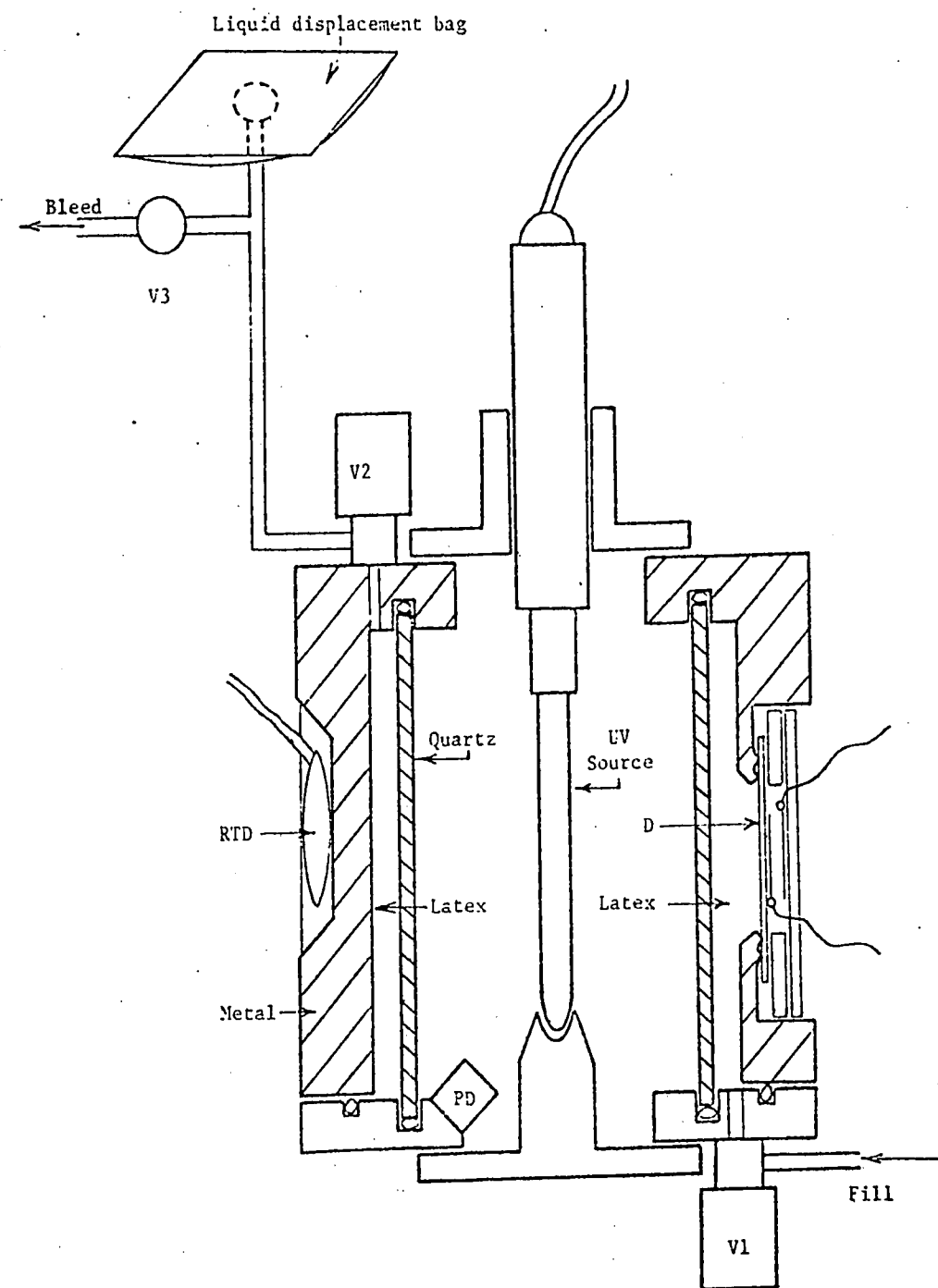


Figure 3.1 Cross-sectional view of the cylindrical vessel proposed for photoinitiated emulsion polymerizations in SPAR experiments. V1, V2, and V3 are valves, RTD is a resistance temperature detector, PD, a photodiode light sensor, and D, a flexible diaphragm sensor for volume change measurement (General Electric).

uring the intensity of the UV radiation after it has passed through the fluid. Fifth, the components of the cell in contact with the fluid were necessarily inert with respect to all components of the polymerization recipe, and sixth, the cell had to be simple enough to be designed and built in a relatively short period of time. These conditions were, for the most part, met by the cell illustrated in Figure 3.2. It consists of three machined teflon blocks which hold two circular quartz windows a fixed distance apart. This distance could be varied by replacement of the middle block with another machined to the desired dimension. This interchangeable component would allow for a varying UV pathlength through the fluid and, in effect, would also change the cell volume. The quartz window on the far side from the UV source could be replaced by a Plexiglas window having three thermistors imbedded in the top, center, and bottom for monitoring temperatures of the fluid during polymerization. Aluminum blocks were used in order that sufficient pressure could be applied to prevent leakage. An exploded diagram is shown in Figure 3.3 and the entire apparatus is depicted in Figure 3.4. A cathetometer was used to measure the change in the fluid level in the capillary tube. The latter was calibrated by measuring the weight and length of varying amounts of mercury drawn into the capillary at a known room temperature. The ultraviolet light source used for activation of the photoinitiator was a low-pressure mercury vapor lamp (Model C-15-61, Oriel Corp.), 5cm. long, having a power of 4.6 watts. The parallel distance between the lamp and the cell could be varied to a minimum of 3.7cm. from the quartz

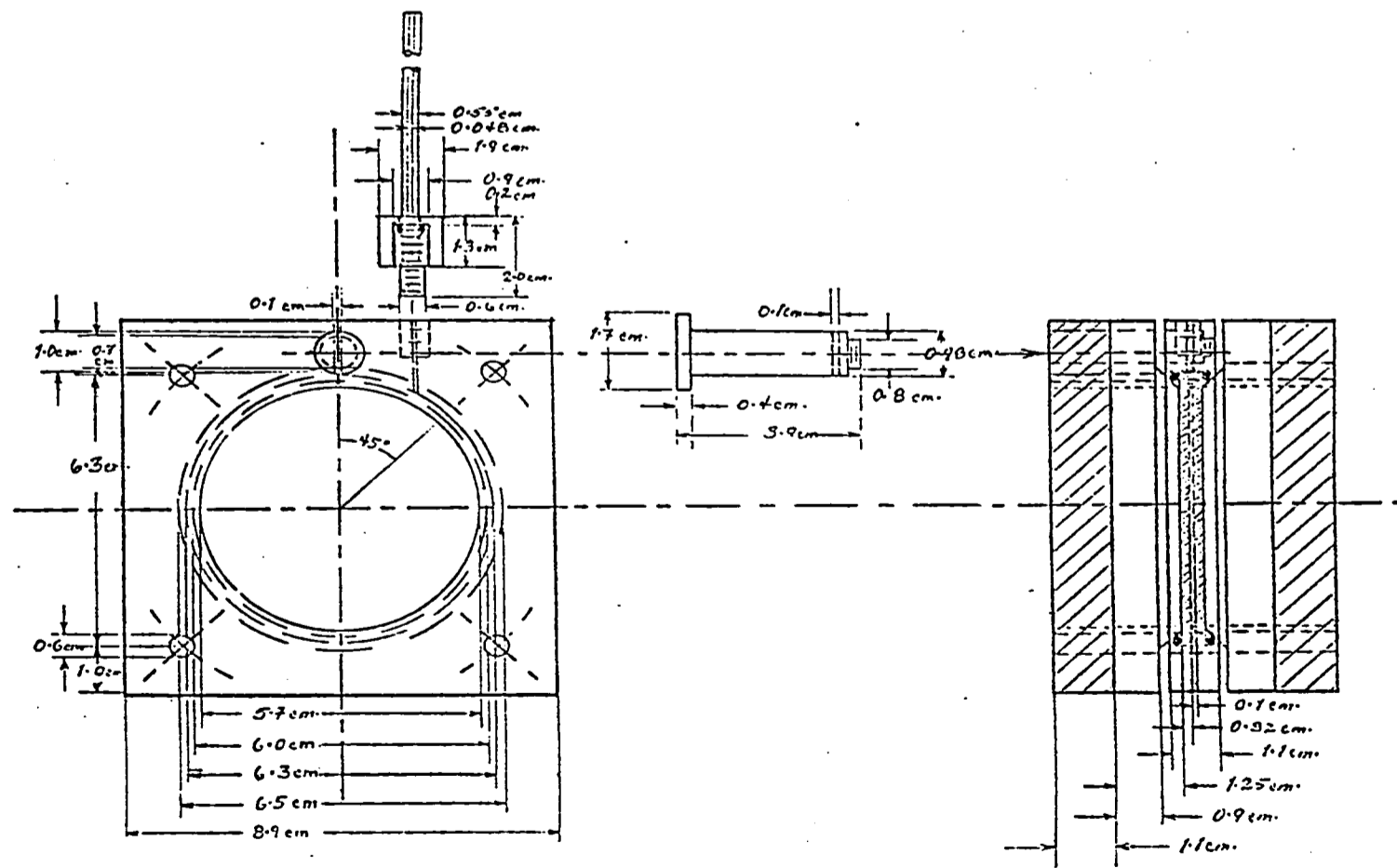


Figure 3.2 Design specifications and dimensions of the LU laboratory vessel for initial photoinitiated emulsion polymerization experiments. Front and side views.

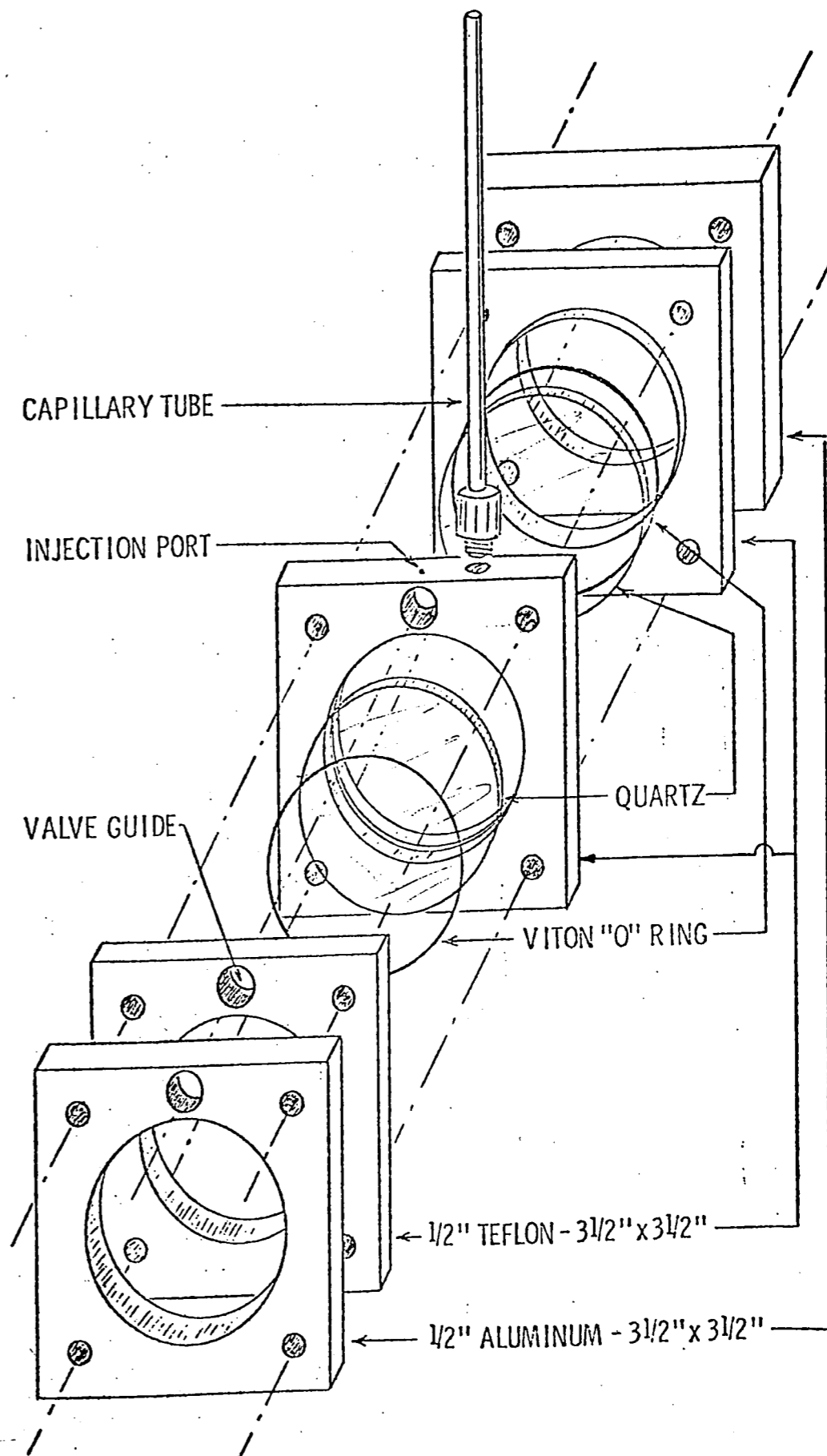


Figure 3.3 LU laboratory polymerization vessel - exploded diagram.

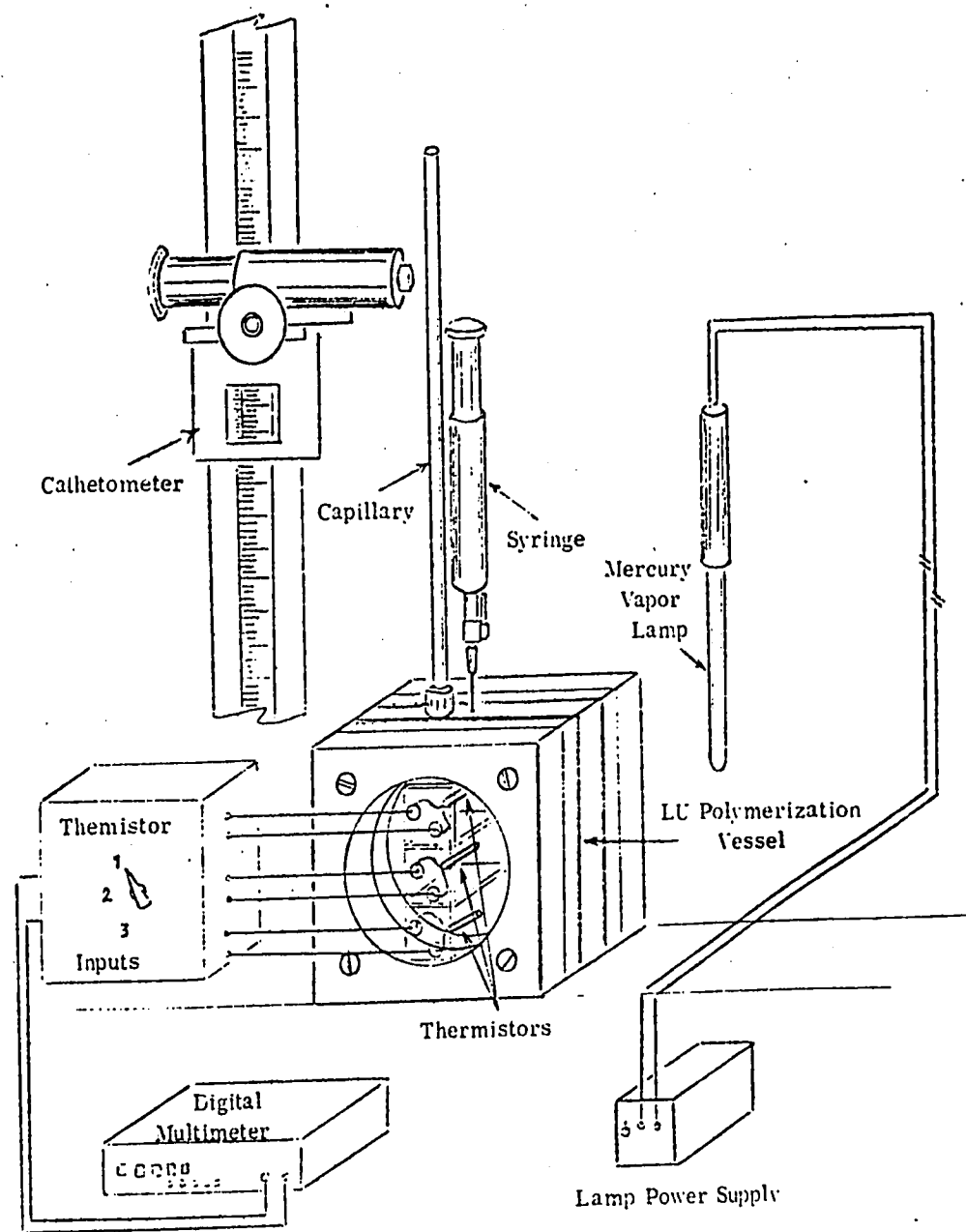


Figure 3.4 Schematic of the LU cell with equipment necessary for conducting kinetic studies of photoinitiated emulsion polymerizations.

window. A multimeter was used to measure resistances of the three thermistors, previously calibrated, to obtain temperatures.

The completed LU cell, used for the preliminary experiments, had a cell thickness of 0.091cm and a volume of 2.45cc. Reasonable polymerization results were obtained with this configuration, the lamp having been positioned at its minimum distance. It should be noted that experiments were conducted with the lamp positioned diagonally closer to the cell with no significant improvements in the results. The final dimensions for the GE laboratory prototype were chosen as illustrated in Figure 3.5. The annular fluid space had a width of 0.1cm and the radius measured from the center to the fluid was 2.7cm. These dimensions do not follow exactly from those of the LU cell but were felt to be a sound choice in light of the preliminary polymerization results. These will be discussed in Part IV. The volume of the GE vessel was 9.15cc, being slightly greater than what is calculated using these dimensions (8.6cc) due primarily to the non-uniformity of the quartz glass cylinder.

#### B. Polymerization Procedure

The polymerization recipes were all prepared in a similar manner. The sodium lauryl sulphate (SLS) emulsifier plus co-emulsifier, if used, were mixed with distilled de-ionized water which had previously been boiled and subsequently cooled under a nitrogen atmosphere to remove any dissolved oxygen. This mixture was sonified using the Sonifier Cell Disruptor (Model W-350, Branson Sonic Power Co.) for approximately one-half minute, then the styrene monomer together with UV initiator was added and again sonified for several minutes. The styrene had



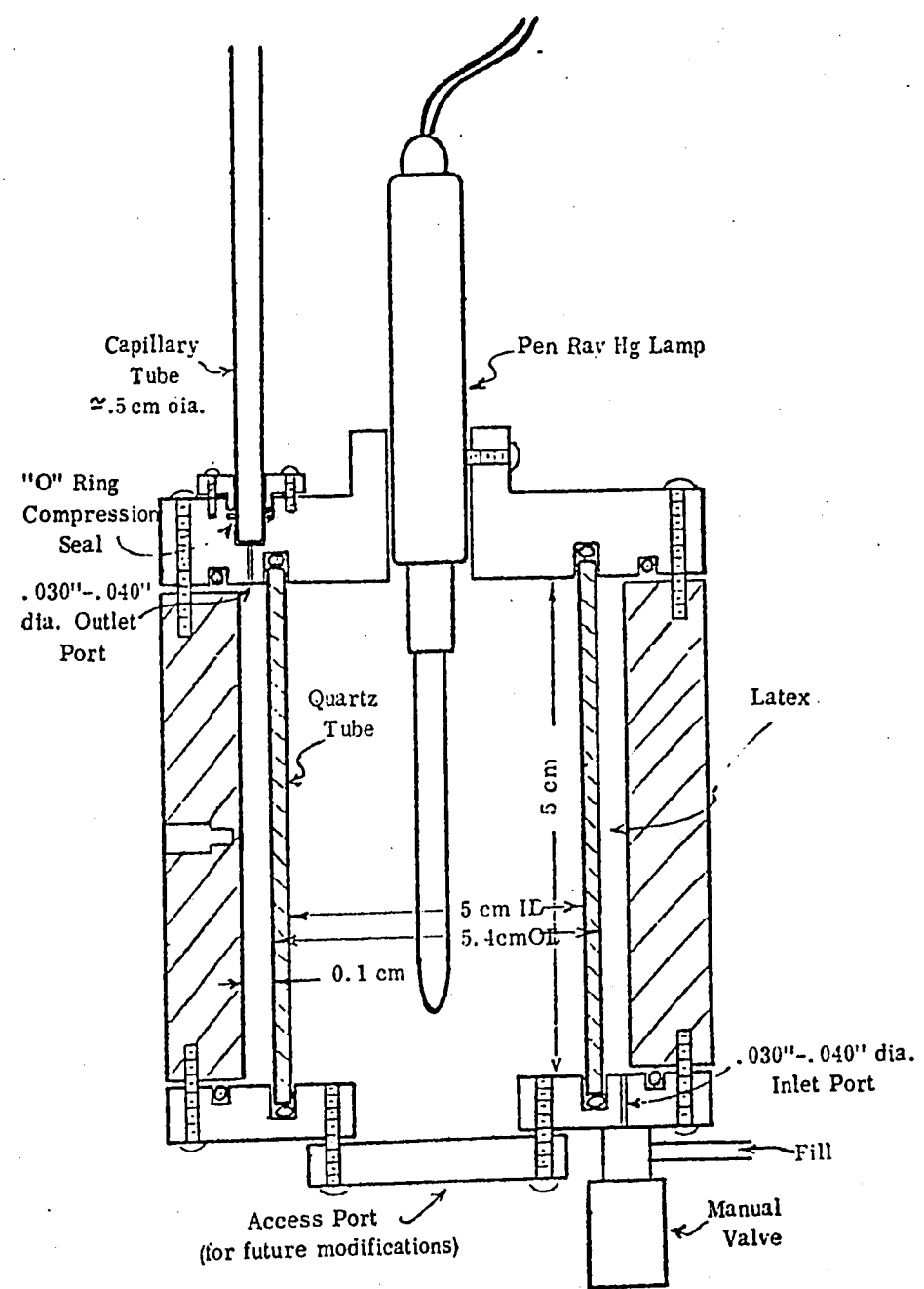


Figure 3.5 GE laboratory prototype polymerization vessel, a modified version of Figure 3.1 (General Electric).

previously been washed with sodium hydroxide and distilled. The emulsion was then cooled under aspirator vacuum or nitrogen prior to being charged into the cell. In the experiments conducted with the GE cell, the sonifier was not needed due to the high levels of SLS, instead the mixture was stirred via a magnetic bar and loaded directly into the cell.

Each cell was charged with the emulsion by means of a syringe and the fluid was continuously forced out of the capillary tube until air bubbles were no longer observed. The cells were tilted during this procedure in order that all the air would rise to the capillary and be expelled. Removal of all air bubbles from the vessels was imperative if accurate dilatometric data was to be obtained. The capillary fluid height was then monitored for change due to equilibration in the cell. When the fluid had reached a constant level the experiment was begun by simultaneously switching on the UV lamp and a timer, first having recorded the capillary height read from the cathetometer, the room temperature, and the thermistor readings from the cell. Note that the LU cell thermistors were located within the reaction fluid while the thermistor location in the GE cell was approximately 0.15cm removed from the fluid within the stainless steel body of the vessel. This can be seen in Figure 3.5. Capillary fluid height and thermistor resistances were recorded at half minute intervals. The experiments were either 20 or 7 minutes in duration, with data being taken for an additional 5 minutes after the lamp was shut off. The latex product was removed from the cell via a syringe and

stored in a labelled container. Samples were taken from these in order to obtain percent conversion of styrene to polystyrene gravimetrically and also some samples were chosen from which were obtained particle size and molecular weights of the products.

### C. Analysis of Polymerized Samples

Percent conversion, obtained dilatometrically and gravimetrically was determined for each sample, and the particle size and the polymer molecular weight were determined for various selected samples.

#### 1. Conversion

(a) Dilatometry - The percent conversion of styrene to polystyrene was determined by dilatometry by knowing the following: 1) the densities of styrene ( $\rho_s$ ) and polystyrene ( $\rho_{ps}$ ), 2) the weight fraction of styrene monomer in the polymerization recipe,  $W_s$ , 3) the inner diameter of the capillary tube,  $d$ , 4) the volume of the reaction vessel,  $V$ , 5) the change in the fluid height in the capillary tube,  $\Delta h$ .

The conversion was calculated via the following equation,

$$\% \text{ conversion} = \frac{100 \pi d^2}{4 W_s V (\frac{1}{\rho_{ps}} - \frac{1}{\rho_s})} \Delta h \quad (9)$$

In using this equation it was assumed that since water was the chief ingredient (~90%) the fluid weight and volume are approximately the same and  $V$  could be substituted for the total weight of the fluid in the cell. The values for the constants used in this equation are

$$\rho_s = 1.05 \text{ gm/cc}$$

$$\rho_{ps} = 0.905 \text{ gm/cc}$$

$$V_{LU} = 2.45\text{cc}$$

$$V_{GE} = 9.15\text{cc}$$

$$d = 4.84 \times 10^{-2}\text{cm}$$

(b) Gravimetrically - In determining the percent conversion by this means, a small sample was weighed in a syringe and then deposited in a tared drying tin and either short stopped with a 0.3% hydroquinone - isopropyl alcohol solution or flocculated with an excess amount of methanol and then dried to a constant weight at 70°C. From the net fluid weight (S), the weight of the dried residue (R) and the corrections for the non-volatile and non-polymeric solids (N), the percent conversion could be determined from the following equation,

$$\% \text{ conversion} = ( RT/S ) - N \quad (10)$$

where T is the total parts of all ingredients charged, based on 100 parts monomer. The corrections amount, N, was determined from the amount of SLS added in the polymerization recipe and by the amount of the photoinitiator added,  $\alpha,\alpha$ -diethoxyacetophenone (DEAP). DEAP being a liquid, it was not known how much of it was incorporated into the polymer, the limits being used, by which a conversion range was computed. The value of the upper limit assumes that all of the initiator was evaporated while the lower limit assumes that all of it is present with the polymer and SLS in the drying tin.

## 2. Particle Size

The determination of particle size was attempted using three methods, hydrodynamic chromatography, electron microscopy, and light scattering. Each of these presented some limitations.

(a) Hydrodynamic Chromatography (HDC) using Packed Porous Silica-

In order to use this chromatographic separation method, a calibration curve of particle size versus the difference in elution volume between the particles and a marker species was constructed using Dow monodisperse latex samples of 880Å, 1090Å, 1760Å, and 2340Å diameters. The marker species was sodium dichromate,  $\text{NaCr}_2\text{O}_7$ . The concentration of the latex samples was approximately 0.1 weight percent solids, these being dilutions of the original latexes with distilled deionized water. A calibration curve is presented in Figure 3.6. Note that the curve has been extrapolated into the smaller particle region. This is necessary due to the small size of the latex particles obtained in this study. Because extrapolation is necessary, the accuracy of the method is doubtful, even though the precision is good. These results can only be considered in light of the electron microscopy results. This method is good, however, for obtaining relative sizes and trends. A more complete description of this method can be found in the literature<sup>15</sup>.

(b) Electron Microscopy - Selected latex samples were prepared for these studies by two methods. The first of these simply involved the dilution of a drop of sample about 40x and placing a drop of this on a grid prepared for use in an electron microscope. This method did not prove to be highly definitive in that the high emulsifier levels in the latex did not allow for good definition of the latex particles. Subsequently, samples were prepared in which the SLS level was reduced using the serum replacement technique<sup>16</sup>. This method allows for the

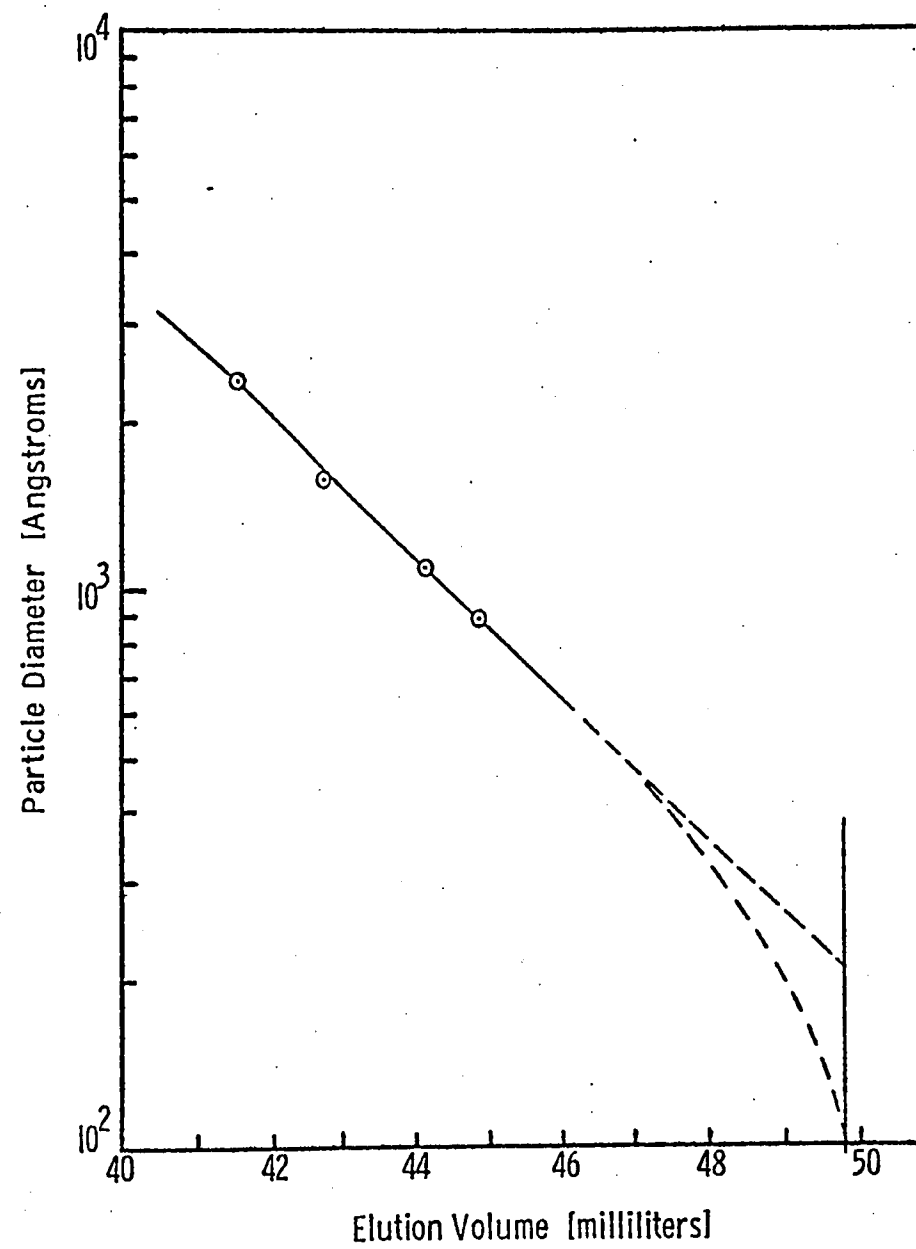


Figure 3.6 Calibration curve for Hydrodynamic Chromatography (HDC) through packed porous silica. Eluting solution is 0.55mM SLS in deionized water. Standards are Dow uniform latexes.

replacement of the latex serum without loss of particles by use of a filtration arrangement. In this case a 0.02wt.% Aerosol MA solution was used to replace the SLS solution in the latexes. These samples were then used in preparing grids for examination by TEM (Transmission Electron Microscope).

(c) Light Scattering - Several latex samples were chosen to be studied by this technique of particle size determination. The specific method of light scattering chosen, known as the transmission or turbidity method, makes use of measurements of transmitted monochromatic light through suspensions of known concentration. This method is a complicated function of particle size and refractive index. The samples used in these experiments were also ones in which the SLS serum had been replaced by a 0.02 wt.% Aerosol MA (AMA) solution. This was necessary because SLS absorbs light in the wavelength region to be used in these measurements and therefore, would interfere and result in false particle size determinations.

Experimentally, a series of measurements of transmittance was made on samples of 0.02 and 0.01 weight percents polymer solids. At each concentration, the transmittance was measured at four wavelengths, 320nm, 340nm, 360nm, and 380nm. The device used to measure this was a variable wavelength photometer (Laboratory Data Control - Spectro-Monitor II). The instrument was zeroed by filling the detection cell with deionized water. The cell was then filled with the latex sample and measurements were made at each successive wavelength.

The data recorded was then used to calculate the average particle

diameter. A sample calculation using the data from one of these experiments can be found in Appendix A.

### 3. Molecular Weight

Gel permeation Chromatography (GPC) was the method used in the determination of the weight average molecular weights of the polymer produced as a result of these photoinitiated emulsion polymerizations. As in the case of HDC, a calibration curve was required for the determination. Seven standard polystyrene samples were used, having molecular weights ranging from 3600 to 2,700,000 with very low dispersity indices. Toluene was used as the polymer solvent and eluting fluid. Samples were prepared by first drying a known amount of latex, dissolving in toluene drawn from the GPC system, and filtration to remove any gelled material or insoluble particles. The final polymer concentration in the samples ranged from 0.1% to 0.6%. It was found that to ensure a reasonable reliability, the calibration curve had to be reconstructed each time the samples were run. Several calibration curves are presented in Figure 3.7, to illustrate how these curves can shift from one run to another

From the chromatographic data, number, weight, and z average molecular weights could be determined. A sample calculation can be found in Appendix B.



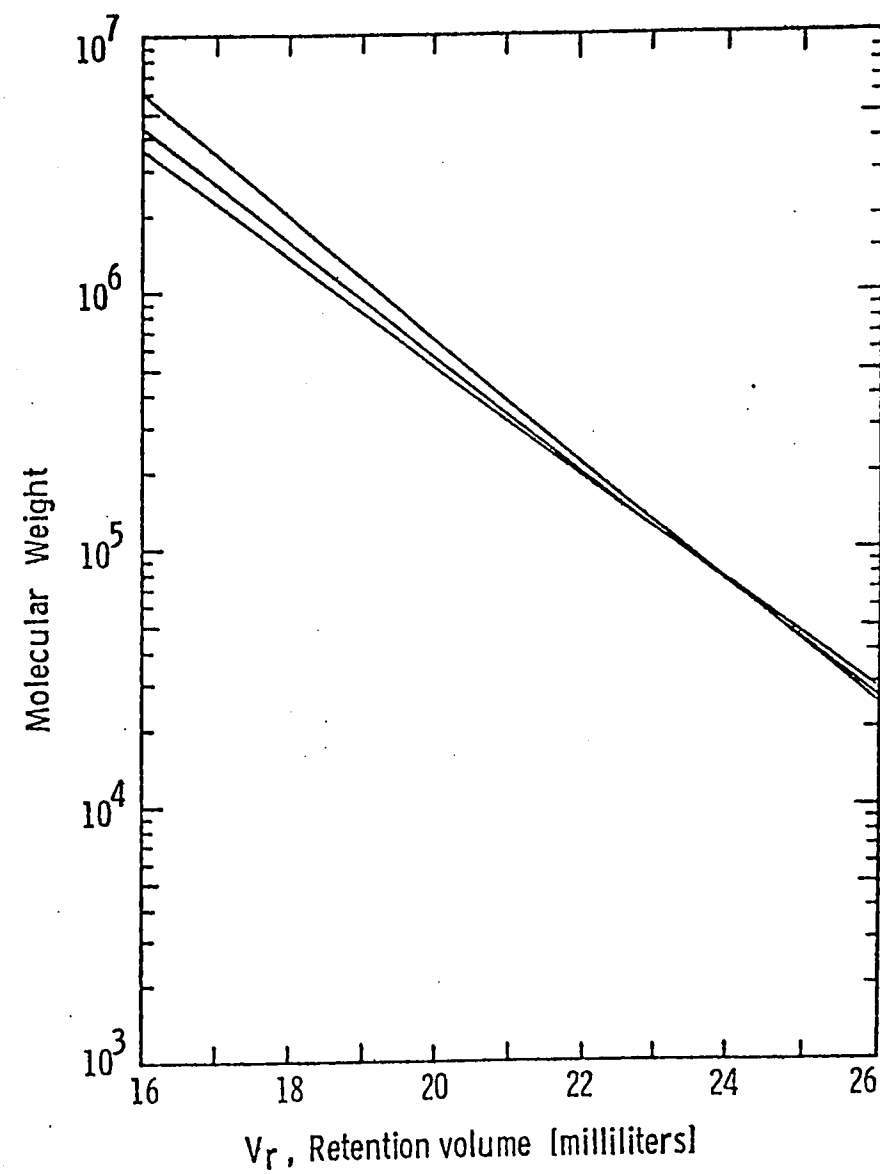


Figure 3.7 Calibration curves for Gel Permeation Chromatography (GPC) illustrating the changing calibration. Eluting liquid is toluene.

A. LU Cell

The primary variable in the photoinitiated emulsion polymerization of styrene to polystyrene was necessarily the polymerization recipe, once the reaction vessel was constructed and the laboratory setup completed. The cell dimensions and the path-length of the UV source to the vessel were fixed after preliminary studies were made to determine the critical dimensions of the GE prototype polymerization vessel. These dimensions have been reported in the previous Experimental section (PART III). The emulsion recipe consisted of water, styrene monomer, sodium lauryl sulphate (SLS) emulsifier, a co-emulsifier, either hexadecane or decanol, and a photoinitiator. These were the variables investigated with the object of obtaining a high degree of conversion in a given time limit.

As a result of the initial experiments two variables were eliminated somewhat arbitrarily. First, the amount of styrene in the emulsion formulation was fixed at 3 wt.% based on the entire recipe. This decision was based on the results of several experiments in which the amount of styrene was reduced from approximately 6% to 3% with an increase in the percent conversion from 3% to 7%, all other variables being fixed. Note that the percent photoinitiator was based on the amount of monomer and not the entire recipe, that is, here the percent photoinitiator used, based on styrene, was constant while it did vary based on the entire recipe. Second, the photoinitiator species was chosen to remain the same throughout the study, only vaying in concen-

tration, this being  $\alpha,\alpha$ -diethoxyacetophenone, abbreviated DEAP (Union Carbide). The structure of this compound has previously been given in PART II. This decision was based on the results of experiments comparing this species with another (VICURE 30 - Union Carbide), in which the recipes were the same except in the structure of the initiator. It was found that the use of DEAP resulted in more than three times the conversion than that found for VICURE 30, at the same concentration. Also, the absorption of UV radiation by DEAP was shown to be favorable, as is illustrated in Figures 4.1a and 4.1b. The absorption with increasing wavelength was measured in a differential spectrophotometer (Laboratory Data Control Spectro Monitor II - 1202), dilute DEAP/SLS solution being injected into the sample cell, with the same SLS solution being in the reference cell (ie. without DEAP). The strongest absorption is at approximately 252nm. The bar graph of Figure 4.1b the typical irradiance of the light source used in these experiments (Ultra Violet Products, Inc. - Pen Ray Model SCT 1). Note that the high intensity at 253.7nm is quite close to the 252nm peak absorption of the DEAP. This appears to make the lamp/photoinitiator combination quite suitable for this work.

All of the polymerization experiments in the LU cell were carried out for 20 minutes, that is, the emulsions were exposed to the UV radiation for these 20 minutes. Data was recorded over this period and an additional 5 minutes after exposure was terminated.

#### 1. Variation in the Recipe for Photoinitiated Emulsion Polymerization

Table I shows the results for a series of experiments conducted

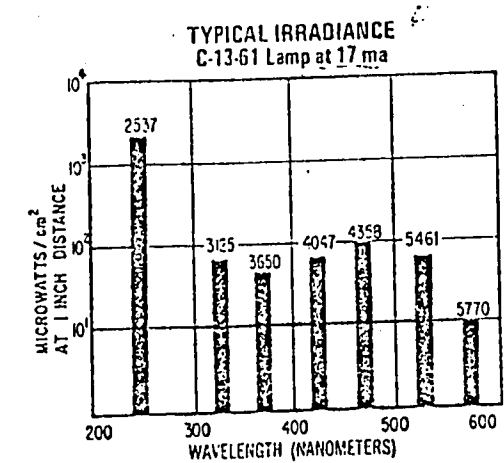
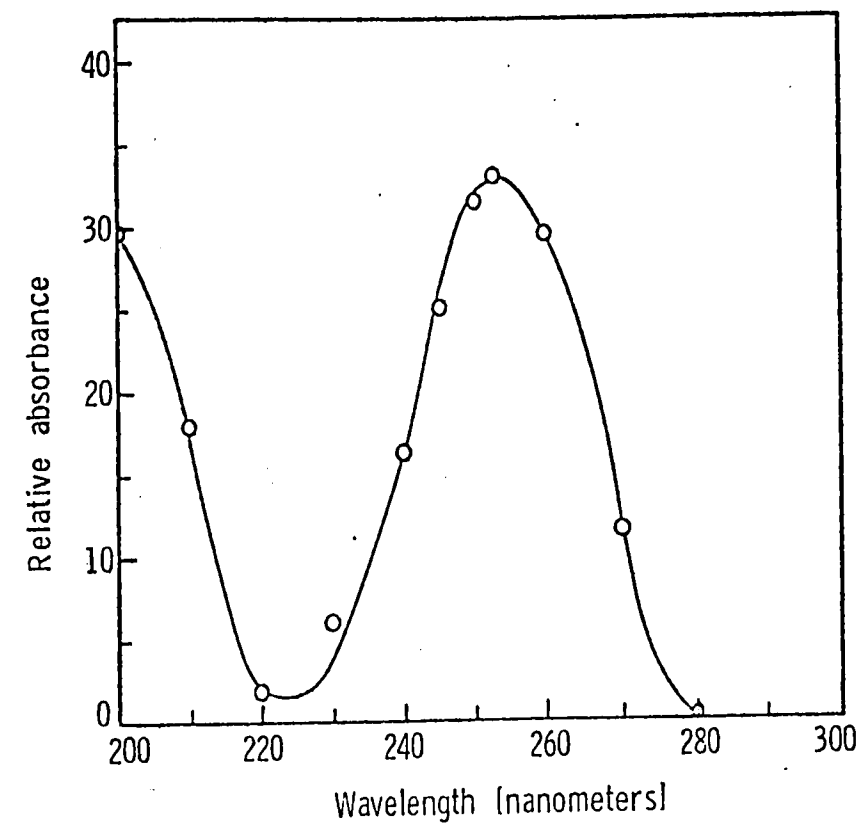


Figure 4.1a (top) Relative absorbance of the photoinitiator, DEAP, showing a peak at 252nm.

Figure 4.1b Typical irradiance of a UV lamp, similar to that used for photoinitiated polymerizations.

TABLE I

Photoinitiated Emulsion Polymerization of Styrene as a Function of Recipe Parameters  
(3% styrene monomer)

Sample	Percent Sodium Lauryl Sulphate	Percent Co-emulsifier	Percent Photoinitiator	Percent Conversion 20 minutes	
				minimum	maximum
10	3.0	0.0	1	31	32
12	3.0	0.0	4	30	34
13	3.0	0.0	10	50	60
13-2	3.0	0.0	10	54	64
14	3.0	0.0	15	27	42
14-2	3.0	0.0	15	51	66
17	3.0	0.05	0	5	5
15	3.0	0.05	10	55	65
16	1.5	0.05	10	42	52
18	3.0	1.50	10	13	23
19	3.0	1.50	10	58	68
20	3.0	1.50	15	60	75
21	3.0	1.50	20	75	95
21-2	3.0	1.50	20	49	69
22	3.0	1.50	30	40	70
24	1.5	3.00	20	2	22
25	0.75	1.50	20	0	20

using the LU cell. Within the table are two series in which the only variable is the photoinitiator concentration, DEAP, 10-14 and 18-22. In the first series, the emulsion recipe consists of 3% styrene monomer, 3% SLS, and no co-emulsifier. The photoinitiator concentration varies from 1% to 15% based on the 3% styrene in the system. The rate of fluid fall in the capillary dilatometer versus time for this series is given in Figure 4.2. and the fluid height in the capillary versus time is shown in Figure 4.3. Several observations can be made about these. First, as might be expected, the rate increases with increasing initiator concentration and the peak rate shifts from approximately 4.5 to 2.5 minutes in the sequence of initiator concentrations from 1% to 15%. Qualitatively, these trends are expected. However, as can be noted in Figure 4.3, the capillary fall is not a reliable gauge of the percent conversion (right hand scale) in the reaction. Samples 13 and 14-2 had recorded capillary drops which were greater than that possible for a volume change due to the reaction alone. Run 12 is the only experiment in this sequence in which the dilatometric conversion correlates well with the conversion determined gravimetrically. The prime reason for this lack of consistency is attributed to the difficulty in obtaining a leak proof seal in the LU cell. Any minute leak would readily become apparent in the capillary fluid height. If it could be assumed that the leakage rate was constant, a means of compensation is possible by the following. Assuming that the conversion is approaching a limit near the end of the experiment, a line drawn tangent to the capillary height - time curve in this

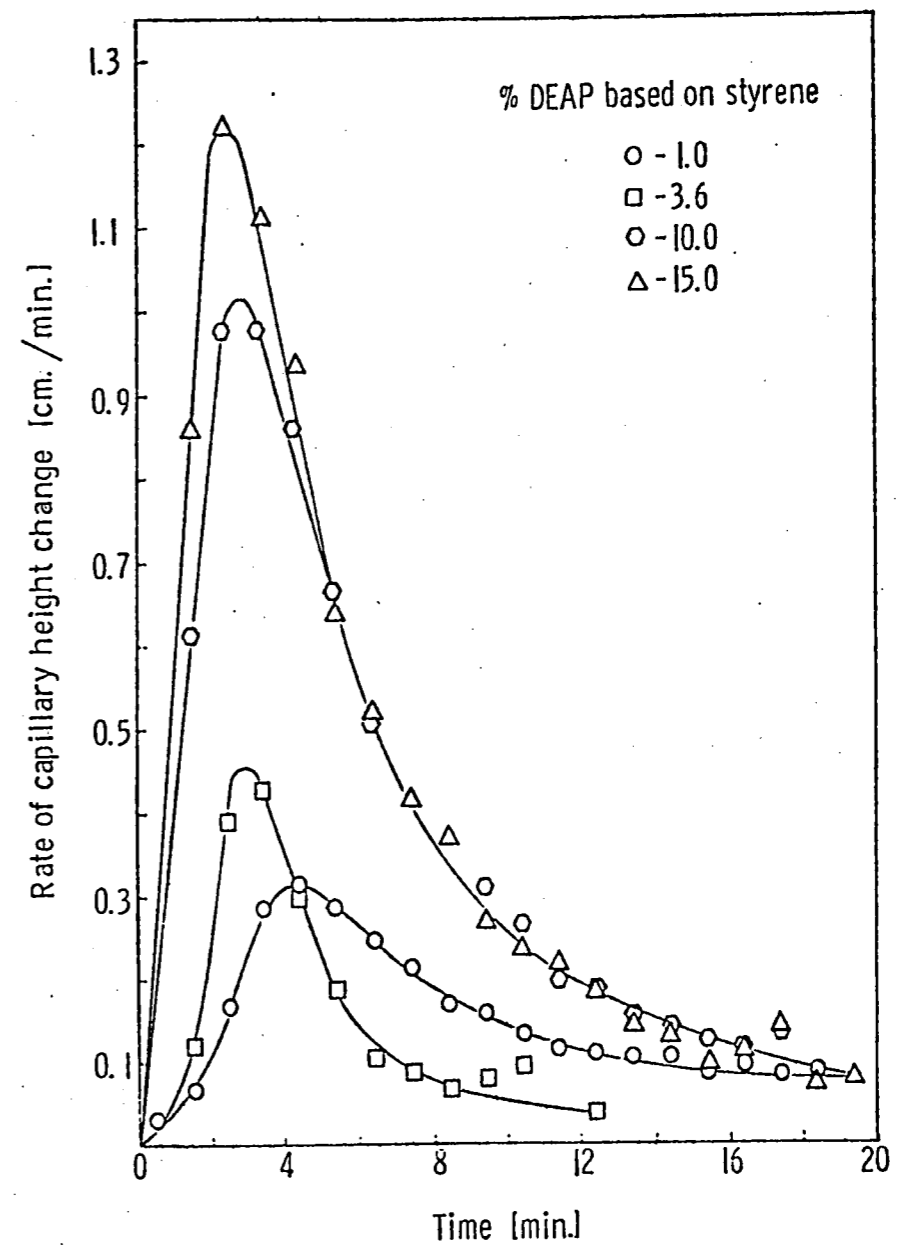


Figure 4.2 Rate of capillary fall versus time for an emulsion consisting of 3% styrene and 3% SLS as a function of the percent photoinitiator, DEAP, based on styrene (samples 10, 12, 13, 14).

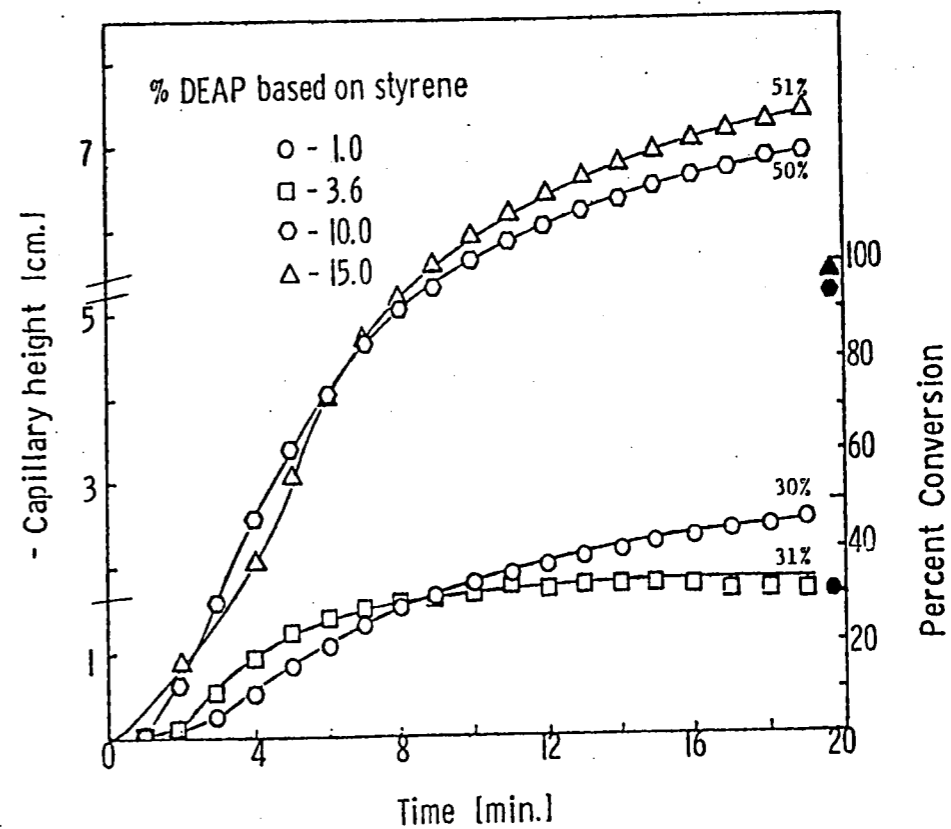


Figure 4.3 Capillary height-time relationships for the data in Figure 4.2; percent conversion is represented on the right hand axis. The solid points represent the results of constant leakage corrections and the percentages above each curve are the gravimetrically determined minimum conversions (samples 10, 12, 13, 14).



region would give a constant rate of capillary fall which, if assumed to be constant throughout the experiment, could be used to correct the given data. This method was attempted in Figure 4.3 (solid data points) and only proved successful for the case of sample 10, meaning that the rate of leakage was not always constant in the experiments but sometimes decreased. This is a problem which continued throughout the use of the LU cell, as exemplified by the reproducibility studies of Figures 4.4 and 4.5, in which samples 13 and 14 are rerun. Notice that in the first of these the reproducibility is quite good, despite obtaining false dilatometric conversion data. Here, the leakage was also reproducible. The latter case shows this same inability to obtain good dilatometric agreement with gravimetric conversion but also behind this is the reason for which this series was discontinued, instability. This series (10,14-2) showed evidence of separation while the emulsion was in the cell for only a short period of time. Also, separation was evident in sample 14 prior to loading into the cell. This sample was shaken just before loading and rerun (14-2). The difference between the two reactions is obvious in Figure 4.5, where the shaken sample shows a higher rate and apparent conversion, this being due to the higher concentration of reactants which had been redispersed. This sequence of polymerizations was characterized by a change in the appearance of the emulsion from a milky white to a translucent latex, this product being quite stable.

To increase the stability of the emulsion, a co-emulsifier was included in the recipe. Figure 4.6 gives capillary rate-time data for

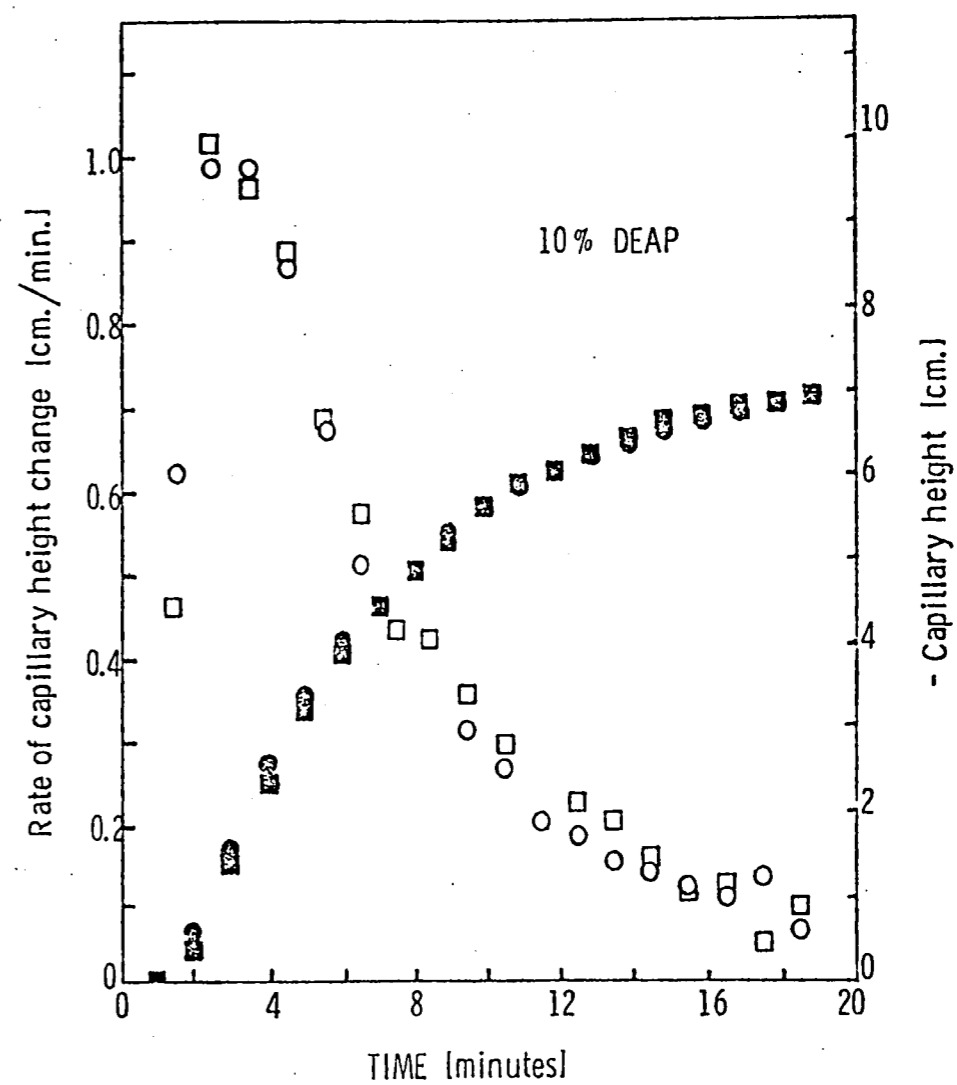


Figure 4.4 Reproducibility experiment of a system consisting of 3% styrene, 3% SLS, and 10% DEAP based on styrene, showing good agreement despite dilatometric inaccuracy. Solid points correspond to the right hand axis (samples 13, 13-2).

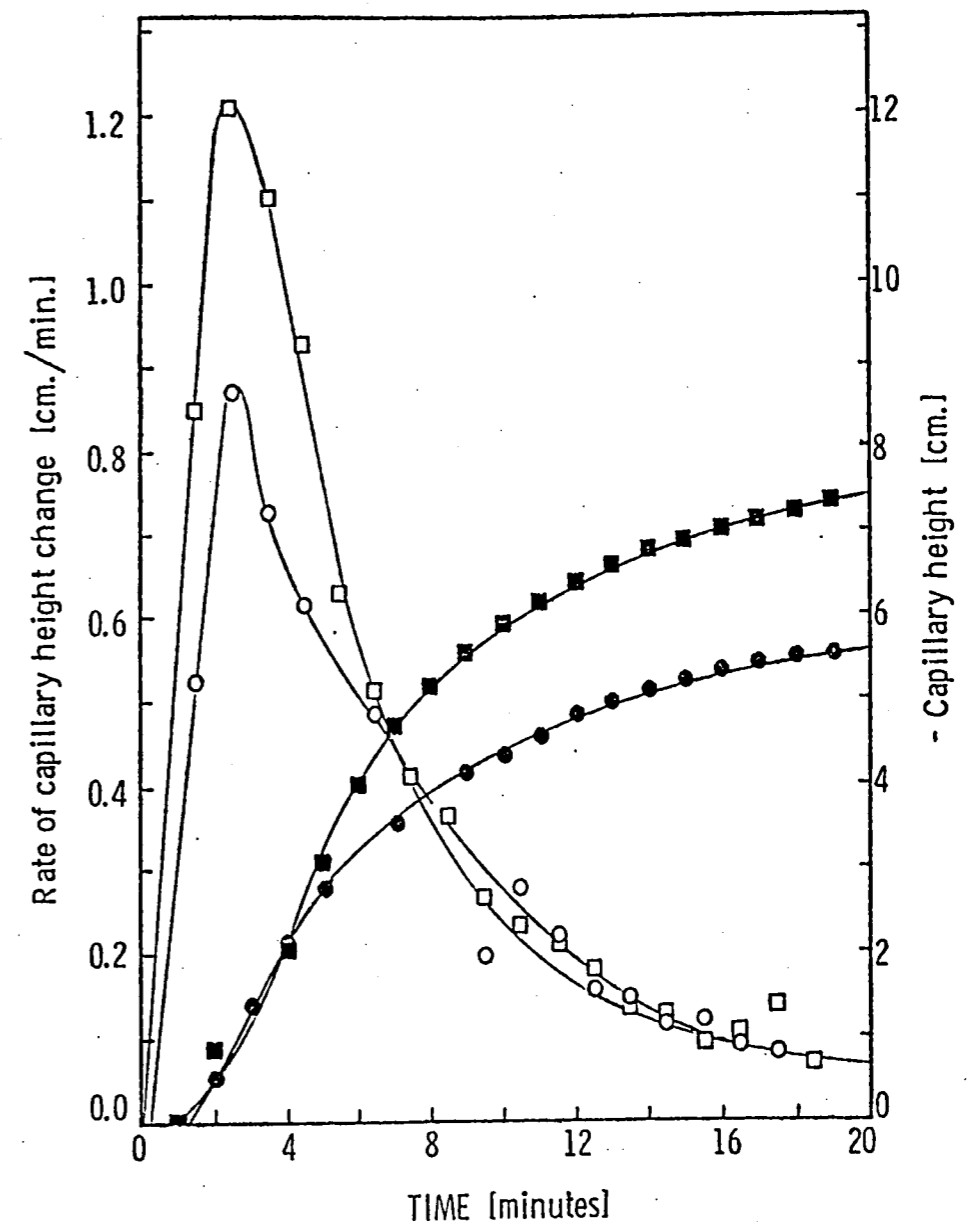


Figure 4.5 Reproducibility experiment of a system consisting of 3% styrene, 3% SLS, and 15% DEAP based on styrene. Differences are primarily due to the instability of the system, one having been agitated just prior to the experiment (14-2, □), while the other was used having evidence of separation (14, ○). Solid points correspond to the capillary height.

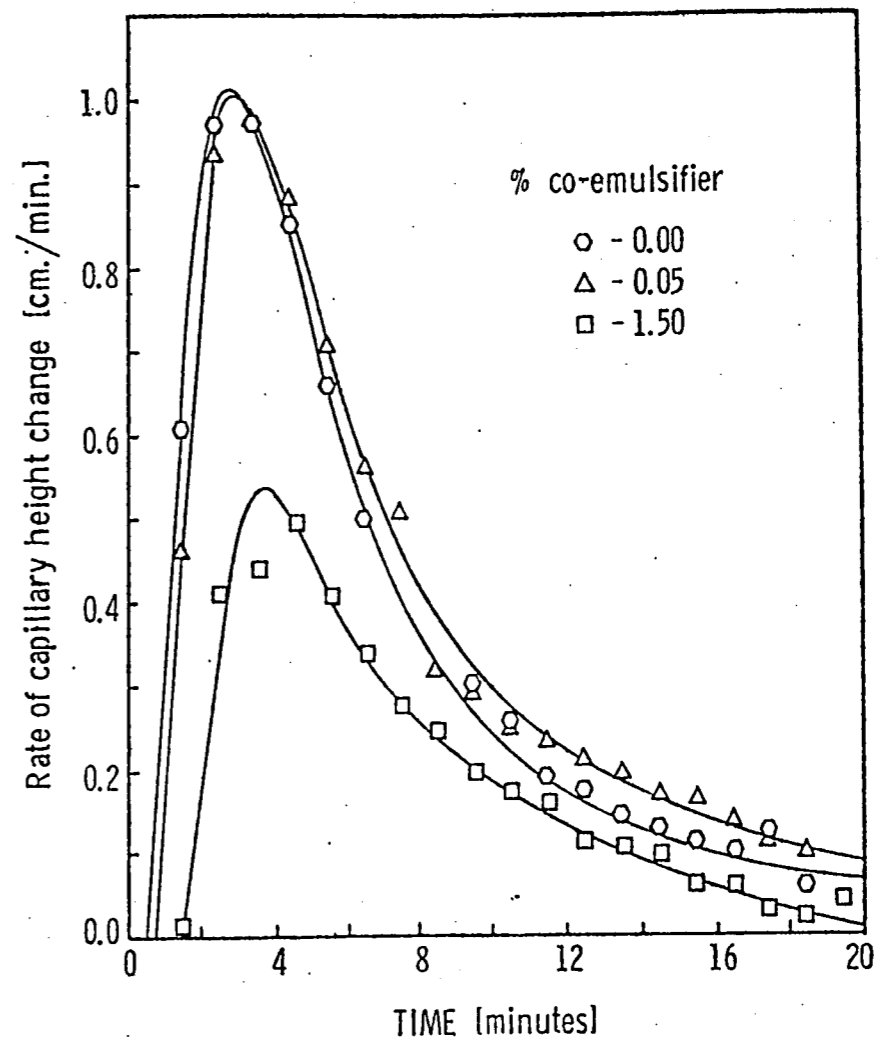


Figure 4.6 Effect of co-emulsifier content (hexadecane) on the polymerization rate of a system consisting of 3% styrene, 3% SLS, and 10% DEAP based on styrene, with varying amounts of hexadecane (samples 13, 15, 18).

two concentrations of hexadecane. For comparison, a zero co-emulsifier concentration curve is also given. In the case of this system, stability was increased slightly with the addition of the co-emulsifier but not to a degree sufficient for the needs of the experiment. Also, as a result, the rates and conversions were decreased substantially with the increased addition of the co-emulsifier (Table I, compare percent conversion for samples 15 and 18). It is interesting to note that there seems to be some correspondence between the emulsion stability and rate of conversion for this photoinitiated free radical polymerization. This phenomenon will be seen again when the effect of SLS concentration is presented.

For increased stability a second co-emulsifier was also tried, decanol. Recipes including this alcohol are represented in Table I by samples 19-25. The first of these (19-22) recipes contained SLS and decanol in a weight ratio of 2:1. Rate-time and conversion-time curves for increasing photoinitiator, DEAP, are presented in Figures 4.7 and 4.8. Note that the extrapolation technique, described earlier for the correction of the conversion-time curves, works for one and not for the other curve outside the predicted region. These data indicate that the reaction rate increases with increasing photoinitiator concentration (10%→20%) and then decreases (30%). This trend is also reflected in the values reported for the final conversion. Possible reasons for this phenomenon will be discussed further on in the report. These recipes exhibited a much improved stability over all the previous ones. This was tested by loading the cell and observing the contents over a period of two days. Only slight separation was

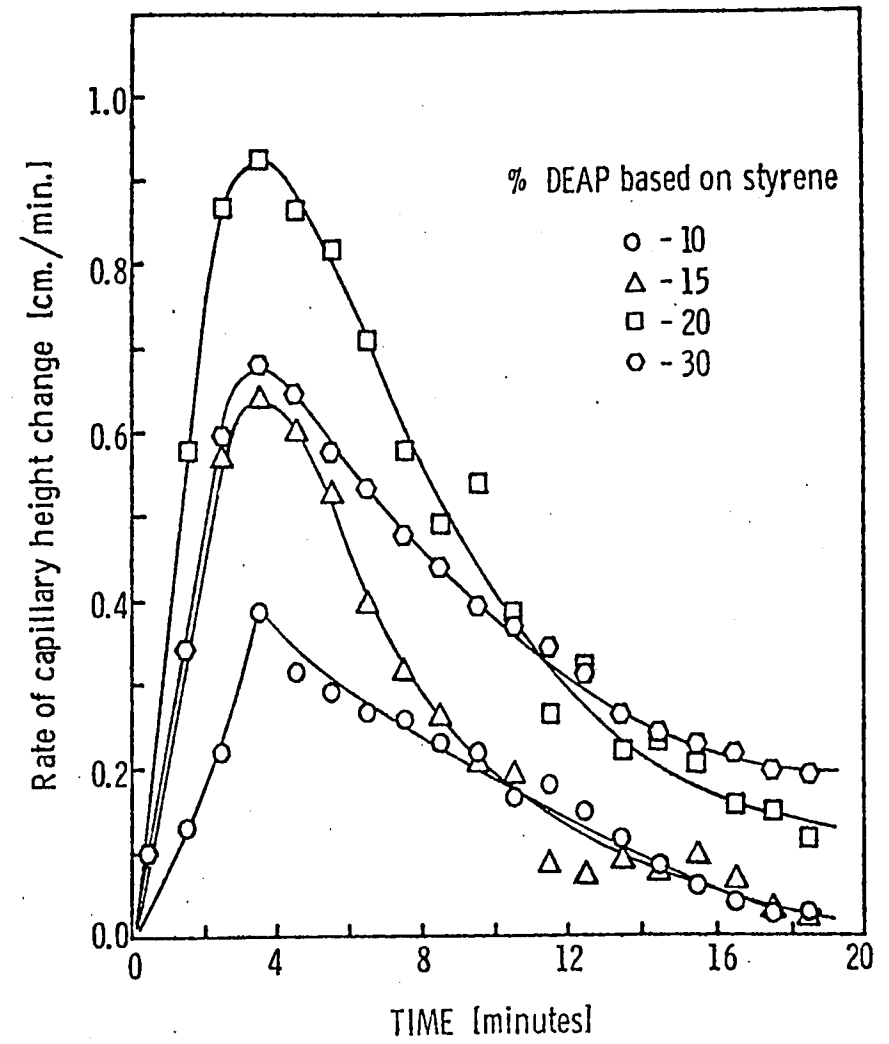


Figure 4.7 Rate of capillary fall as a function of the percent DEAP based on styrene for a system consisting of 3% styrene, 3% SLS, and 1.5% decanol co-emulsifier (samples 19, 20, 21, 22).

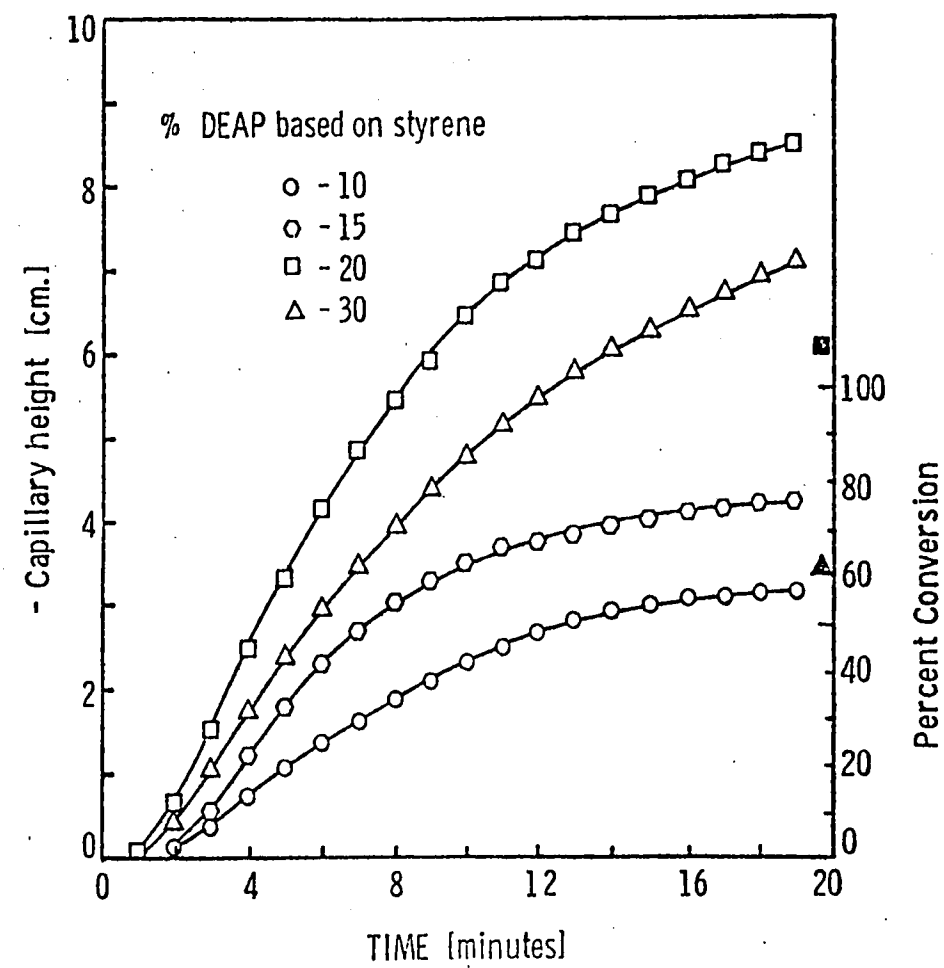


Figure 4.8 Capillary height-time as a function of the percent DEAP based on styrene for the data in Figure 4.7. Solid points represent the results of constant leakage corrections.

noted at the end of this period. This fact, plus the high reaction rates with the maxima being at  $\sim 3.5$  minutes into the reaction, made this system a good candidate for future experiments in the GE prototype polymerization vessel. As noted in some previous experiments, the polymerizations involving this system were characterized by a change in the appearance of the fluid in the cell, from a milky white emulsion to a translucent latex. This phenomenon can be attributed to the disappearance of monomer droplets, 1-10 $\mu\text{m}$  in diameter, and the growth of the much smaller polymer particles ( $< 0.05\mu\text{m}$ ). In order to quantify this visual opacity change in the course of the reaction, the intensity of the UV radiation passing through the cell was measured by means of a UV detector (IL 745 UV Curing Radiometer - International Light Inc.). The results are given by Figures 4.9 and 4.10 in which the rate of change in the intensity of the UV radiation and the intensity itself are compared to the rate of capillary fluid height change and fluid height respectively. Note that the rate curves follow each other initially as the rates increase, then the rate of intensity change falls to near zero in six minutes while the rate of reaction falls only gradually. These observations seem to indicate that the rates of monomer drop-size decrease and intensity and reaction rate increase are closely related, being directly proportional to each other. Also, it indicates that when the droplet size reaches a certain minimum, it no longer affects the intensity of the transmitted UV radiation. This seems to indicate that the monomer droplets do not disappear when the intensity reaches a constant, since the



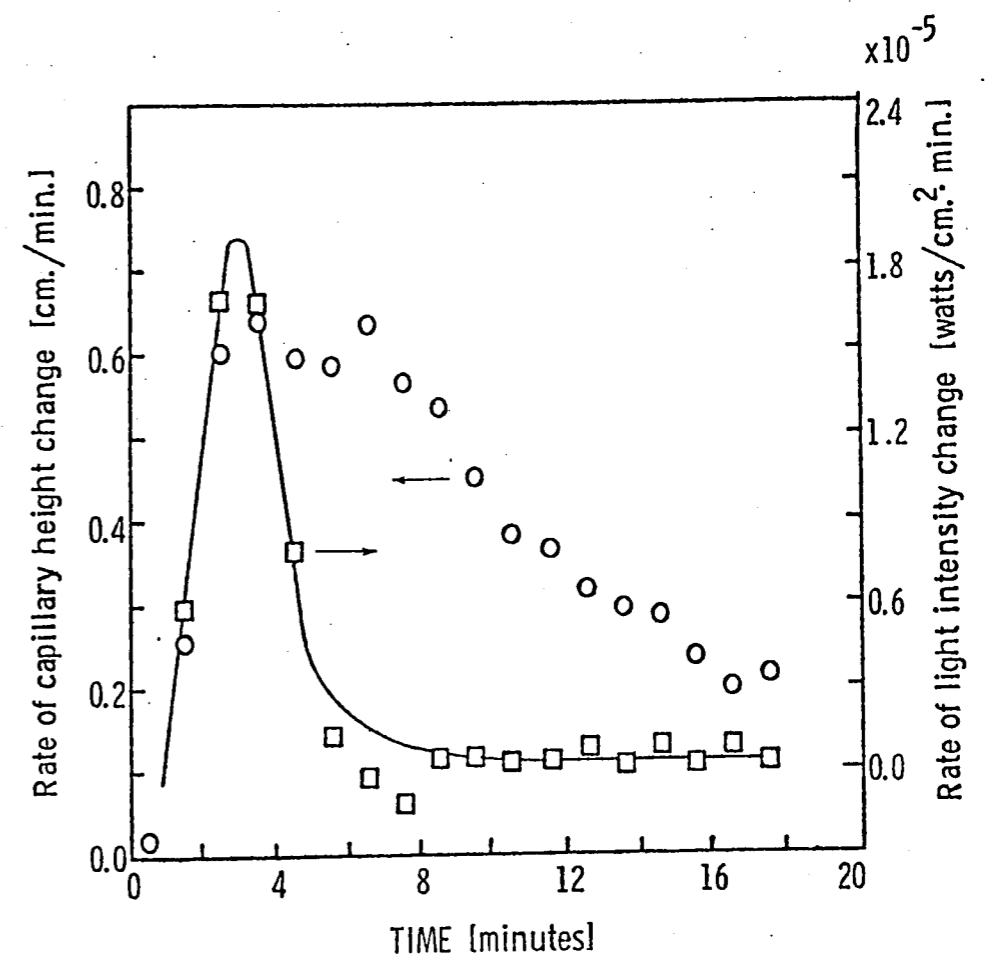


Figure 4.9 Rate-time relationships for capillary height (O) and UV intensity transmitted through the cell (□) during polymerization (sample 22).

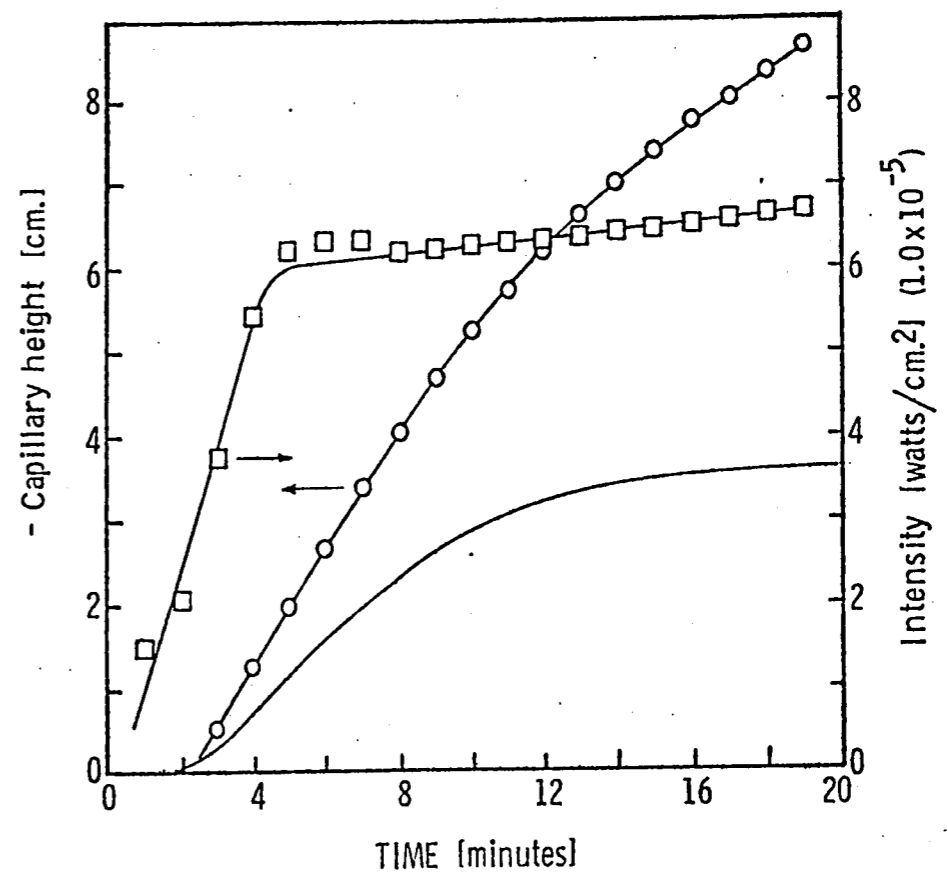


Figure 4.10 Capillary height and UV intensity-time relationships for the data in Figure 4.9. Solid line is the capillary height curve corrected for a constant leakage rate.

curves do not follow each other after the first three minutes. Monomer droplet disappearance may therefore occur after five minutes has elapsed. This fits in well with what is known about the emulsion polymerization of styrene, since it is reported that the monomer droplets disappear at conversions from 25% to 35% for this monomer<sup>14</sup>. The corrected curve in Figure 4.10 shows a conversion of approximately 30% at the five minute mark.

It might be conjectured that the time required for the lamp intensity to increase to its normal operating level, may be influencing the initial shape of the reaction rate curves. This, however, has proven to be of little importance as the lamp quickly reaches full intensity as shown in Figure 4.11. This curve was produced in the same way as that in Figure 4.10, with the exception that water was used in the cell in place of the emulsion. Two points from Figure 4.10 are also included to show the relative values of intensity and the arrow represents the final intensity measured during the experiment. This indicates that most of the radiation is being absorbed in passing through the fluid sample, even when it appears to be translucent to the eye.

Other experiments using the same emulsifier combination proved less successful as give by samples 24 and 25 in Table I. In these cases the ratio of SLS to decanol was reversed (1:2), this ratio being known to give very stable emulsions<sup>17</sup>. The system was indeed quite stable but gave little or no conversion over the twenty minutes of UV exposure. The rate and capillary height curves are given in

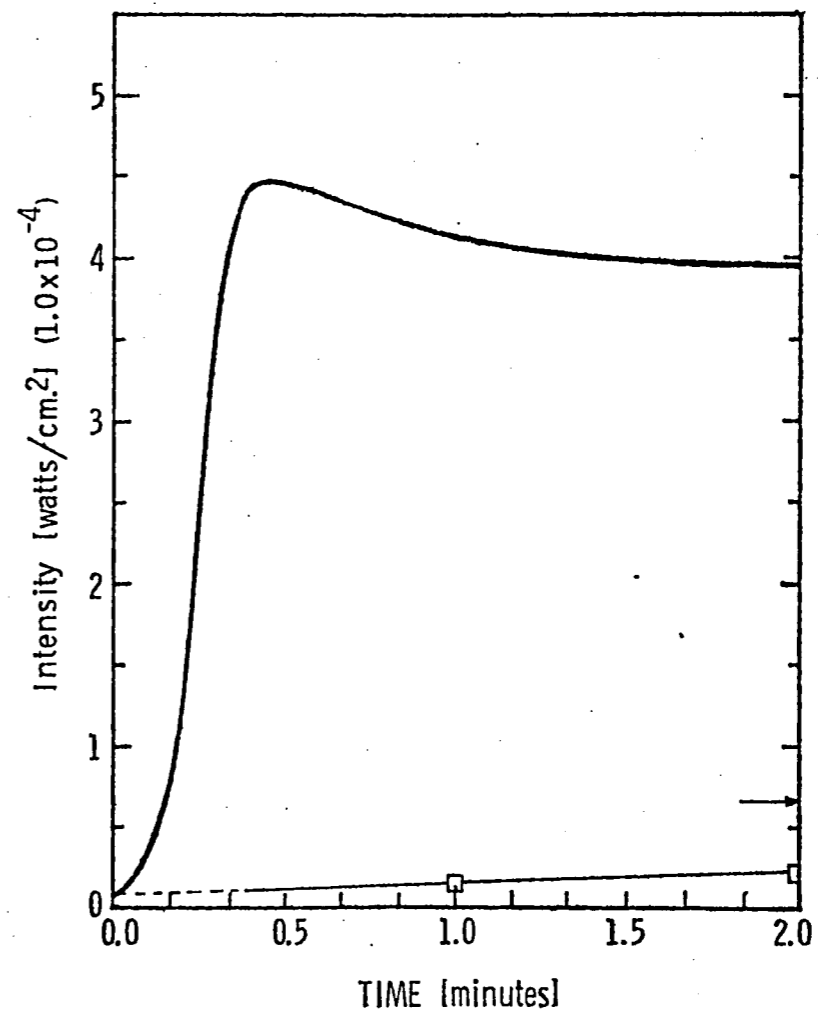


Figure 4.11 UV intensity versus time measured through the LU cell containing deionized water. For comparison, data from Figure 4.10 are also given ( $\square$ ). Arrow indicates the intensity recorded at the end of the latter experiment.

Figure 4.12, again illustrating the problem of obtaining accurate and reproducible dilatometric data in the LU cell. Originally it had been considered that if these curves represented the conditions of no conversion they could be used to correct other data obtained from the LU cell. However, it was subsequently found that no consistent correlation could be made.

In order to observe the effect of increased SLS emulsifier in a given system, the rate curves for samples 15 and 16 are presented in Figure 4.13. This is a system which employs a co-emulsifier and a 10% DEAP concentration based on styrene. From these curves it is apparent that sample 15, having the highest emulsifier concentration, is the better of the two from the point of view that its rate is greater and peaks earlier (3 vs. 6 minutes) than sample 16. This seems a logical outcome in that in the former system there are more micelles present and therefore more sites for particle nucleation. One observation that cannot be made from this Figure is that sample 16 proved to be the more stable of the two systems. Again there seems to be some correlation between the stability and the success of the polymerization within a given system.

Having noted the increase in polymerization rate due to an increase in the SLS concentration, a system was prepared in which there were equal molar concentrations of styrene and SLS, that is, for every styrene molecule there was one SLS molecule. No co-emulsifier was used. This system may be better classified as a micellized system rather than an emulsion, since monomer droplets, at least in the range

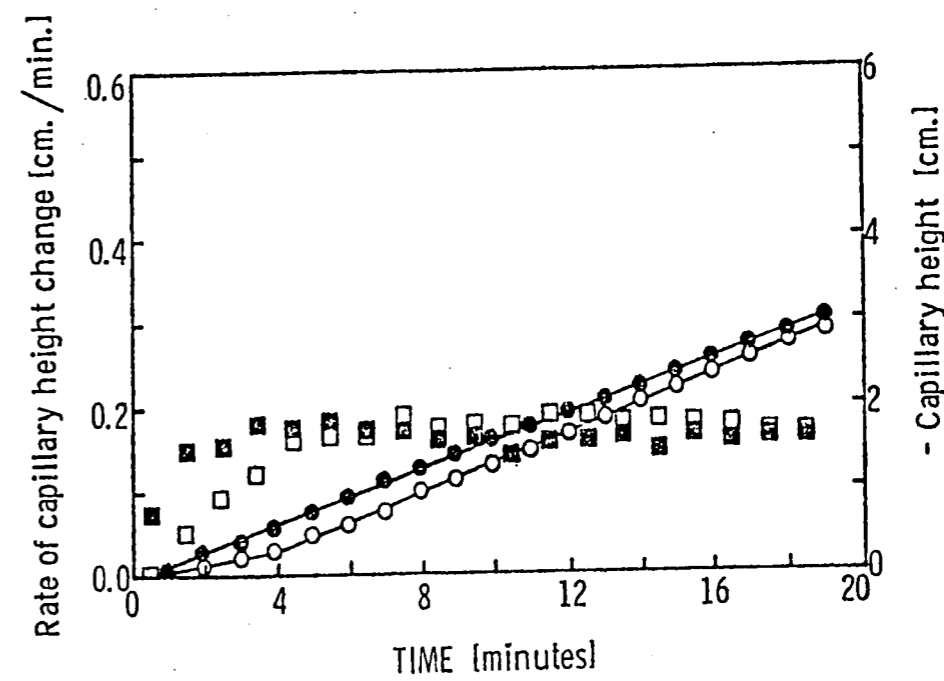


Figure 4.12 Capillary height (○, ●) and its rate of change (□, ■) for a system consisting of 3% styrene and 20% DEAP based on styrene, with a 1:2 ratio of SLS to decanol (sample 24, 1.5% SLS ●, ■ and sample 25, 0.75% SLS ○, □).

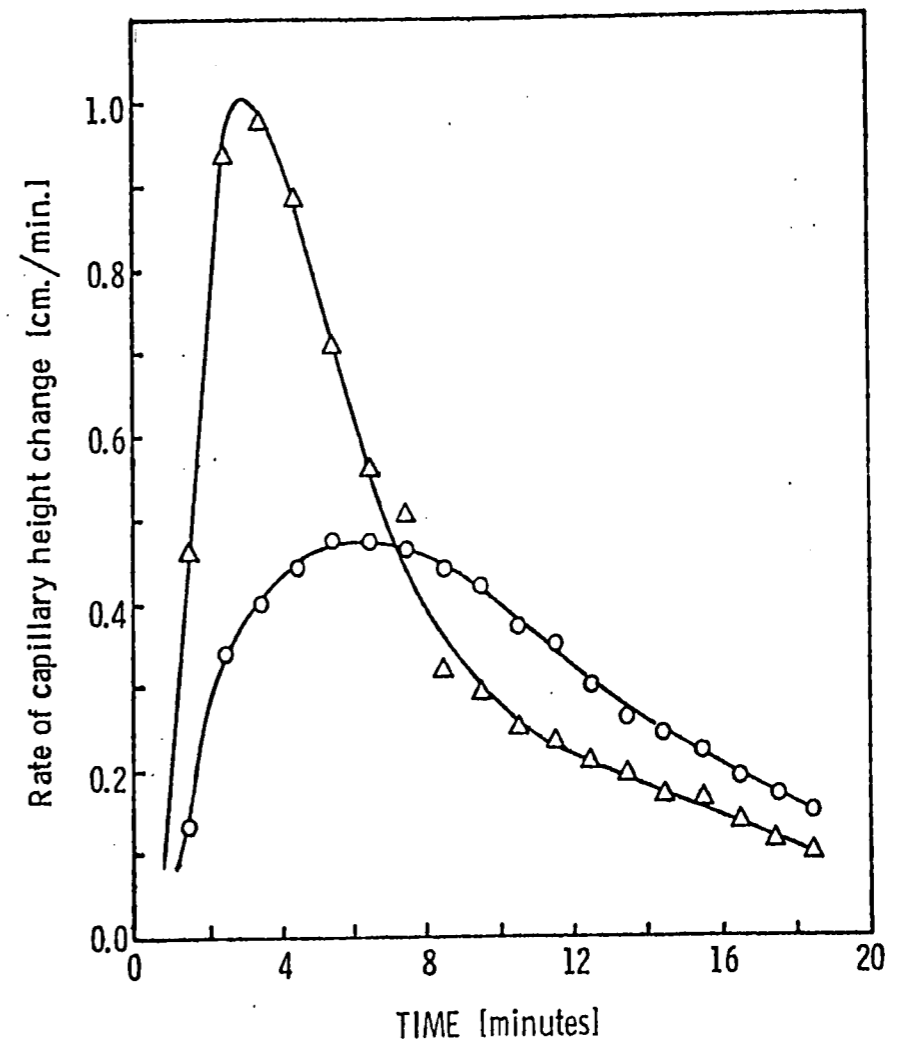


Figure 4.13 Rate of capillary height change as a function of the SLS content, the system containing 3% styrene, 0.05% decanol, and 10% DEAP based on styrene with 3% SLS ( $\Delta$ ) or 1.5% SLS ( $\circ$ ) (samples 15 and 16, respectively).

1-10 $\mu$ m, do not exist in such a system. This system appears translucent and not the typical milky white of an emulsion, this being verification of the absence of large monomer droplets. This system, including 20% DEAP, sample 28, was run in the LU cell, giving dilatometric data as shown in Figure 4.14. The correction method, described previously, was applied to this data with reasonable results. The open points ( $\square, \circ$ ) represent the original data while the solid ones ( $\blacksquare, \bullet$ ) represent the corrected data. The maximum final conversion, determined gravimetrically, was 70% as compared to 78% taken from the corrected curve. The rate curves can be compared to those in Figure 4.13, noting again the increased rate maximum and the shorter time in reaching this peak ( $\sim 1.5$  minutes) with increasing SLS concentration. The shelf-stability of this equimolar styrene/SLS system did not follow the trend toward less stability, as was the case for samples 15 and 16. The presence of a co-emulsifier in the latter systems makes the comparison less relevant however. With this increased stability and improved polymerization characteristics, this system became a good candidate for the more detailed work planned for the GE SPAR prototype vessel. At this point in the investigation this vessel became available.

#### B. Transition of Experimentation to the GE Laboratory Prototype -

##### 1. Scale-up

With the arrival of the GE vessel, came an end to the work being done on optimizing a recipe formulation with regards to the emulsifier level and combinations with co-emulsifiers. Initial experiments were



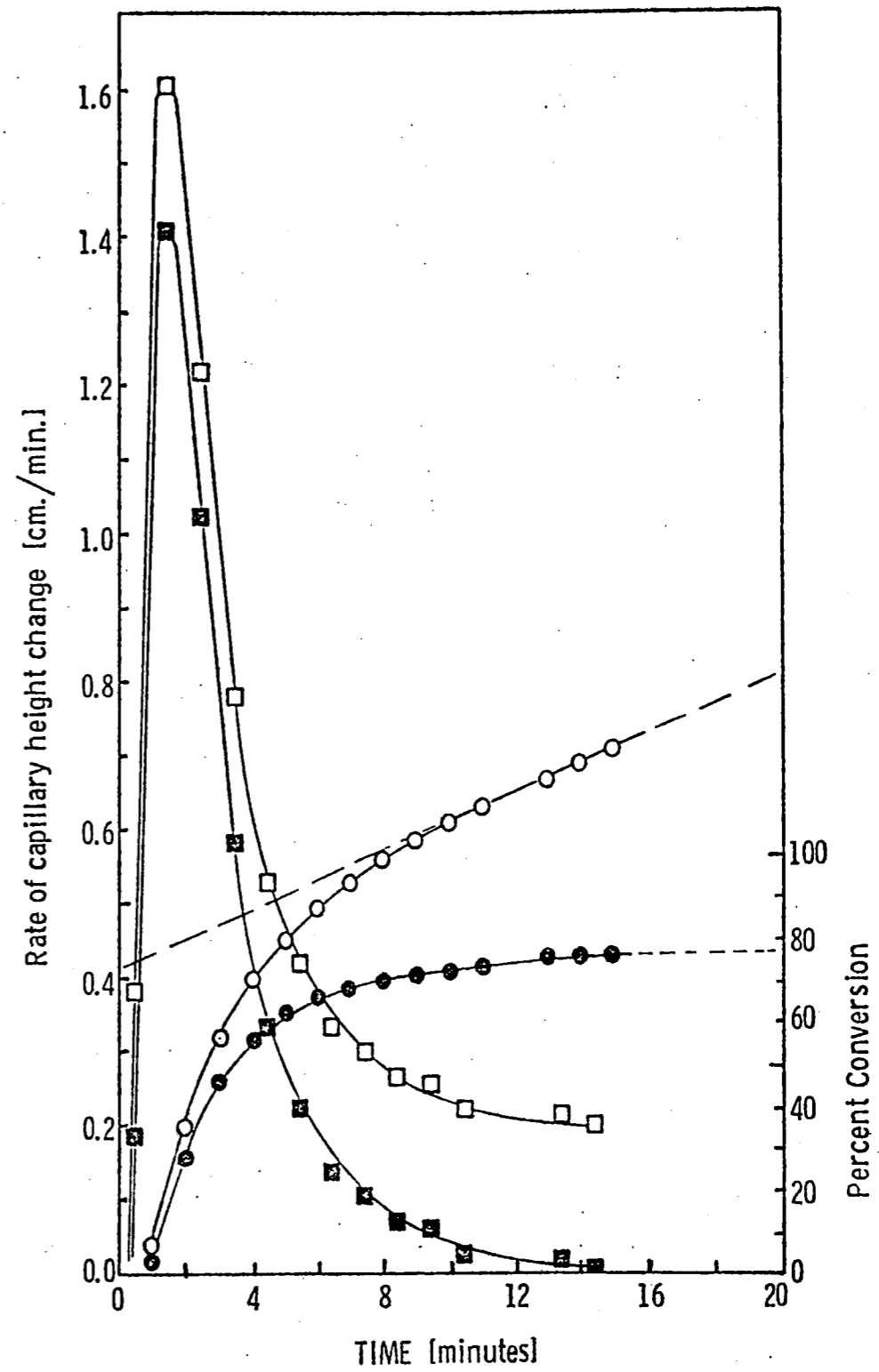


Figure 4.14 Rate of capillary height change ( $\square, \blacksquare$ ) and percent conversion ( $\circ, \bullet$ ) for a system consisting of 3% styrene, 8.3% SLS, and 20% DEAP based on styrene. Solid points represent corrected data (sample 28).

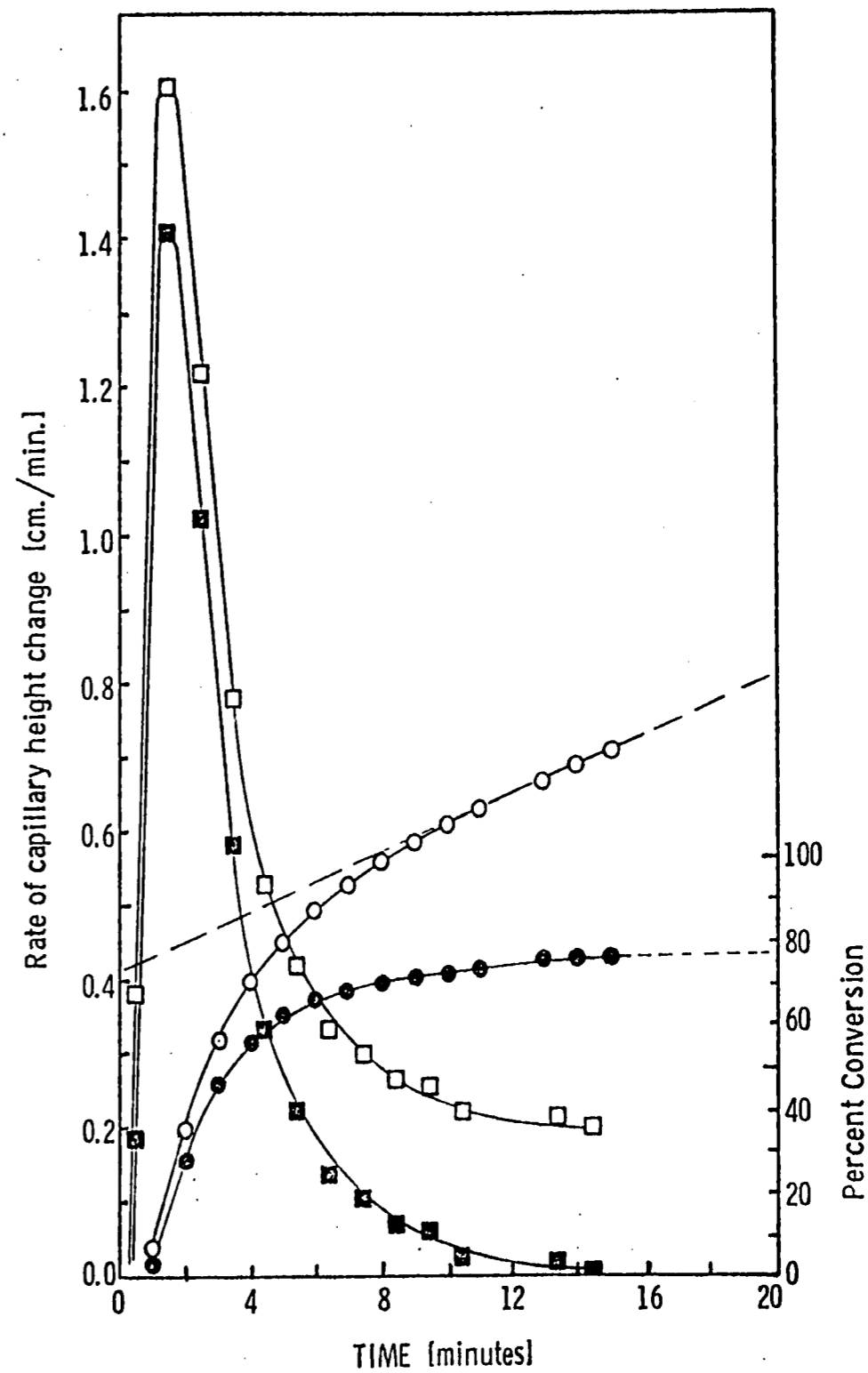


Figure 4.14 Rate of capillary height change (□, ■) and percent conversion (O, ●) for a system consisting of 3% styrene, 8.3% SLS, and 20% DEAP based on styrene. Solid points represent corrected data (sample 28).

carried out in the GE vessel in order to determine what changes in the polymerization would occur with the change in the cell configuration. The same micellized recipe prepared for sample 28 was run in the GE cell. It should be noted, however, that the sample was then four days old, having been stored in a dark place between uses. As with all of the experiments in the LU cell, the exposure of the fluid to the UV radiation was set at twenty minutes. The dilatometric data is given in Figure 4.15 (sample 32). First, notice that the same correction method, as applied to previous data obtained with the LU cell, is used here. The need for this correction was attributed to a constant rate of fluid leakage from the vessel, this resulting from the lack of familiarity with the proper assemblage of the vessel. The correction was used only for the first two experiments, those following not having this problem. The limits for conversion, set by gravimetric determination, were 49 - 69%. The uncorrected dilatometric conversion was outside of this range, while the corrected data resulted in a conversion of 63%, well within the gravimetric limits. This fact represents further justification for the correction.

The similarity of these results with those for sample 28 are quite obvious. The final conversion in the LU cell is essentially the same (69% vs. 70%). In order to more closely compare the data obtained for the same recipe in each vessel, Figure 4.16 was prepared. Since the vessels were of differing configuration, having different volumes and areas for exposure to the UV radiation, they could not be compared directly. Therefore, the rates were converted to rates per unit volume

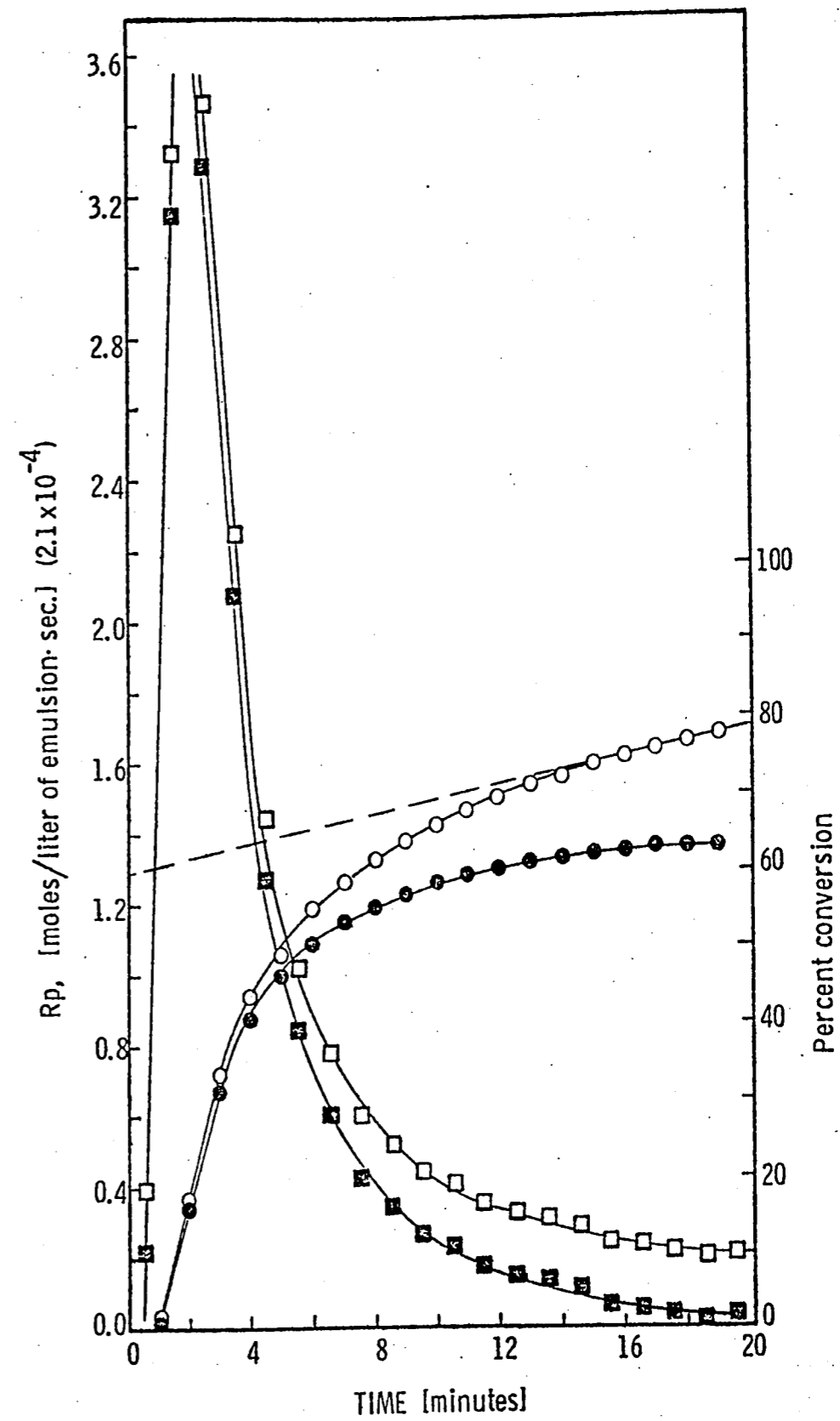


Figure 4.15 Polymerization rate,  $R_p$ , ( $\square, \blacksquare$ ) and percent conversion ( $\circ, \bullet$ ) obtained from the GE vessel, for comparison to Figure 4.14 (LU cell), same recipe. Solid points represent corrected data (sample 32).

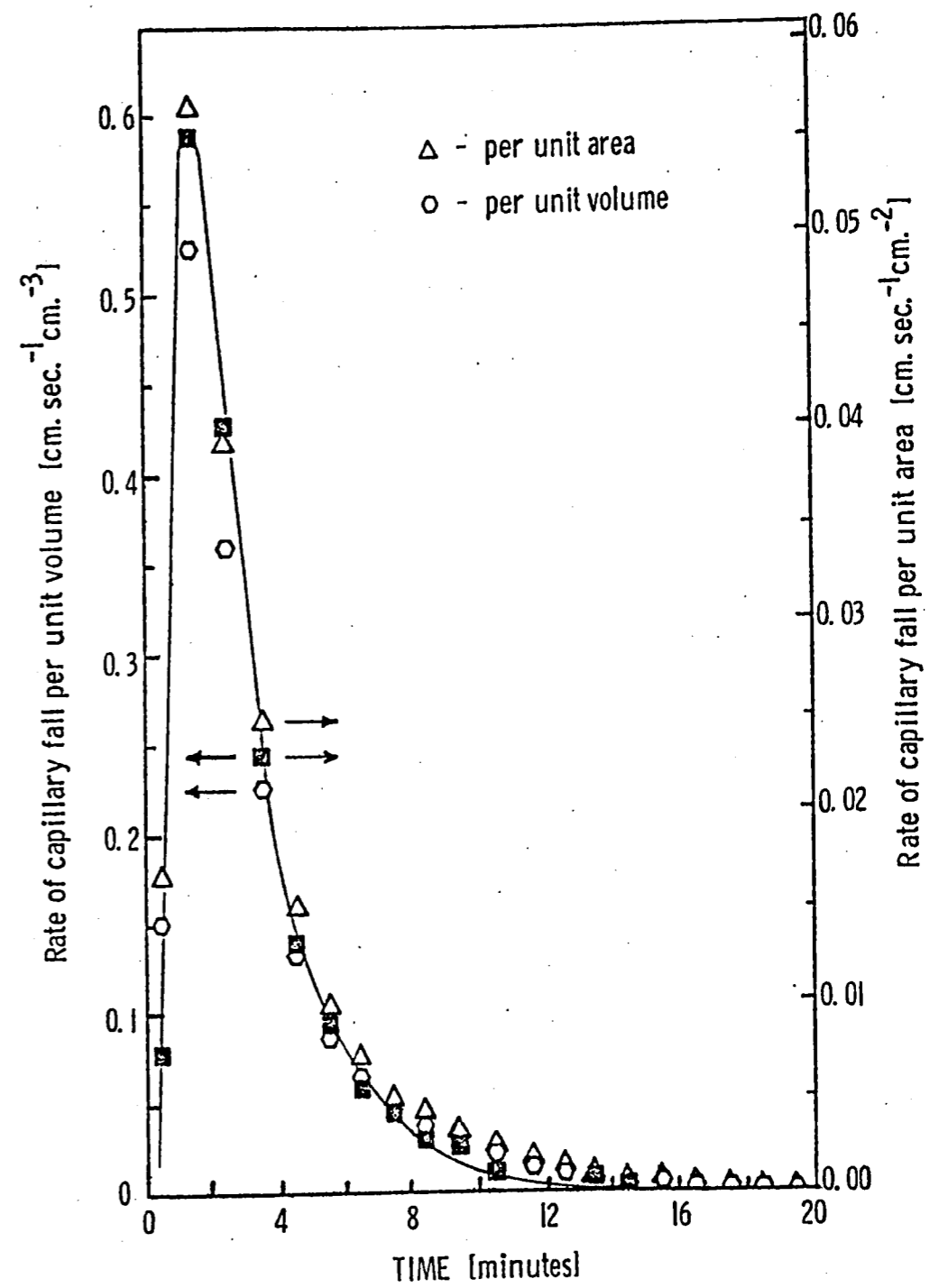


Figure 4.16 Comparison of rate data from the LU cell and the GE vessel, for the same polymerization recipe (samples 28 and 32).

and per unit area (  $\text{cm}/\text{min}/\text{cm}^3$  and  $\text{cm}/\text{min}/\text{cm}^2$  ). Both of these were included with the hope of determining which was more critical, volume or area, in scaling from the LU cell up to the GE vessel. The solid squares represent data from the LU cell (28) which determined the scale on both the left and right axis. The open figures are data from the GE vessel (O - volume basis,  $\Delta$  - area basis). In the early minutes of the reaction the comparison indicates that the rate is closer to being area dependant rather than volume dependant. This behavior is expected since the amount of free radicals produced is dependant on the number of initiator molecules activated by the UV radiation, which in turn is dependant on the surface area of exposure. This influences the rate of polymerization by determining the number of particles formed. As the polymerization proceeds past the rate maximum, particle formation has been completed and the rate becomes a weaker function of the initiation rate. During this stage the rate of polymerization becomes more dependant on the monomer concentration in the polymer particles. Therefore, it is obvious that scaling up to the GE vessel presented no problems as a result of the change in vessel configuration.

## 2. Time Restriction Check

In the proposed SPAR experiments, it became apparent that there would be a significant time delay between the loading of the experimental package and the actual microgravity experiments. Indications were that up to a 48 hour delay period was possible. Therefore, an experiment was carried out in which the GE vessel was loaded 48 hours prior to running the 20 minute polymerization. The results can be

found in Table II. The final conversion, as given by the gravimetric and dilatometric data, show a significant increase over the sample run just after loading. Note, however, that gravimetrically the increase is approximately 24% while dilatometrically the increase is only about 11%. This is a good indication that some polymerization had taken place in the sample prior to exposure to the UV radiation. Also note that sample 32-2 had been in dark storage a net nine days longer than 32. It is reasonable to expect some polymerization even under these storage conditions, due to exposure to ambient light during preparation and some thermal decomposition of the initiator species at room temperature. The amount of polymerization during 48 hours of storage could, in the limit, be as high as 10%. This could be a problem, in that an inhibitor would have to be found and incorporated into the polymerization recipe. This would have to be done without consequences to the five minute polymerization in the SPAR experiment.

In order to more closely approximate the time restriction involved in the free fall period of the experiment, a seven minute period for sample exposure to UV radiation was chosen. This time was chosen somewhat arbitrarily, in that the extra two minutes were added to allow for lamp warmup and possible extra seconds of microgravity that might occur in the experiment. The last point might be considered a rather optimistic point of view. This seven minute restriction was one of the limitations considered when a recipe was chosen for a more complete investigation using the GE vessel.

TABLE II

Photoinitiated Emulsion Polymerization of Styrene as a Function of Conditions and Recipe Parameters  
(3% styrene monomer)

Sample	Percent Sodium Lauryl Sulphate	Percent Co-emulsifier	Percent Photoinitiator	Percent Conversion 20 minutes		Percent Conversion 20 minutes Dilatometry
				minimum	maximum	
28 <sup>†</sup>	8.3 <sub>1</sub>	0.0	20	50	70	72
32 <sub>2</sub>	8.3	0.0	20	49	69	63
32-2 <sub>3</sub>	8.3	0.0	20	73	93	74
32-3	8.3	0.0	20	75	95	84
32-4	8.3	0.0	18	--	--	69
32-5 <sub>3</sub>	8.3	0.0	18	--	--	--
22 <sup>†</sup>	3.0	1.5	20	75	95	--
33	3.0	1.5	20	61	81	94
33-2 <sub>4</sub>	3.0	1.5	20	39	59	75

† polymerization in the LU cell, all others in the GE vessel

1 1:1 mole ratio of styrene to sodium lauryl sulphate

2 4 days old sample

3 vessel charged 48 hours prior to experiment

4 2 days old sample



### 3. Choice of Recipe for Further Investigations

In choosing a polymerization recipe for more detailed studies involving the GE vessel, the following criteria were used. The emulsion was required to have a high degree of stability prior to the polymerization and likewise the resulting latex. High polymerization rates and conversions were needed and these had to be insured for a seven minute polymerization as described previously. Also, no significant polymerization could be allowed for in the time period prior to the actual free fall experiments.

Two recipes have previously been indicated as good candidates for this further study. These are represented by the formulations of samples 28 and 22 as given in Table II. These recipes were run in both the LU cell and the GE vessel. For comparison, the kinetics of the experiments in the GE vessel are presented in Figure 4.17 (samples 32, 33). First, notice the difference in the rate curves. The system consisting of the one-to-one mole ratio of styrene to SLS with no co-emulsifier ( $\square$ ) peaks at a much higher rate than the co-emulsifier system ( $\circ$ ). This peak is reached in approximately two minutes for the former system while the latter peaks at around five minutes. The conversion-time curves show that the conversion reached at the end of the twenty minute period is greater for the co-emulsifier system by about 13%. This becomes unimportant, however, when the time restriction of the free fall experiment is considered, in that, if the polymerization is conducted for the 5 to 7 minutes allowed, the degree of conversion will be much greater for the 1:1, styrene/SLS combination. The stabil-

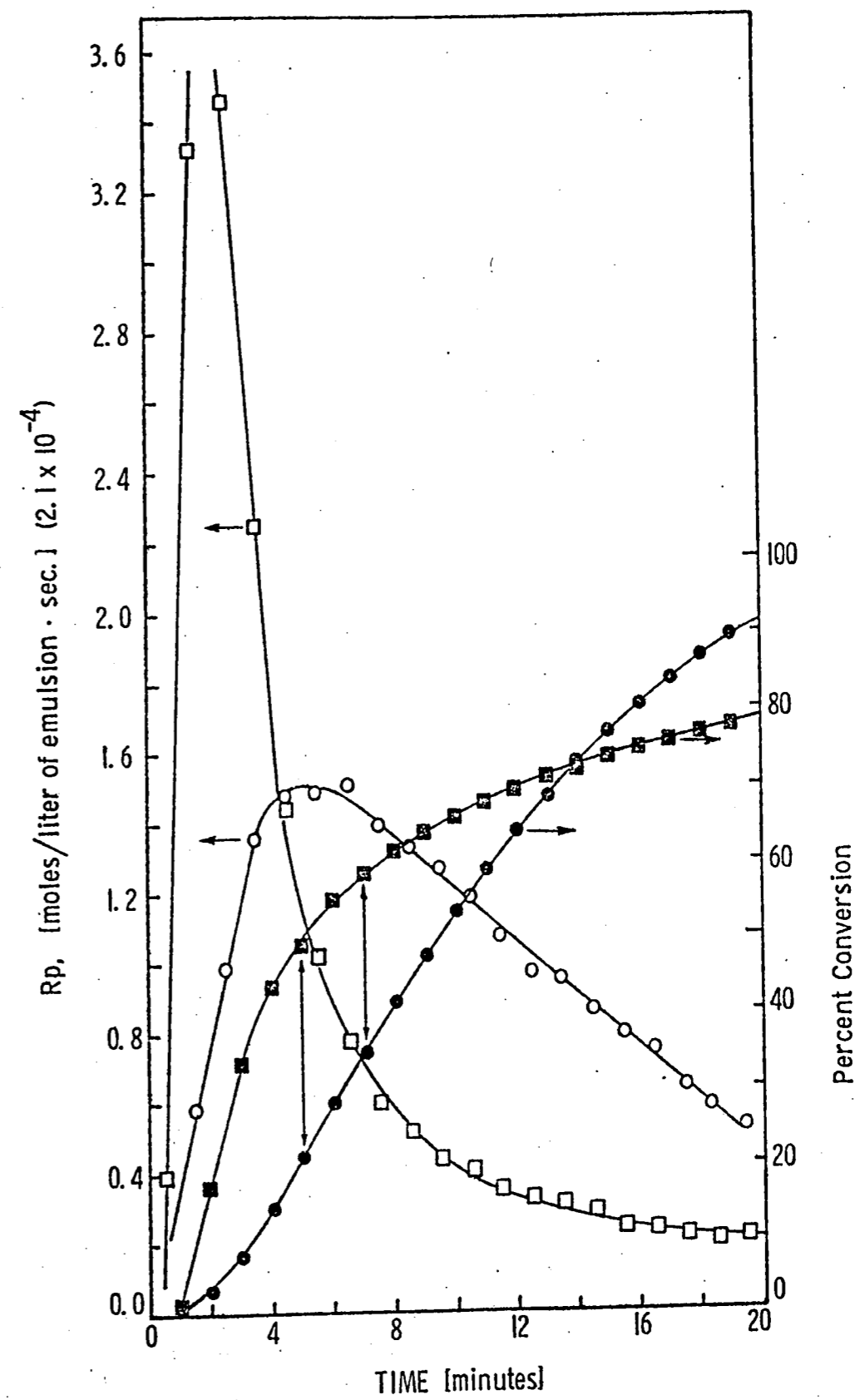


Figure 4.17 Comparison of polymerization rate ( $\square, \circ$ ) and conversion ( $\blacksquare, \bullet$ ) data for samples 32 ( $\square$ ) and 33 ( $\circ$ ), obtained from the GE vessel.

ity of these two systems before and after polymerization were comparable, being quite good for extended periods of time. Therefore, this was not a factor in choosing between these systems.

The choice was made to go with the one-to-one mole ratio of styrene to SLS in view of the facts given above. This system was then used for a more ordered and detailed study of photoinitiated polymerizations in the GE laboratory prototype vessel.

#### 4. Investigation of the One-to-one Mole Ratio of Styrene to SLS

All experiments conducted in the GE vessel using variations of this system were carried out for seven minutes of UV exposure, with dilatometric data being recorded for twelve minutes, an additional five minutes beyond the exposure period. It was determined that the dilatometric data could be used directly for obtaining rate of reaction and conversion-time curves without need for corrections involving cell volume and fluid volume changes with increasing temperature, as a result of lamp irradiation. This was verified by running a blank in the GE vessel. The emulsion was replaced by water and data was collected during twelve minutes of UV exposure, as given in Figure 4.18. Presented here is the capillary height as a function of time and temperature. Note that there is little significant change at the seven minute mark, at which the experiments were terminated with respect to UV exposure. Significant deviations occurred only after approximately ten minutes of exposure.

##### 4a. Rate of Polymerization and Degree of Conversion

In an attempt to optimize this one-to-one styrene/SLS micellized system, a series of polymerizations were performed in which the

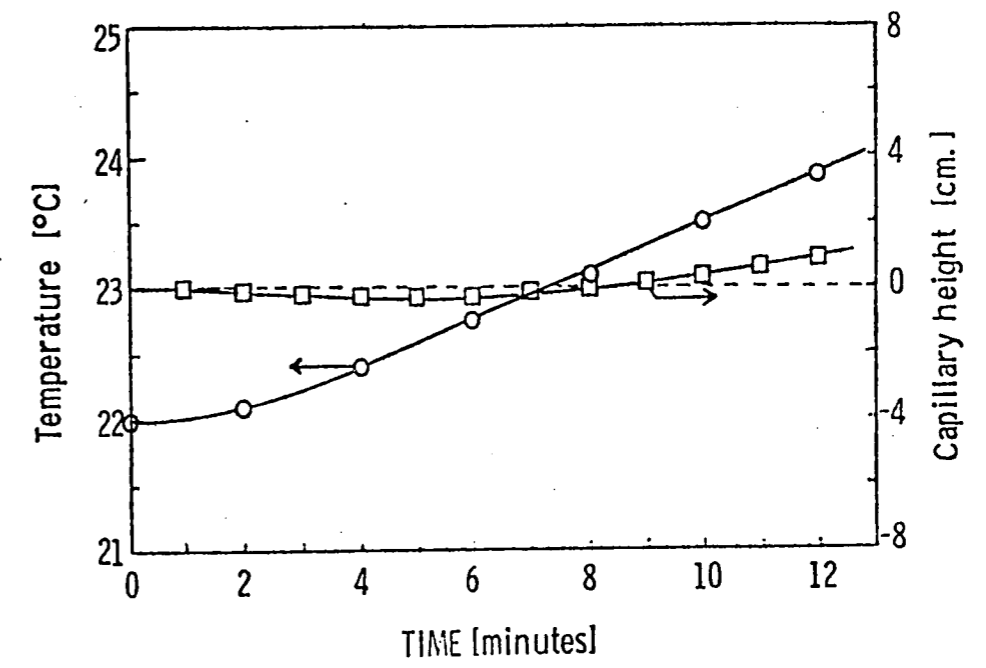


Figure 4.18 Temperature-time and the corresponding capillary change for water, used as a control in the GE vessel.

only variable was the amount of photoinitiator, DEAP, added to the recipe. The amount, based on the three percent styrene, ranged from 0% to 60%. The gravimetric and dilatometric conversion results are tabulated in Table III and graphed in Figure 4.19. Again minimum and maximum conversions are presented for the gravimetric determination, not knowing the amount of the photoinitiator that has been incorporated into the polymer particles. The bars represent the actual limits of the gravimetric determination of conversion, and the circles are the computed conversions from the dilatometric data. A smooth curve has been drawn in an attempt to fit the latter data. Note that this fits the data fairly well with the exception of points representing 12.1% and 15.0% DEAP. One could imagine that an oscillating curve might better fit this data, but studies have shown that the reproducibility is not high due to variations in environmental conditions and experimental techniques. (Examples are given in Appendix C.) These include factors such as the time between sample preparation and the actual experiment, the amount of exposure to ambient light, and the temperature of the solution prior to and during the experiment. This conversion versus initiator curve, as drawn, indicates a maximum in the the region between 20% and 25% DEAP. It is possible, however, that the curve levels out at a constant conversion between 50% and 70%. For purposes of optimization, the highest conversion with the least amount of initiator is desirable, as long as the time restrictions are fulfilled.

In order to locate this optimum with more assurance, a better comparison would be the polymerization rate curves at various initial

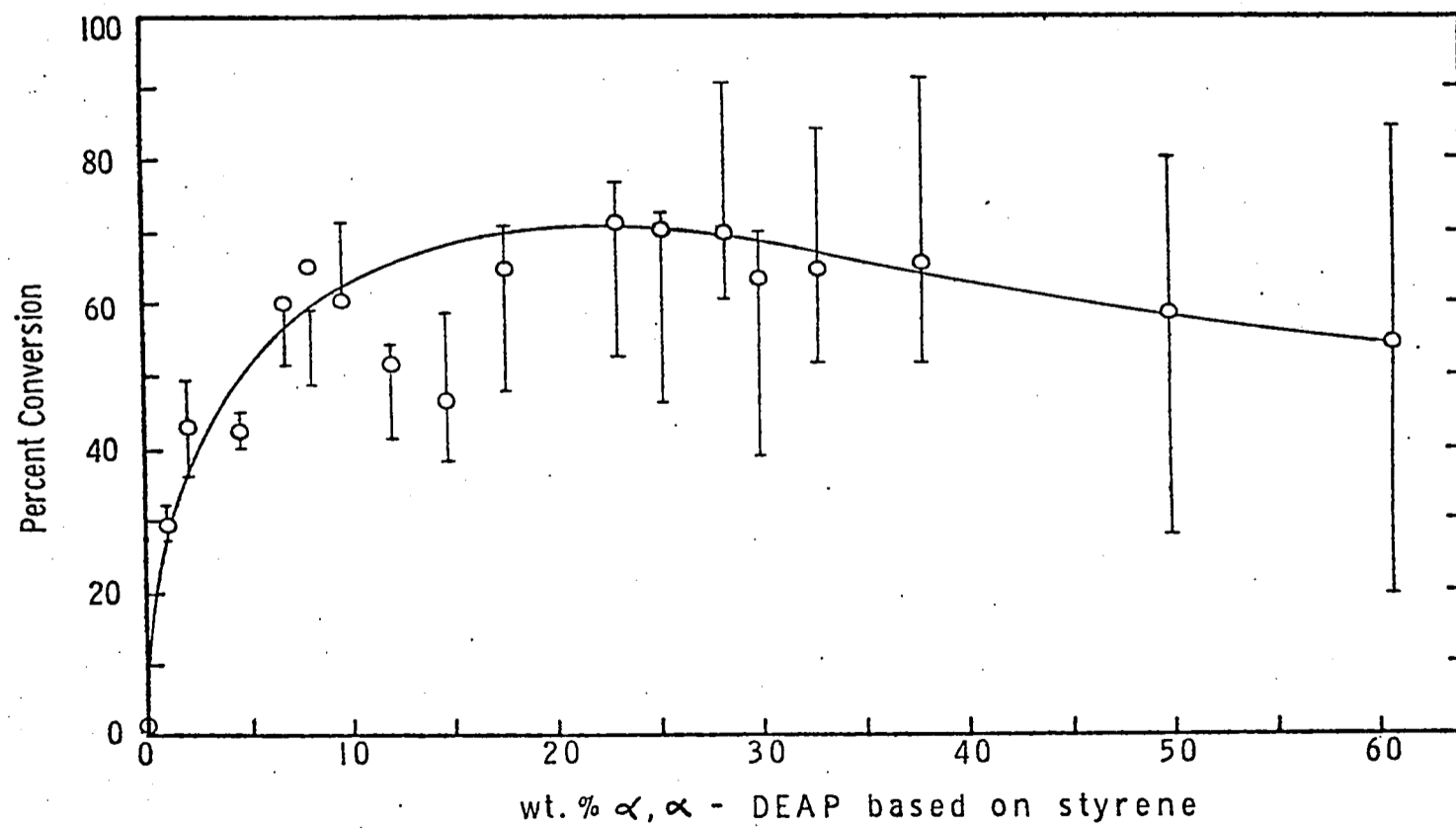


Figure 4.19 Percent conversion as a function of photoinitiator content, DEAP, for the micellized system consisting of 3% styrene and 8.3% SLS. Circles indicate dilatometric conversions while the bars are the limits of conversion determined gravimetrically.

TABLE III

Photoinitiated Emulsion Polymerization of Styrene as a Function of Initiator Concentration  
(3% styrene monomer)

Sample	Percent Sodium Lauryl Sulphate	Percent Photoinitiator	Percent Conversion minimum	Percent Conversion maximum	Percent Conversion Dilatometry
42	8.36	0.0		2.3	1.78
52	8.36	1.1	27.1	32.5	29.14
43	8.36	2.1	36.8	50.0	43.37
37	8.33	4.6	40.3	45.6	42.31
44	8.35	6.5	51.0	60.9	60.14
45	8.34	8.1	49.0	59.1	65.51
34	8.19	9.7	60.3	71.4	60.57
48	8.34	10.4	53.4	63.8	59.90
40	8.33	12.1	41.7	54.9	51.42
35	8.16	15.0	38.5	59.0	46.64
51	8.33	15.5	49.7	65.2	61.62
50	8.32	17.6	55.9	73.5	62.53
41	8.32	17.6	48.0	71.4	65.04
39	8.31	20.5	39.1	67.3	54.36
38	8.30	25.2	46.5	72.6	70.50
36	8.30	30.0	39.2	70.3	63.52
56	8.30	40.0	29.6	71.6	53.25

initiator concentrations. A series of these are given in Figures 4.20 and 4.22. Note in the first of these that as the amount of DEAP is increased, the curve maxima shift to shorter times (6.5 min.-1.1% DEAP, 4.5 min.-2.1%, 2.5 min.-8.1%) and also to higher rates ( $2.6 \times 10^{-4}$ ,  $4.2 \times 10^{-4}$ ,  $8.8 \times 10^{-4}$  moles/liter·sec.). The dilatometric conversion-time curves are given in Figure 4.21. This shift to shorter times becomes less noticeable after ~15% DEAP, while the rates continue to increase up to 25% DEAP and then decreases for 30% DEAP (Figure 4.22). In order to more clearly illustrate the effect increasing initiator has on the polymerization rate,  $R_p$ , a graph has been constructed relating this  $R_p$  at 1.5 minutes into the polymerization, to the amount of DEAP. This is presented in Figure 4.23. The time of 1.5 minutes was chosen because it represents the first reliable rate-time data point available with data recorded in minute intervals. The peak rate may seem more suitable, however, extrapolation to a maximum lacks accuracy. The rates given were determined over the 1 - 2 minute interval during polymerization. Note again that a maximum is observed between 20% and 25% DEAP (~23%) except that in this case it is much more distinct, with less scatter in the data.

How can these various results and observations be explained based on what is known about emulsion polymerization? First of all, this system is not conventional. The level of emulsifier, 8.3% with 3% styrene (1:1 mole ratio), is extremely high compared with typical systems. This can be termed a micellized or solublized system, in that only swollen micelles apparently exist, the styrene and initiator being sol-



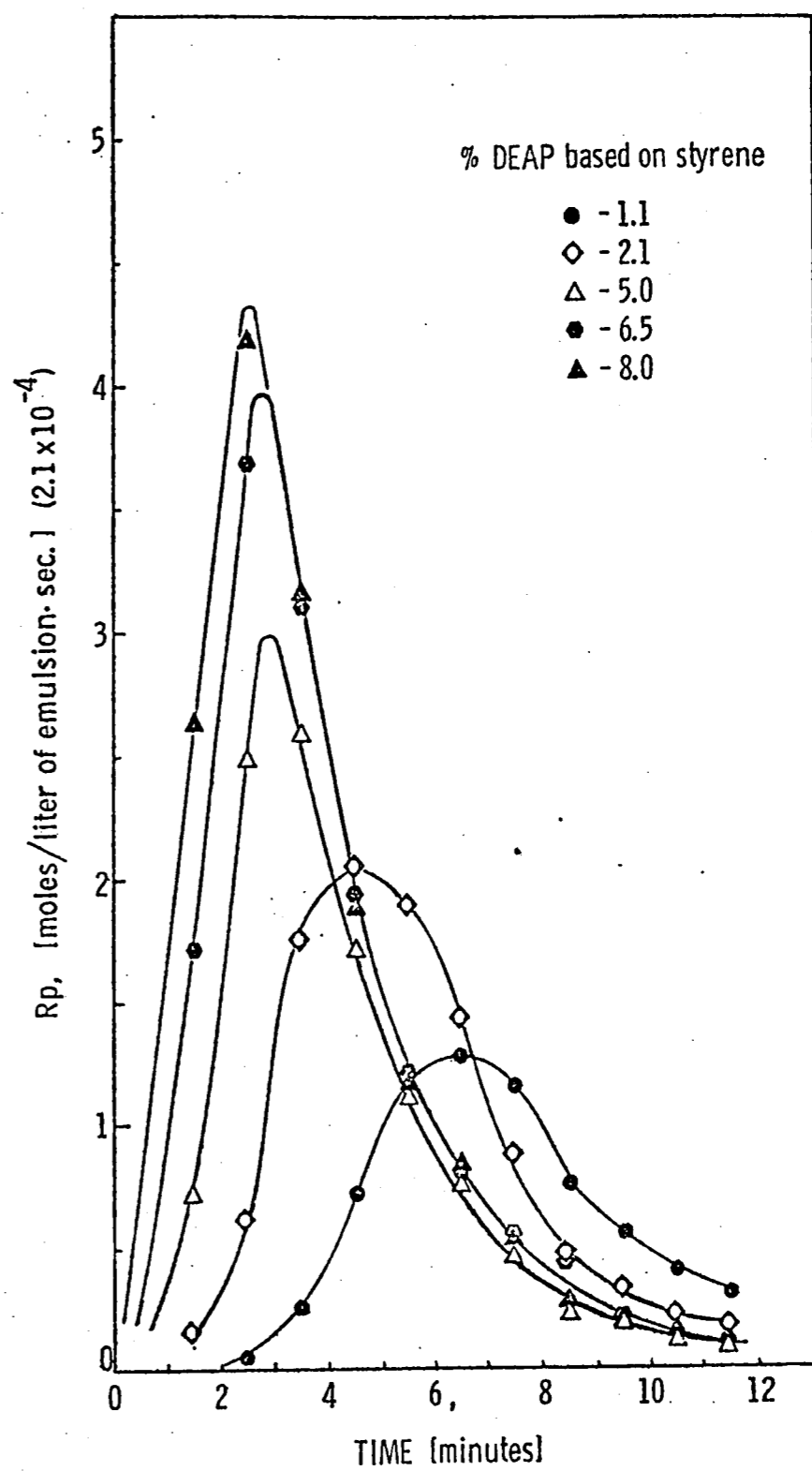


Figure 4.20 Polymerization rate curves for increasing photoinitiator DEAP, in the micellized system ( samples 52, 43, 37, 44, 45).

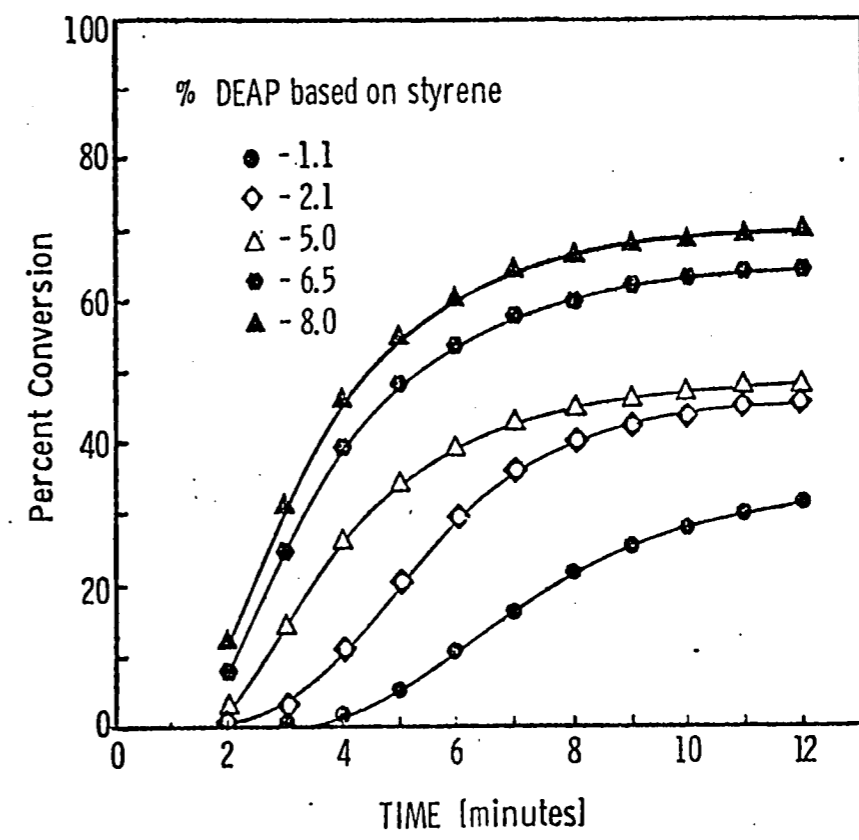


Figure 4.21 Conversion histories corresponding to the data in Figure 4.20.

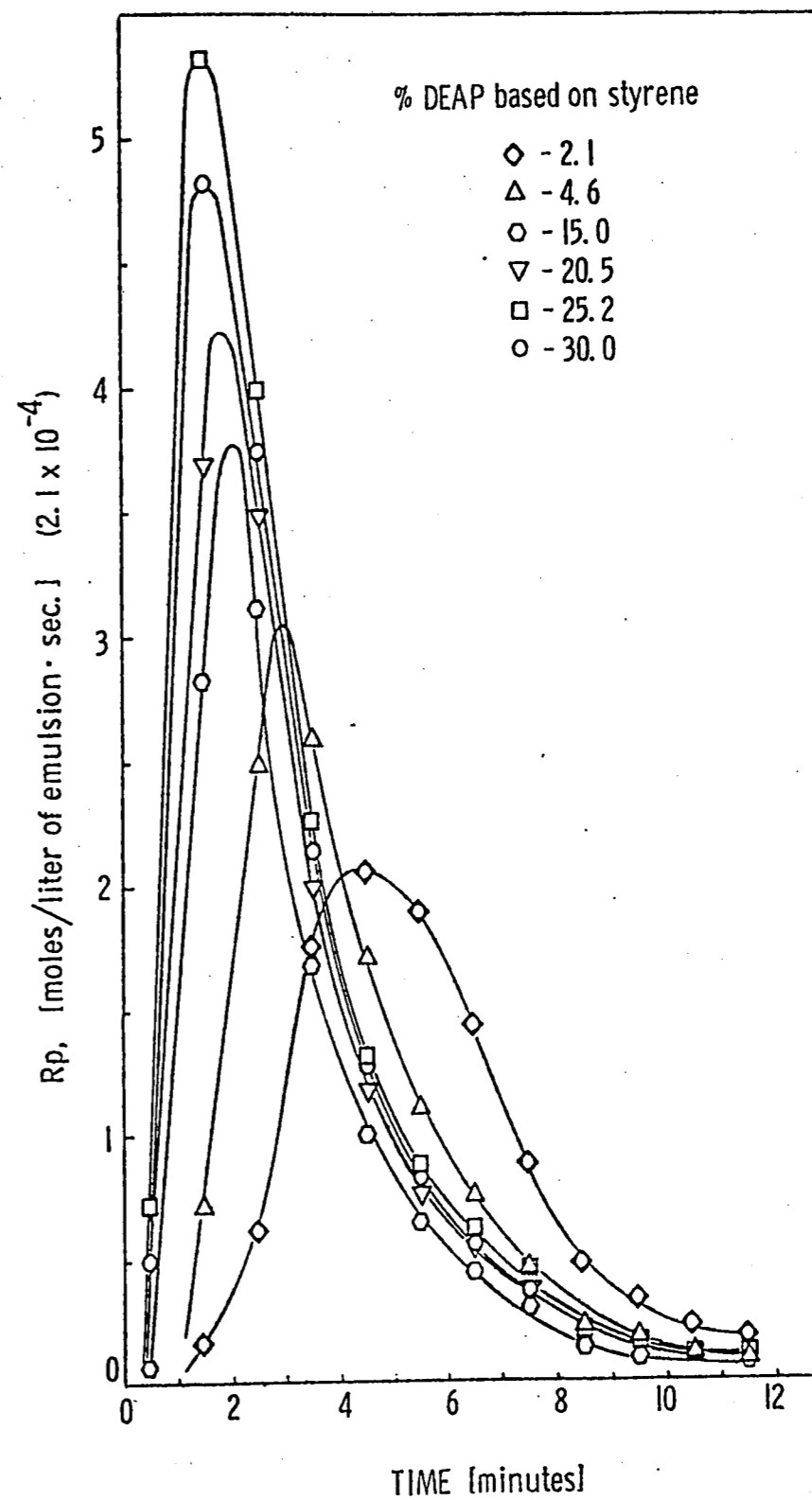


Figure 4.22 Polymerization rate curves for increasing photoinitiator, DEAP, in the micellized system (samples 43, 37, 35, 39, 38, 36).

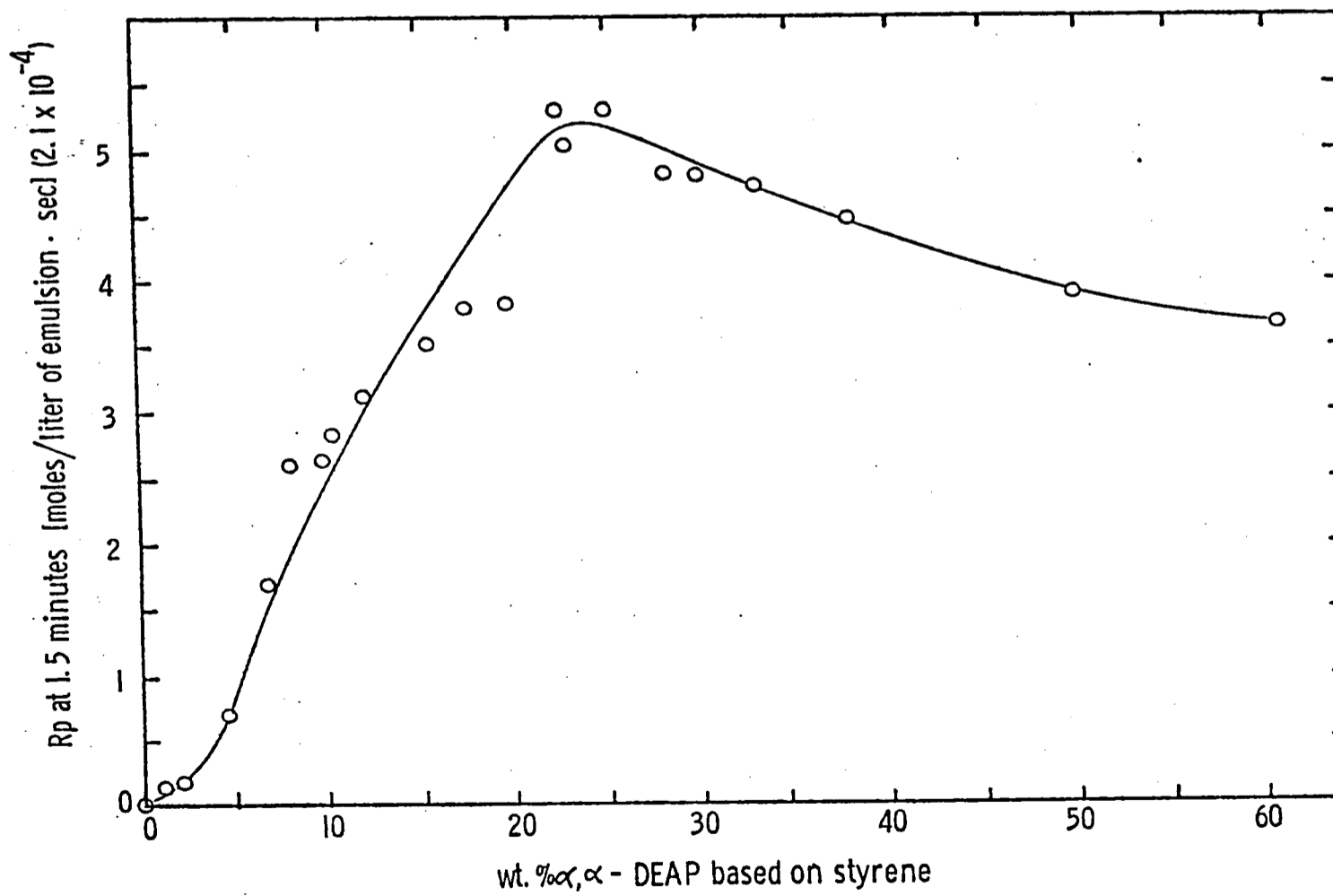


Figure 4.23 Rate of polymerization,  $R_p$ , at 1.5 minutes as a function of the photo-initiator content, DEAP, for the micellized system consisting of 3% styrene and 8.3% SLS.

ubalized inside these micelles. This implies that there are no monomer drops present. This is born out by the visual observation of near transparency of the prepared recipe prior to the polymerization. Also with this being the case, stage two of Harkins' conceptualization of emulsion polymerization would not exist for this system with the absence of monomer droplet resevoirs. The lack of an observable constant rate period in the kinetic curces does not conflict with this line of reasoning.

The shape of the initial rate versus initiator concentration curve can be understood by using the following reasoning. The increase in the initial rates with initiator can be due to the formation of increasing numbers of particles, as previously indicated by equations (5) , (6), and (7) in Part II. The rate of polymerization increases with the number of particles formed. The reason behind the subsequent decrease in the rates is less clear. The amounts of initiator used are much greater than what is commonly employed in conventional emulsion polymerization. At this high level, the effect of the oil soluble initiator as a diluent, reducing the monomer concentration, may outweigh that of increasing particle number. Also the number of particles generated may become less a function of initiator concentration at such extremely high concentrations. Therefore, as the initiator concentration increases the monomer concentration decreases and thus, the rate of polymerization. Another factor which may come into play is the shielding ability of the photoinitiator, that is, a cell thickness effect. To illustrate this, the intensity of transmitted UV radiation

at 350nm wavelength, was measured as a function of increasing DEAP concentration in the same micellized SLS system, no monomer being present. Figure 4.24 shows a decreasing intensity with increasing initiator. It is not known, however, if this influences the rate of polymerization via reduction in the rate of radical production or particle number. As will be shown, particle size, which is a function of number, is not a very sensitive function of the initiator level.

Another question raised concerns the limiting conversion reached in the polymerization. Note that the conversion-time curves begin leveling out even prior to the seven minute shut off time, revealing no perceptible discontinuity due to the termination of the UV radiation. Significant increases in the conversion would not be likely with increased exposure. No attempt was made to determine the actual amounts of initiator consumed in polymerization. It is assumed that the extreme levels used, rules it out as a limiting reactant, at least after the 23% for the maximum conversion of 70%. One possible reason may lie in the ability of the continuing forming polystyrene to shield the initiator from the UV radiation. With increasing conversion would come increased shielding. This assumes that the initiator species does not prefer to be near the surface of the particles but rather inside.

Another explanation given for limiting conversions, is the reduction in the termination rate constant due to the gel effect<sup>14</sup>. This occurs with the approach to the glass transition ( $T_g$ ) of the monomer/polymer. The  $T_g$  for polystyrene is 85°C<sup>14</sup>. This decreases with the introduction of monomer, acting as a plasticizer. In this case, the

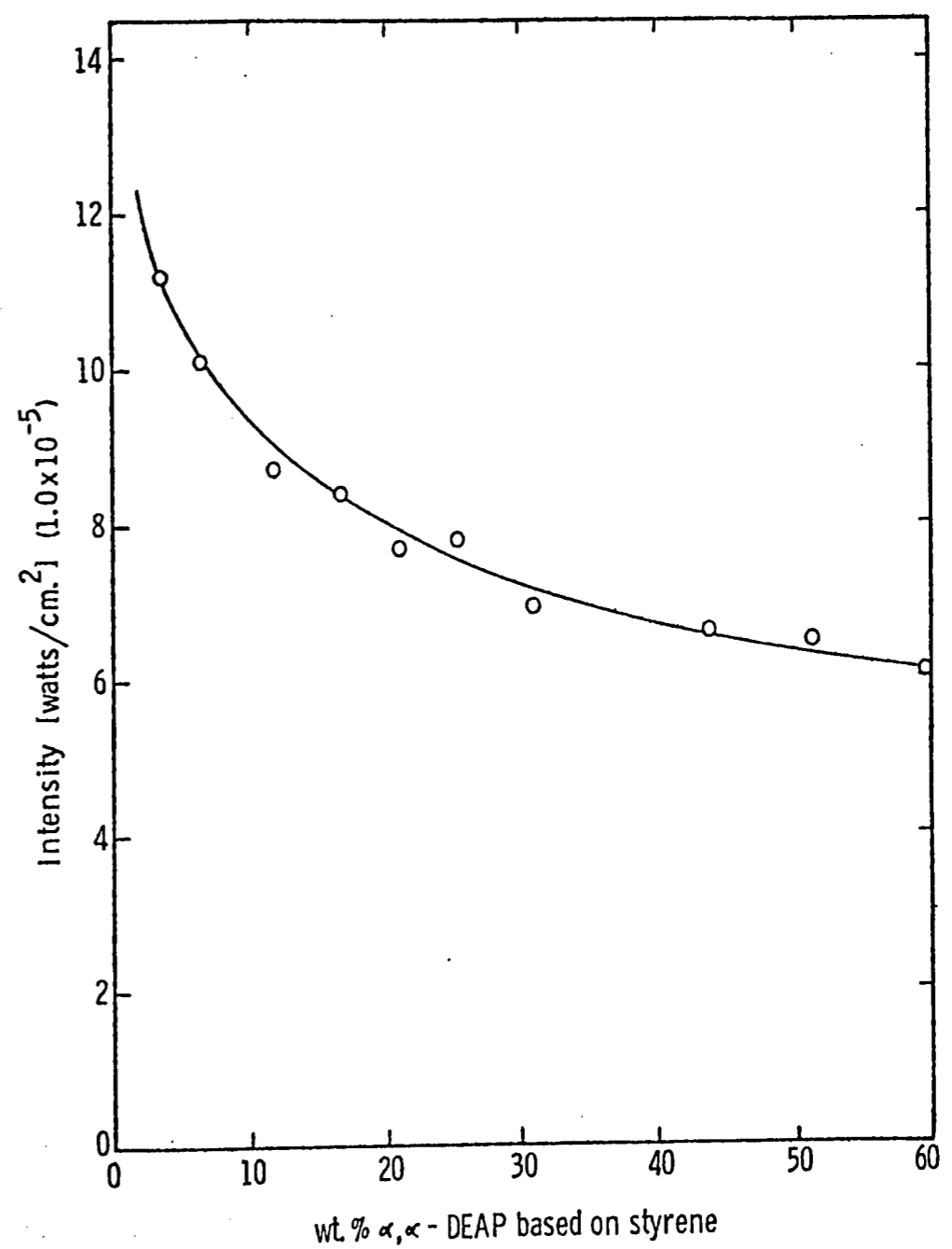


Figure 4.24 Intensity of UV radiation transmitted through the micellized system, no styrene present, as a function of the photoinitiator content, DEAP.

oil soluble initiator would also play a role in reducing the  $T_g$ . For this effect to be valid for this system, the particle composition at the limiting conversion would have a  $T_g$  around room temperature (20 - 25°C). This seems unlikely in view of data indicating that at 20°C, the  $T_g$  for polystyrene/styrene would have a composition in the neighborhood of 90%/10%, which is far from the 70% conversion limit obtained experimentally. The effect of the initiator on the  $T_g$  of the polymer is not known, however. Another point opposing this argument, is that there is no evidence of an acceleration in the polymerization as the  $T_g$  is approached (gel-effect), which has been shown to be the case for polystyrene<sup>14</sup>.

#### 4b. Particle Size and Molecular Weight

The average particle diameter and the weight average molecular weight have also been determined as a function of the amount of photoinitiator present in the 1:1 mole ratio system of styrene and SLS. The first of these is shown in Figure 4.25. The data represented by the circles and bars were obtained by use of the chromatographic system described in Experimental (Part III). The squares were determined from the light scattering experiments, a sample calculation being given in Appendix A. The difference in the results of the two methods can be attributed to the uncertainty of obtaining accurate sizes from HDC, the calibration curve not being well defined in this particle size region (see Figure 3.6). The sizes are correct relative to each other, but the curve should be shifted to smaller particle sizes. In any case, the particle size does not appear to be a strong function of the initi-



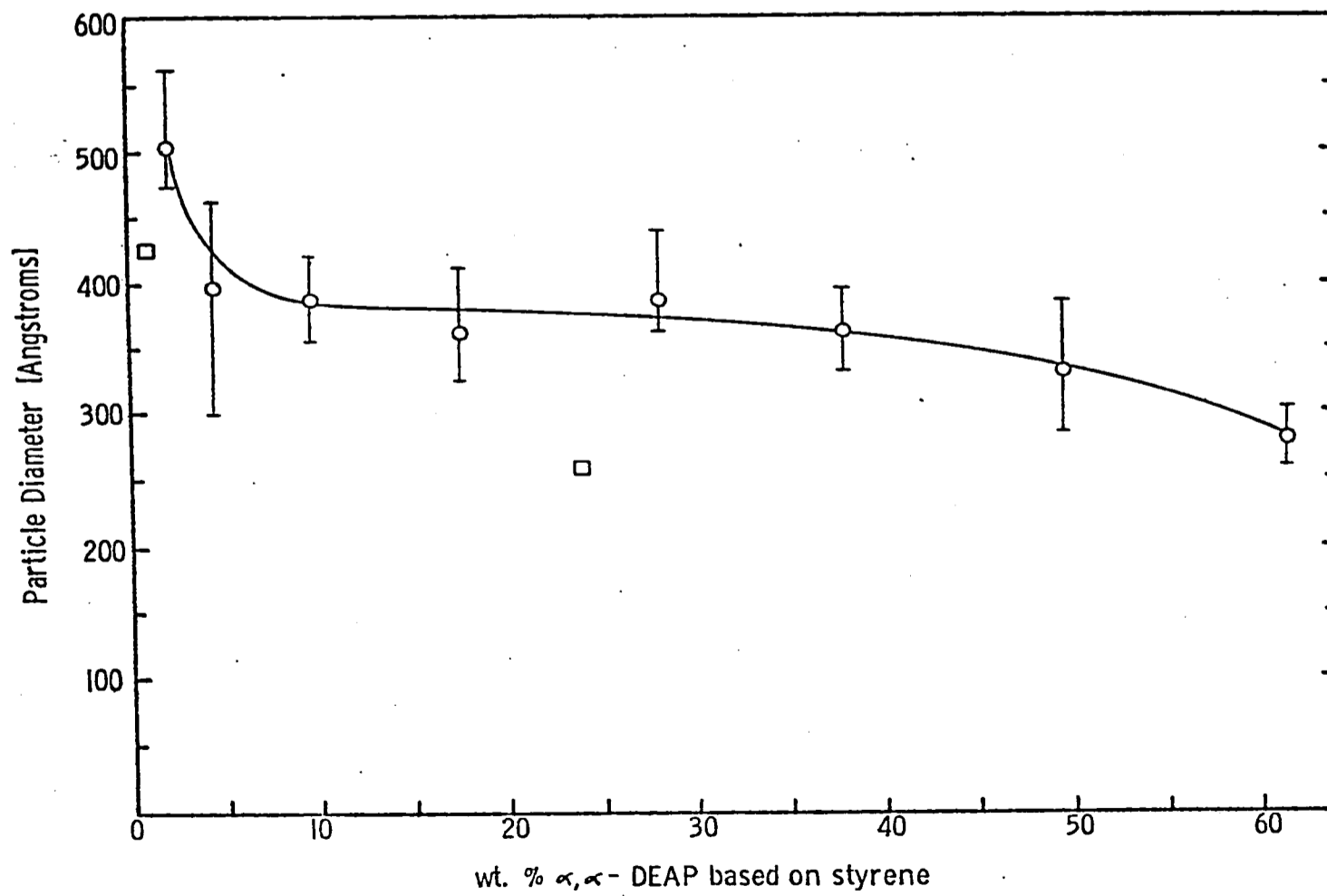


Figure 4.25 Average particle size as a function of the photoinitiator content, DEAP. Circles represent values obtained from HDC, the bars indicating the limits on these measurements. Squares were obtained from light scattering.

ator concentration, with the possible exception of levels under 5%. This may be deceptive, however, in that the particles could contain an ever increasing amount of initiator, which would tend to make the particles appear increasingly larger. The solubility of the initiator in water was not determined quantitatively, and therefore, the amount in the particles is unknown for the diluted samples used in these measurements.

Particle size determination by electron microscopy proved difficult with such small particles. Even though the serum replacement technique was used in order to "clean" the latex system from excessive emulsifier, particle definition was poor. This can be seen in Figures 4.26, a and b, for particles produced using 1% DEAP based on styrene. The particle size distribution represented in these micrographs would be rather broad, averaging near  $0.03\mu\text{m}$  (300Å). A particle count was not attempted. This sample is the same as that used in the light scattering measurements which resulted in a computed size of  $0.0425\mu\text{m}$  (425Å), this being somewhat larger than those represented in the micrographs.

These particle size results do indicate a decrease in particle size with increasing initiator which lends support to the concept of increasing particle number. The maximum in the rate curve of Figure 4.23 would not be expected for an ever increasing number of particles. This, however, does contribute support to the argument of reduced rate of polymerization based on monomer dilution.

The average molecular weights of selected samples were determined from GPC data, such as given in Figure 4.27. From these were calcu-

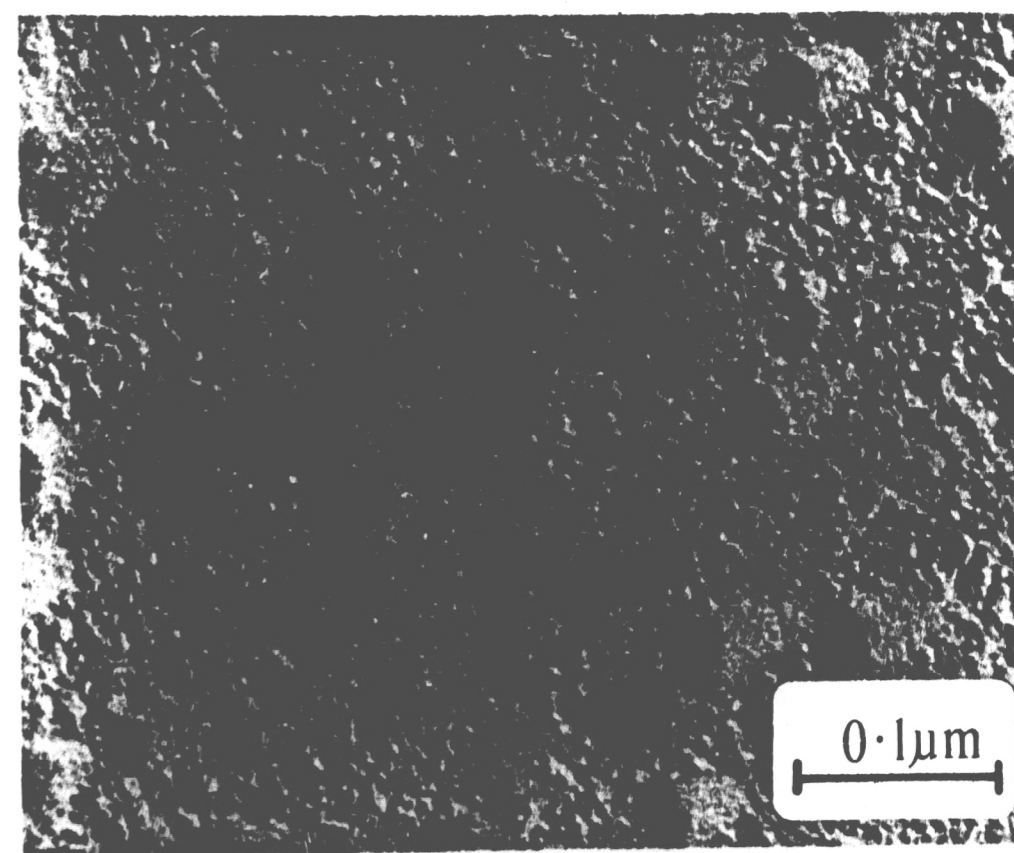
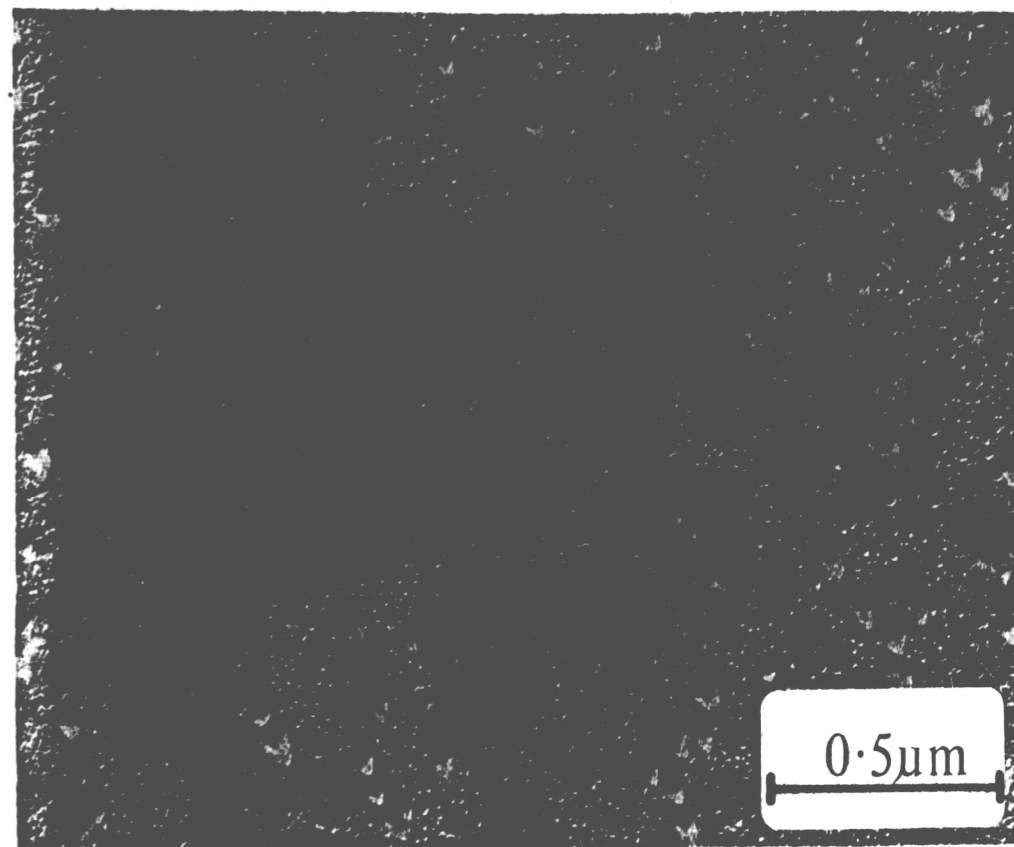


Figure 4.26 a,b Electron micrographs of the latex particles produced in the system consisting of 3% styrene, 8.3% SLS, and 1.1% DEAP based on styrene (sample 52).

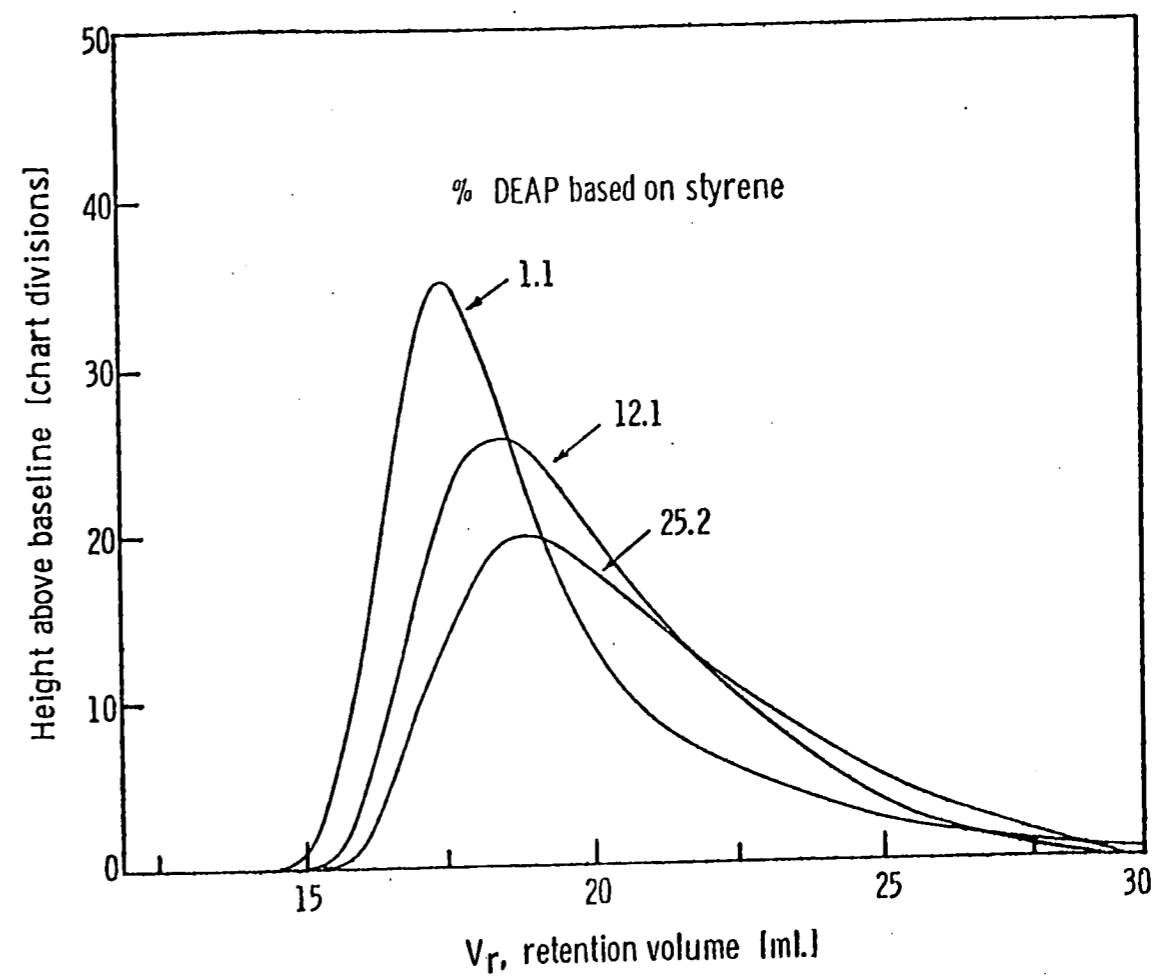


Figure 4.27 Examples of GPC chromatograms obtained for the micellized system with increasing photoinitiator content, DEAP.

lated the number and weight average molecular weights. Figure 4.28 illustrates the decreasing  $\bar{M}_w$  with increased photoinitiator concentration. The data represented by the blackened circles are an average of three measurements, the bars indicating the limits. The open circles represent only one measurement. This curve was drawn showing  $\bar{M}_w$  becoming less sensitive to increasing amounts of initiator, DEAP. In actuality it may continue to decrease. This would be expected in view of the increased number of free radicals generated with increasing amounts of initiator, terminating growing chains more often, thereby resulting in lower molecular weights. The calculated values for the number average molecular weight,  $\bar{M}_n$ , are also plotted on the same Figure, the squares having the same meaning as given above for the circles. The relationship is similar, but shows even a lesser sensitivity to the initiator level.

## 5. Other Kinetic Considerations

### 5a. Temperature Effect

In order to determine whether the variation in the ambient temperature conditions contributed significantly to the scatter in the conversion and rate versus percent initiator data, several experiments were conducted using three sample of the same emulsion, polymerized at different temperatures. These temperatures were reached by placing the entire GE vessel in a constant temperature bath with only the capillary tube above the water level, so that the kinetic measurements could be made via the cathetometer. The experiments were begun once

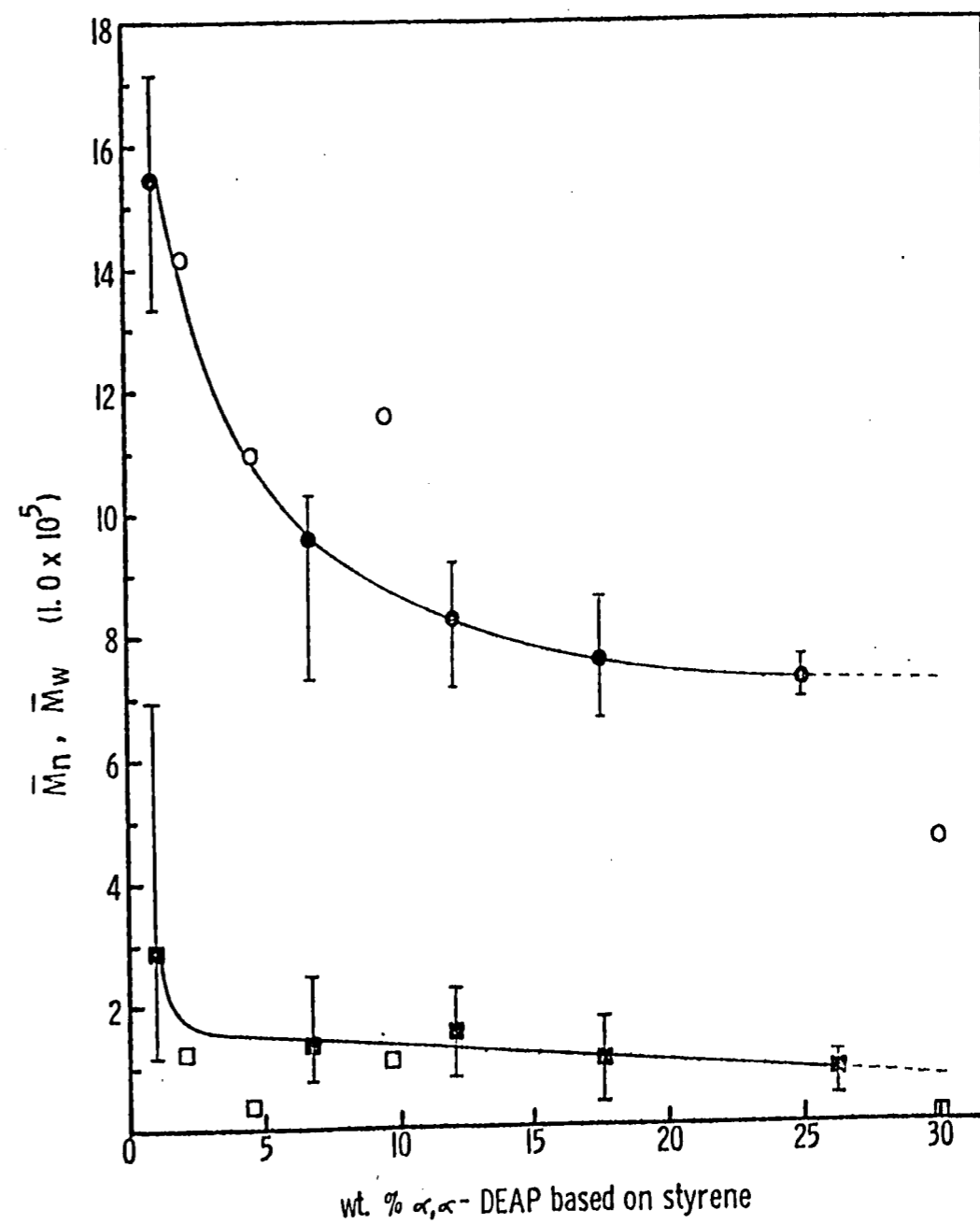


Figure 4.28 Number ( $\square, \blacksquare$ ) and weight ( $\circ, \bullet$ ) average molecular weights determined as a function of photoinitiator content, DEAP, for the micellized system.

the capillary fluid height reached a constant level, equilibration being assumed.

The rate-time and conversion-time curves are given by Figures 4.29 and 4.30. As expected qualitatively, the higher temperatures give greater rates and conversions. These results are illustrated in another way by Figure 4.31. Despite these effects, it appears doubtful that ambient temperature variations could have caused the scatter alone since the experimental temperature varied only between 20°C and 25°C. The final conversion changes by only about 3% in this range which is small when compared to the wide scatter in Figure 4.19. Procedural and preparative effects are more likely to contribute to this scatter and lack of consistent reproducibility. Some examples of reproducibility variations are given in Appendix C.

As an aside, one can check the Arrhenius dependence of the rate on the temperature from this data by using the following arguments and simplifying assumptions. The rate of polymerization,  $R_p$ , for an emulsion polymerization has previously been given by equation (8).

$$R_p = k_p [M_p] \bar{n} N_p \quad (8)$$

The average number of radicals per particle,  $\bar{n}$ , can vary from being much smaller than unity to much greater. In either case, it is found to be proportional to  $(1/N_p)(R_I/k_{tp})^{0.5}$ . This assumes that termination in the aqueous phase, and desorption of free radicals is negligible in the case of this system. Substituting this into (8), the proportionality is obtained,

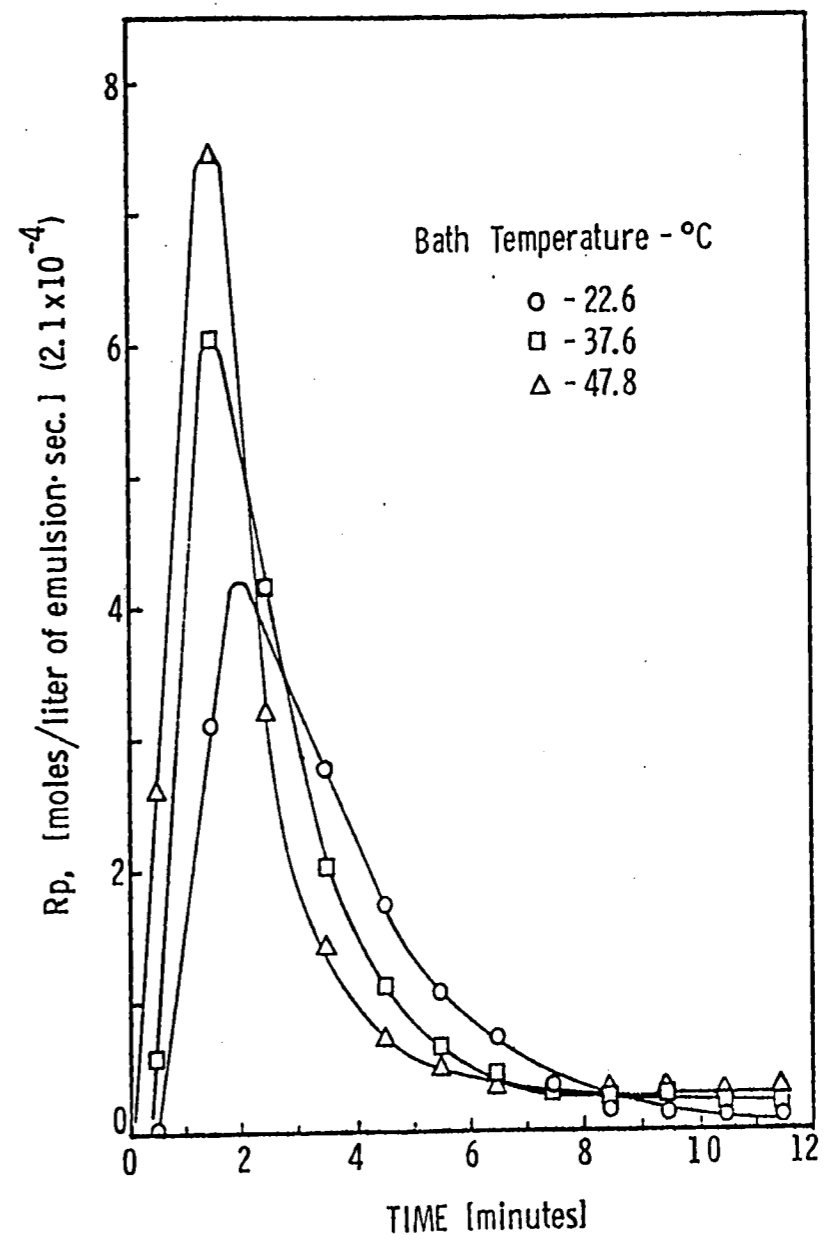


Figure 4.29 Polymerization rate curves as a function of the polymerization temperature for the system 3% styrene, 8.3% SLS, and 17.6% DEAP based on styrene.



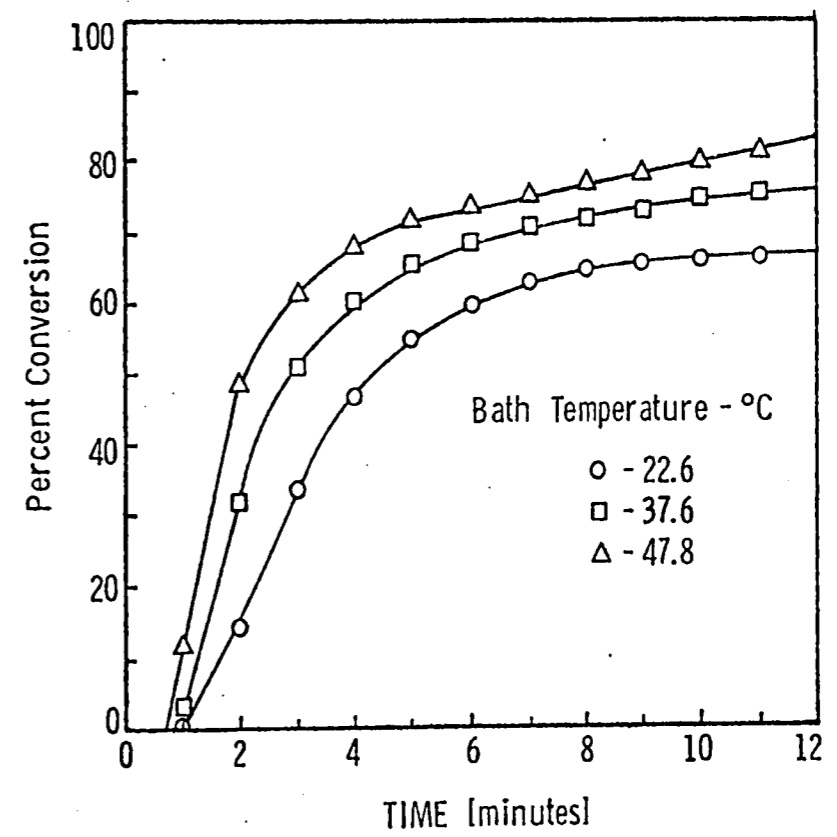


Figure 4.30 Conversion histories corresponding to the data in Figure 4.29.

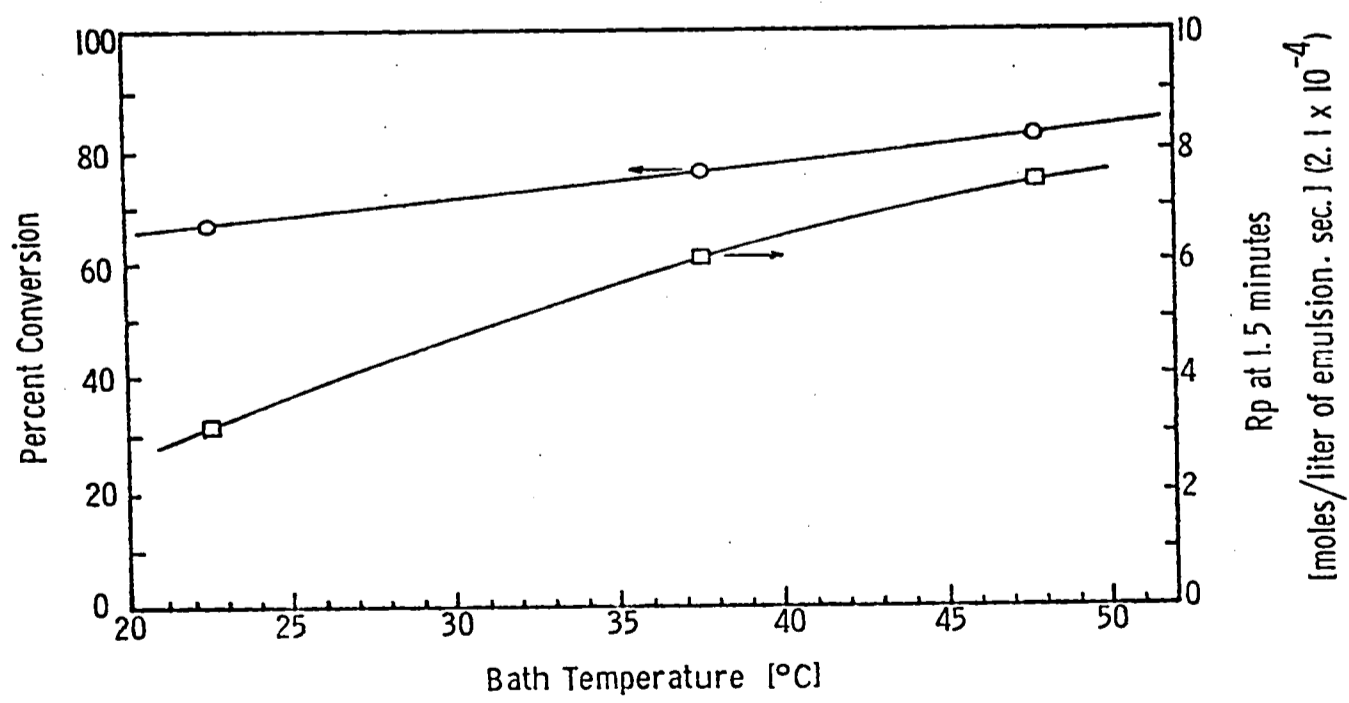


Figure 4.31 Percent conversion and rate of polymerization,  $R_p$ , at 1.5 minutes, as a function of temperature, obtained from the data in Figures 4.29 and 4.30.

$$R_p \propto \frac{k_p}{k_{tp}^{0.5}} [M_p] (R_I)^{0.5} \quad (9)$$

For a photoinitiated polymerization, the polymerization rate depends on the ratio,  $k_p/k_{tp}^{0.5}$ . The temperature dependence of this ratio can be obtained by combining the two Arrhenius equations into one,

$$\ln \left[ \frac{k_p}{k_{tp}^{0.5}} \right] = \ln \left[ \frac{A_p}{A_{tp}^{0.5}} \right] - \frac{[E_p - (E_{tp}/2)]}{RT} \quad (10)$$

Combining (9) and (10),

$$\ln(R_p) \propto \ln \left[ \frac{A_p}{A_{tp}^{0.5}} \right] + \ln([M_p](R_I)^{0.5}) - \frac{E_R}{RT} \quad (11)$$

from which  $E_R$  can be obtained from the slope of a plot of  $\ln(R_p)$  versus  $1/T$  as given in Figure 4.32. From the graph  $E_R$  is computed to be 6.6 kcal/mole. The literature values of  $E_p$  and  $E_{tp}$  for styrene are 7.3 kcal/mole and 1.9 kcal/mole respectively<sup>11</sup>, giving  $E_R = 6.45$  kcal/mole, which is remarkably close to the experimental value obtained here, considering the assumptions made to reach it.

#### 5b. Dependency of the Rate on Monomer and Initiator Concentrations

The rate of polymerization is proportional to the first power of the monomer concentration in the particles and to the one-half power of the rate of initiation or initiator concentration. This latter point is true only if the intensity of the UV radiation within the fluid does not vary appreciably with the thickness. Relatively good agreement is

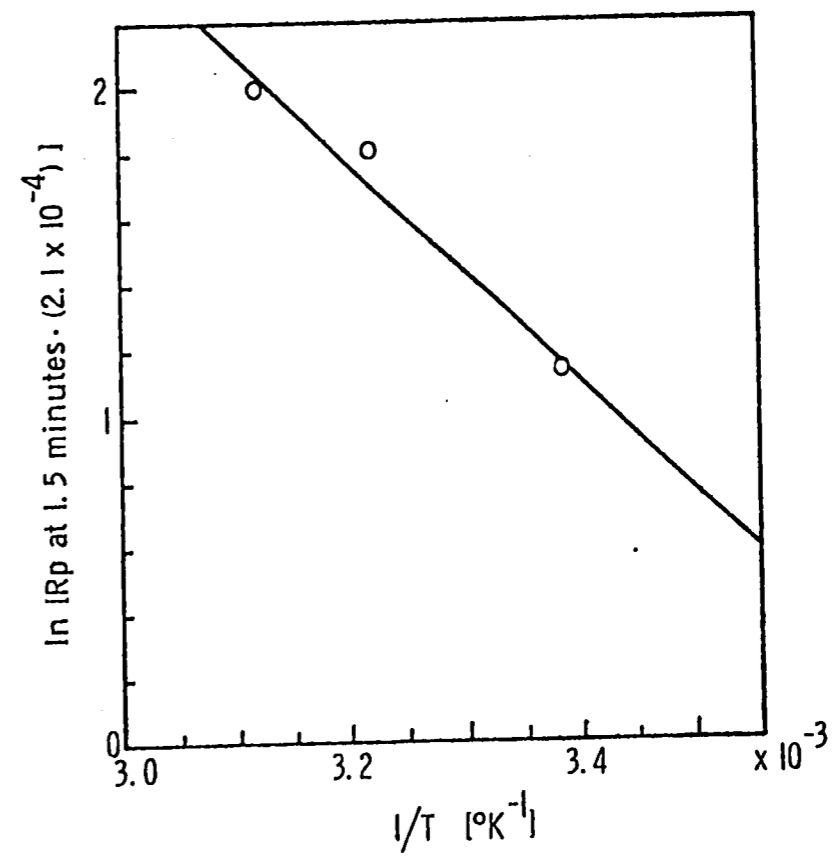


Figure 4.32 Arrhenius dependence of the rate of polymerization on the temperature. The line represents the least squares fit of the data.

found with experiment, as given in Figures 4.33 and 4.34. Note that the rate versus conversion (or monomer concentration) follows a linear relationship only after the peak in the rate curve has been reached, that is, after all particles have been formed. This would imply that after this point the monomer concentration continues to decrease in the particles. The fit in Figure 3.34 seems reasonable for this relationship, in the least, not disputing the predictions.

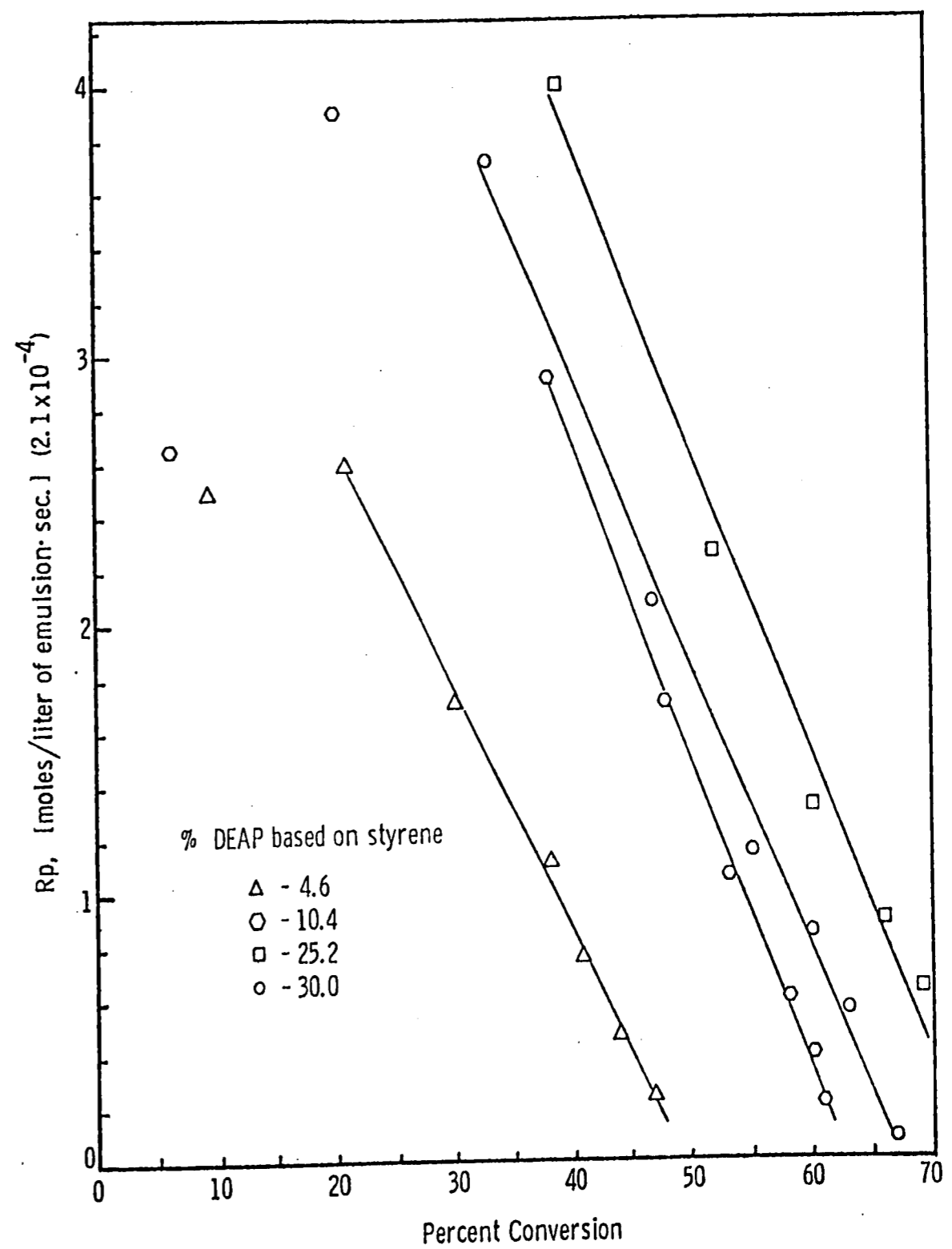


Figure 4.33 Rate of polymerization,  $R_p$ , as a function of the percent conversion (or monomer concentration) for varying amounts of DEAP in the micellized system, 3% styrene and 8.3% SLS.

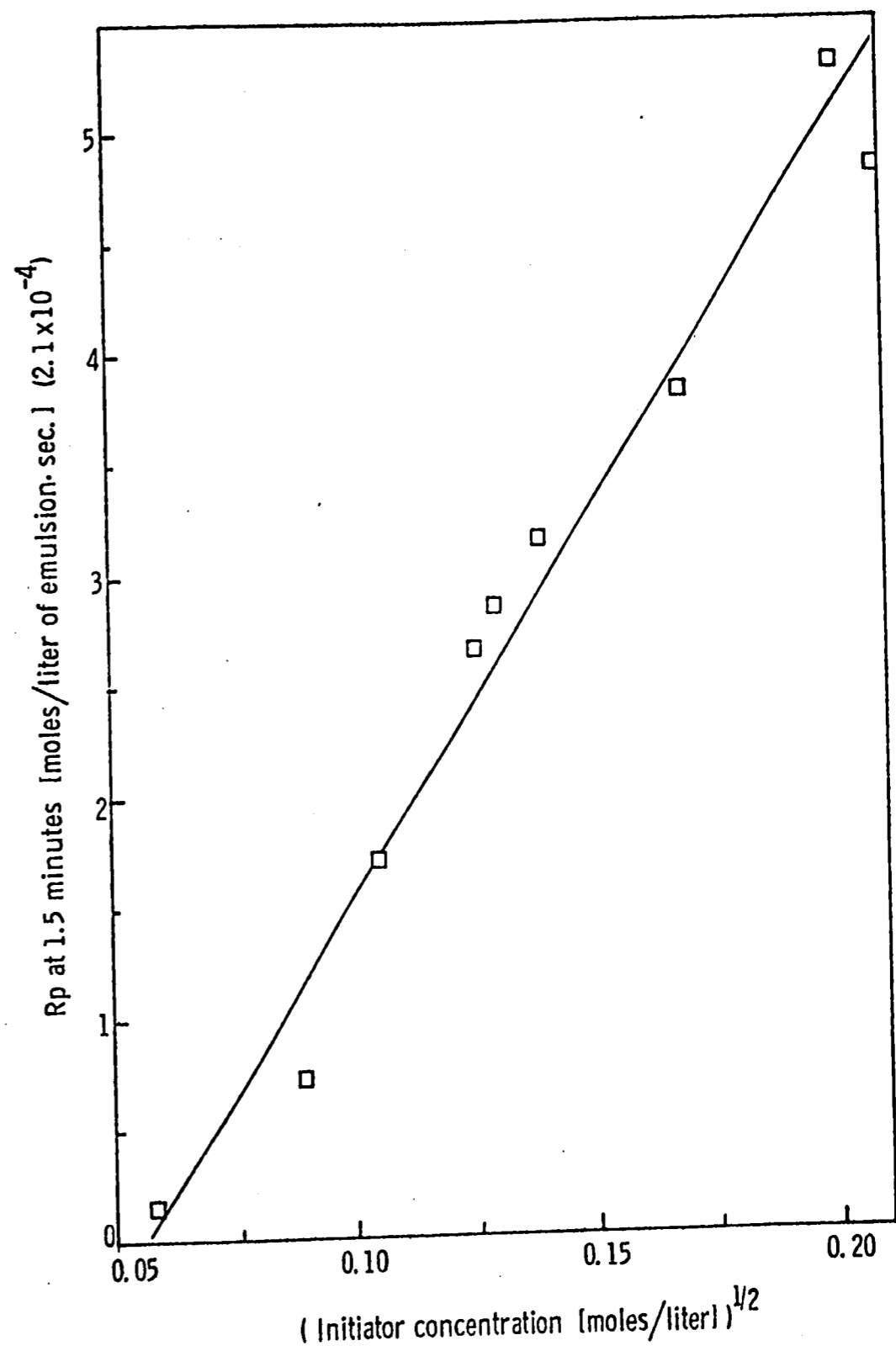


Figure 4.34 Rate of polymerization,  $R_p$ , at 1.5 minutes, as a function of the square root of the initial photo-initiator concentration, DEAP, in the micellized system, 3% styrene and 8.3% SLS.

## PART V - SUMMARY AND CONCLUSIONS

The work described in this report has evolved from a feasibility study designed to investigate the possibility of producing small-particle-size latexes in a GE laboratory prototype vessel of similar configuration to that proposed for the SPAR experiments. This has gone somewhat beyond the original six-month definition study, leading to the following statements concerning the results.

1. The LU cell has proven effective in enabling the establishment of the critical dimensions of the SPAR prototype reactor and also in the development of a recipe for detailed investigation using the GE built vessel.

2. The most effective polymerization formulation with regards to emulsion and product stability, polymerization rate and conversion in seven minutes, was found to be a micellized styrene and SLS system (3 wt% styrene, 8.3 wt% SLS) with  $\alpha,\alpha$ -diethoxyacetophenone as the photoinitiator (23 wt% based on the styrene). A conversion of 70% can be obtained with this system.

3. This recipe was finalized with the use of the GE prototype, which proved comparable to the LU cell in several polymerization kinetic comparisons. The GE vessel, in contrast, has proven reliable for obtaining kinetic information, through capillary dilatometry. Expansion of fluid and vessel due to the UV source and heat of reaction are negligible during the short duration experiments.

4. Conversions determined gravimetrically are not decisive, in that the amount of DEAP incorporated into the polymer is unknown.



5. In the micellized styrene/SLS system, the molecular weight and particle size were found to decrease with increasing amounts of photoinitiator, but with decreasing sensitivity.

6. The polymerization kinetics correlate well with known emulsion polymerization rate expressions.

PART VI - POSTSCRIPT

As a result of this work, NASA has accepted the two phase proposal entitled "Production of Large-Particle-Size Monodisperse Latexes", bypassing the SPAR experiments in favor of the longer duration Space Shuttle experiments. This jump in the proposed sequence has virtually eliminated the need for the short duration photoinitiated polymerizations. More conventional thermal initiators will hence be used instead, in a seeded polymerization sequence to produce large-particle-size monodisperse latexes.

REFERENCES

1. Backus, R.C. and Williams, R., J. Appl. Phys. 19, 1186 (1948);  
ibid. 20, 224 (1949).
2. Alfrey, T., Bradford, E.B., Vanderhoff, J.W., and Oster, G.,  
J. Opt. Soc. Am. 44, 603 (1954).
3. Bradford, E.B. and Vanderhoff, J.W., J. Appl. Phys. 26, 864 (1955).
4. Smith, W.V., J. Am. Chem. Soc. 70, 3695 (1948).
5. Willson, E.A., Miller, J.R., and Rowe, E.H., J. Phys. Colloid  
Chem. 53, 357 (1949).
6. Bradford, E.B. and Vanderhoff, J.W., J. Colloid Sci. 11, 135 (1956).
7. Vanderhoff, J.W., Vitkuske, J.F., Bradford, E.B., and Alfrey, T.,  
J. Polymer Sci. 20, 225 (1956).
8. Vanderhoff, J. W., Preprints, Am. Chem. Soc. Div. Organics & Plastics  
Chem. 24, (2), 223, (1964).
9. For a general description, see Vanderhoff, J.W. in "Vinyl Polymer-  
ization Vol. I, Part II", Ham, G.E., editor, Marcel Dekker, New  
York, 1969, Chapter 1; p. 1-138.
10. Harkins, W.D., J. Am. Chem. Soc. 69, 1428 (1947); J. Polymer Sci.,  
5, 217 (1950).
11. Osborn, C.L. and Stevens, J.J., Amer. Paint & Coatings Journal,  
1, 48 (1977).

12. Ugelstad, J. and Hansen, F.K., Rubber Chemistry and Tech., 49, 3 (1976).
13. Smith, W.V. and Ewart, R.H., J. Chem Phys. 16, 592 (1948).
14. Friis, N. and Hamielec, A.E., ACS Symposium Series 24, 82 (1976).
15. Nagy, D.J., Silebi, C.A., McHugh, A.J., paper presented at the National ACS meeting, Miami Beach, Florida, September 1978.
16. Ahmed, S.M., El-Aasser, M.S., Pauli, G.H., Poehlein, G.W., and Vanderhoff, J.W., accepted for publication in J. Colloid Interface Sci.
17. Ugelstad, J., El-Aasser, M.S., and Vanderhoff, J.W., J. Polymer Sci.: Polymer Letters 11, 503 (1973).

APPENDICES

APPENDIX A

Determination of Average Particle Size from Light Scattering

In light scattering the turbidity or optical density of a dispersion is measured to determine the particle size of the dispersed particles, in this case, polystyrene.

Turbidity is defined by

$$\tau = \ln \frac{I_0}{I} = N R_{\text{ext}} x \quad (\text{A-1})$$

where  $I_0$  = intensity of light through reference medium

$I$  = intensity of light through sample

$N$  = number of particles per unit volume ( $\text{cm}^{-3}$ )

$x$  = pathlength of the light (cm)

$R_{\text{ext}}$  = extinction cross-section ( $\text{cm}^2/\text{particle}$ )

and the optical density is given by

$$\text{O.D.} = \log \frac{I_0}{I} \quad (\text{A-2})$$

Therefore,

$$\text{O.D.} = \frac{N R_{\text{ext}} x}{2.303} \quad (\text{A-3})$$

The number of particles per unit volume is given by

$$\begin{aligned} N &= \frac{\text{weight percent polystyrene}}{(\text{volume of a particle})(\text{density of a particle})} \\ &= \frac{100 w}{(4\pi R_p^3/3) \rho_p} \end{aligned} \quad (\text{A-4})$$

As a first approximation, it is assumed that the radius of the particles is at least 20x smaller than the wavelength of the source in the medium.  $R_{ext}$  is then calculated by the Rayleigh formula for the scattering of light,

$$R_{ext} = \frac{24 \pi^3 (4\pi R_p^3/3) n_m^4}{\lambda_o^4} \left[ \frac{(n_p/n_m)^2 - 1}{(n_p/n_m)^2 + 2} \right]^2 \quad (A-5)$$

where  $\lambda_o$  = wavelength of the source in vacuo  
 $n_p$  = refractive index of the particles  
 $n_m$  = refractive index of the medium  
 $R_p$  = particle radius

For polystyrene the refractive index is given as a function of wavelength by,

$$n_{p,20^\circ C} = 1.5663 + \frac{7.85 \times 10^{-3}}{\lambda_o^2} + \frac{3.34 \times 10^{-4}}{\lambda_o^4} \quad (A-6)$$

and for water,

$$n_{m,20^\circ C} = (1.7650 - 1.3413 \times 10^{-2} \lambda_o^2 + \frac{6.5438 \times 10^{-3}}{\lambda_o^2 - 0.115^2})^{0.5} \quad (A-7)$$

Therefore  $R_p$  is calculated from,

$$R_p = \left[ \frac{(O.D.) (2.303) (\rho_p) (100) (\lambda_o^4)}{(w) (n_m^4) (24\pi^3) (4\pi/3)} \left[ \frac{(n_p/n_m)^2 + 2}{(n_p/n_m)^2 - 1} \right]^2 \right]^{1/3} \quad (A-8)$$

For sample 52 (1% DEAP based on styrene) with 0.00239 wt% solids, measured at a wavelength of 320nm, the O.D. was found to be 0.00957. The density of polystyrene is 1.05gm/cc. With  $n_p = 1.675$  and  $n_m = 1.374$ , the diameter was computed to be 335 Å. Note that this does approximate the assumption of the wavelength being at least 20x larger than the particle radius.



APPENDIX B

Determination of  $\bar{M}_n$  and  $\bar{M}_w$  by Gel Permeation Chromatography (GPC)

The data taken from a GPC chromatogram are the recorder chart readings, height and retention volume,  $V_r$ . The latter is used to obtain the molecular weight from the calibration curve. The chart height readings represent the total concentration of the polymer at a particular retention volume and are proportional to the quantity  $N_i M_i$ , which appears in the calculations of the average molecular weights,

$$\text{number average, } \bar{M}_n = \frac{\sum N_i M_i}{\sum N_i} \quad (\text{B-1})$$

$$\text{weight average, } \bar{M}_w = \frac{\sum N_i M_i^2}{\sum N_i M_i} \quad (\text{B-2})$$

Therefore, the curve height, in chart units, is set equal to  $N_i M_i$ . The retention volume for that point on the curve gives the corresponding  $M_i$ , from which  $N_i$  is calculated. Knowing these, computations can be made for  $N_i M_i^2$ . Making the summation at intervals of the retention volume of 0.05ml,  $\bar{M}_n$  and  $\bar{M}_w$  are computed using equations B-1 and B-2.

Example : Sample 52, 1% DEAP based on styrene

$V_r$ , ml	Height, divisions
15.0	0.05
15.5	0.16
16.0	0.49
16.5	0.92
17.0	1.32
17.5	1.65

V<sub>r</sub>, ml      Height, divisions

18.0	1.91
18.5	2.02
19.0	2.07
19.5	2.00
20.0	1.84
20.5	1.66
21.0	1.45
21.5	1.24
22.0	1.05
22.5	0.87
23.0	0.73
23.5	0.61
24.0	0.49
24.5	0.40
25.0	0.33
25.5	0.27
26.0	0.22
26.5	0.18
27.0	0.15
27.5	0.13
28.0	0.12
28.5	0.10
29.0	0.08
29.5	0.06
30.0	0.04

$$\Sigma \text{Height} = \Sigma N_i M_i = 24.61$$

$$\Sigma N_i = 1.9166 \times 10^{-4}$$

$$\Sigma N_i M_i^2 = 3.287 \times 10^7$$

$$\bar{M}_n = 1.285 \times 10^5$$

$$\bar{M}_w = 1.334 \times 10^6$$

APPENDIX C

Reproducibility Studies

The following pages contain graphs demonstrating the lack of consistency in obtaining reproducible kinetic results for the micellized system containing 3% styrene and 8.3% SLS with varying amounts of photoinitiator, DEAP. Some of these are quite close while others are off by large margins. Each recipe was prepared twice, once for each experiment. It has been noted that the reproducibility on a once prepared sample is quite good and does not show this unreliability.

